Supporting Information

for

Catalysis Activity and Chemoselectivity Control with the *Trans* Ligand in Ru-H Pincer Complexes

Mita Halder,[a] Diana Castillo Cardenas,[a] Angela Chartouni,[a] and Damien B. Culver[a] *

*Email: culver@ameslab.gov

Address where work was performed:
[a]Ames National Laboratory, Ames, IA, 50011, United States

Table of Contents

Purification of 1

In a nitrogen filled glovebox, a 25 mL round bottom flask was charged with 1 g of **1** and 20 mL of dichloromethane. After stirring for 30 minutes at room temperature, the suspension was filtered through a layer of celite. The filtrate was concentrated under reduced pressure resulting in a pale yellow colored solid. The solid was further washed with diethyl ether (3×10 mL) and finally dried under vacuum for 1 hour. Percent recovery of **1** was 46 %. Representative ^{31}P NMR spectra for **1** before and after purification are shown in Figure S1.

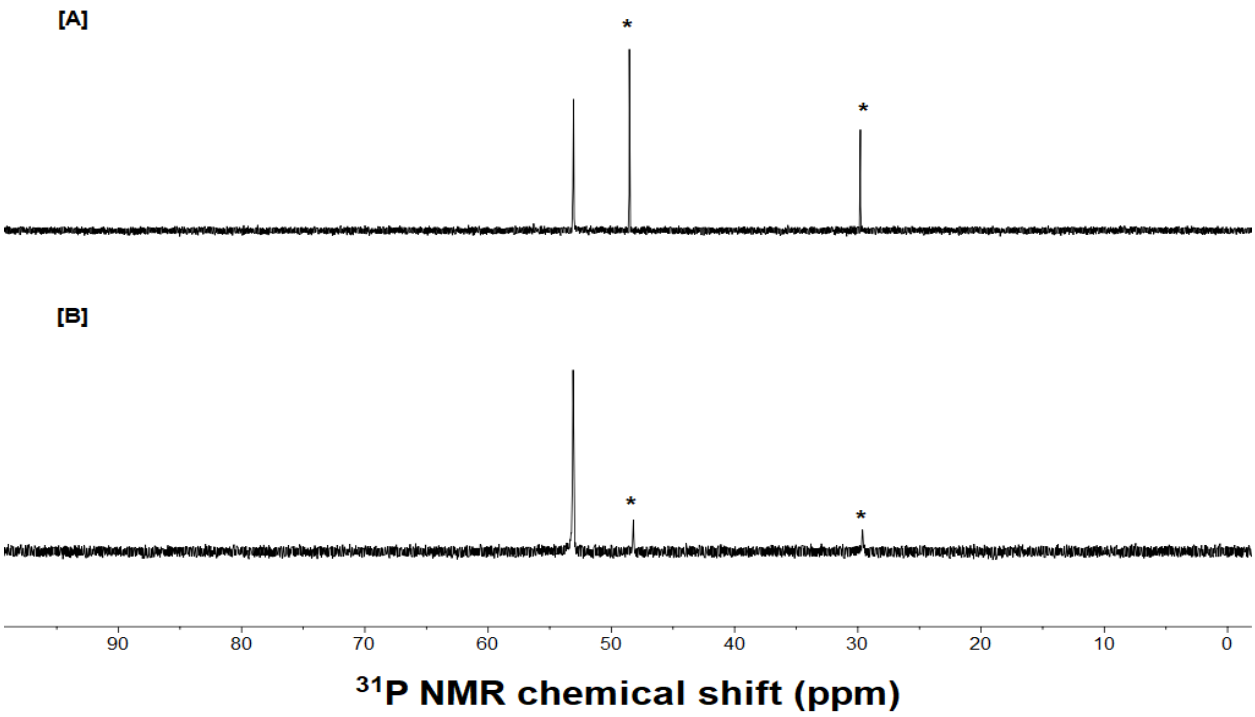

Figure S1. $^{31}P\{^{1}H\}$ NMR spectrum of **1** (A) before and (B) after purification; [*]: residual impurities.

Catalysis data and NMR spectra

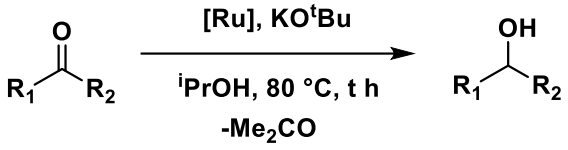

Table S1. Summary of the catalytic transfer hydrogenation of benzophenone reactions.[a]

Entry	**Catalyst**	**Catalyst loading (%)**	**KO^{t}Bu loading (%)**	**Time (h)**	**Yield (%)[b]**
1	**2a**	2	5	1	96.2 (±0.6)
2	**2a**	2	2.5	1	91.8 (±0.4)
3	**2a**	0.5	2.5	1	97.0 (±0.15)
4	**2a**	0.5	0.625	4	97.4 (±0.9)
5	**2a**	0.1	0.625	5.5	97.1 (±1)
6	**1**	0.1	0.625	5.5	96.6 (±1.46)
7	**2a**	0.1	NA	24	<1
8	none	NA	0.625	24	8

a. Reaction conditions: benzophenone (0.15 mmol), ^{i}PrOH (0.4 mL), catalyst, and KO^{t}Bu were combined in an NMR tube along with a benzene-d_6 capillary and heated at 80 °C. b. Yields were determined by ^{1}H NMR spectroscopy and performed in duplicate. The values reported are the average and the errors are reported in the parentheses. NA = not applicable.

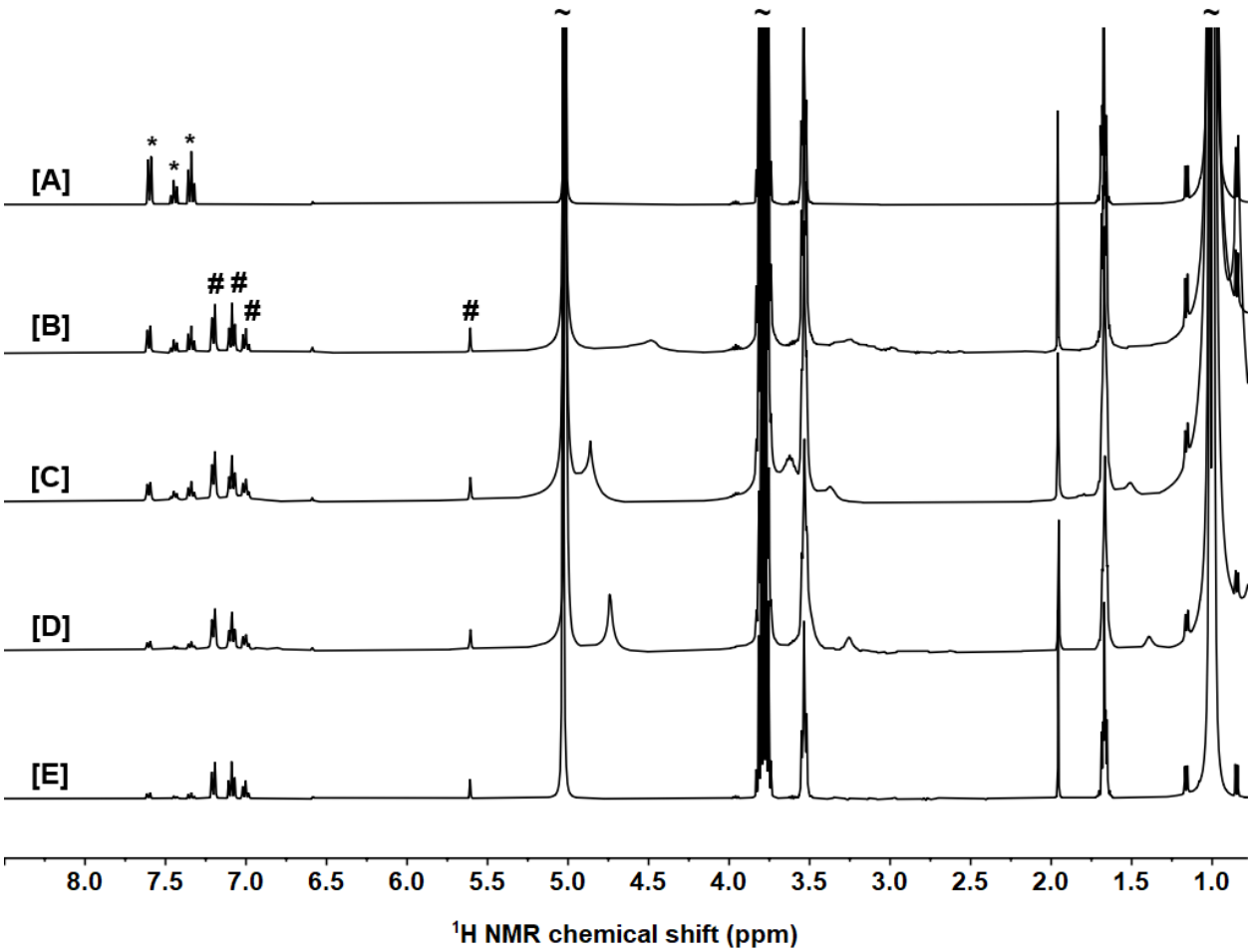

Figure S2. Representative ^{1}H NMR spectra to monitor the progress of the reaction between benzophenone (0.15 mmol) and ^{i}PrOH in presence of **1** (0.1 mol% of Ru), and KO^{t}Bu (0.625 mol%). [A] after 0 minutes; [B] after 75 minutes; [C] after 2.5 h; [D] after 3.45 h; [E] 5.5 h. * = Benzophenone; # = diphenylmethanol. ~ = solvent signal cutoff.

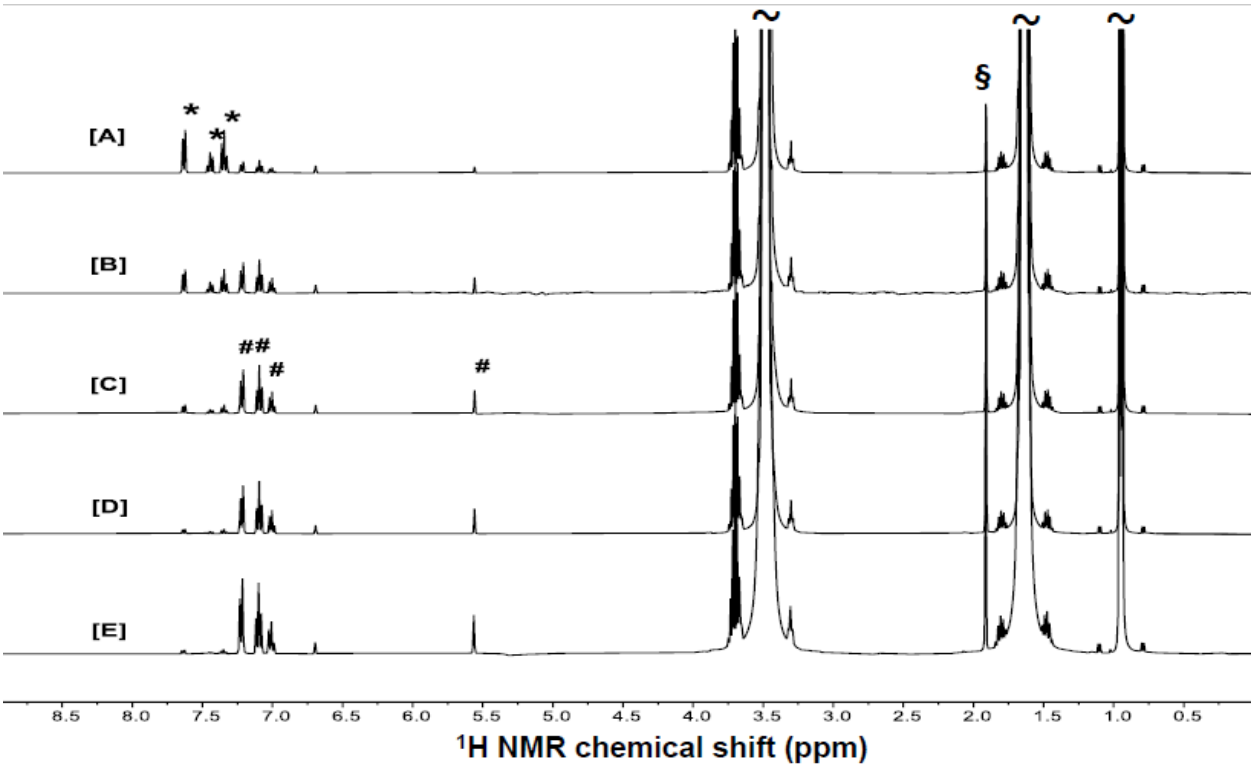

Figure S3. Representative ^{1}H NMR spectra to monitor the progress of the reaction between benzophenone (0.15 mmol) and iPrOH in presence of **2a** (0.1 mol% of Ru), and KOtBu (0.625 mol%). [A] after 15 minutes; [B] after 45 minutes; [C] after 2 h; [D] after 2.45 h; [E] 4.15 h. * = Benzophenone; # = diphenylmethanol, § = acetone. ~ = solvent signal cutoff.

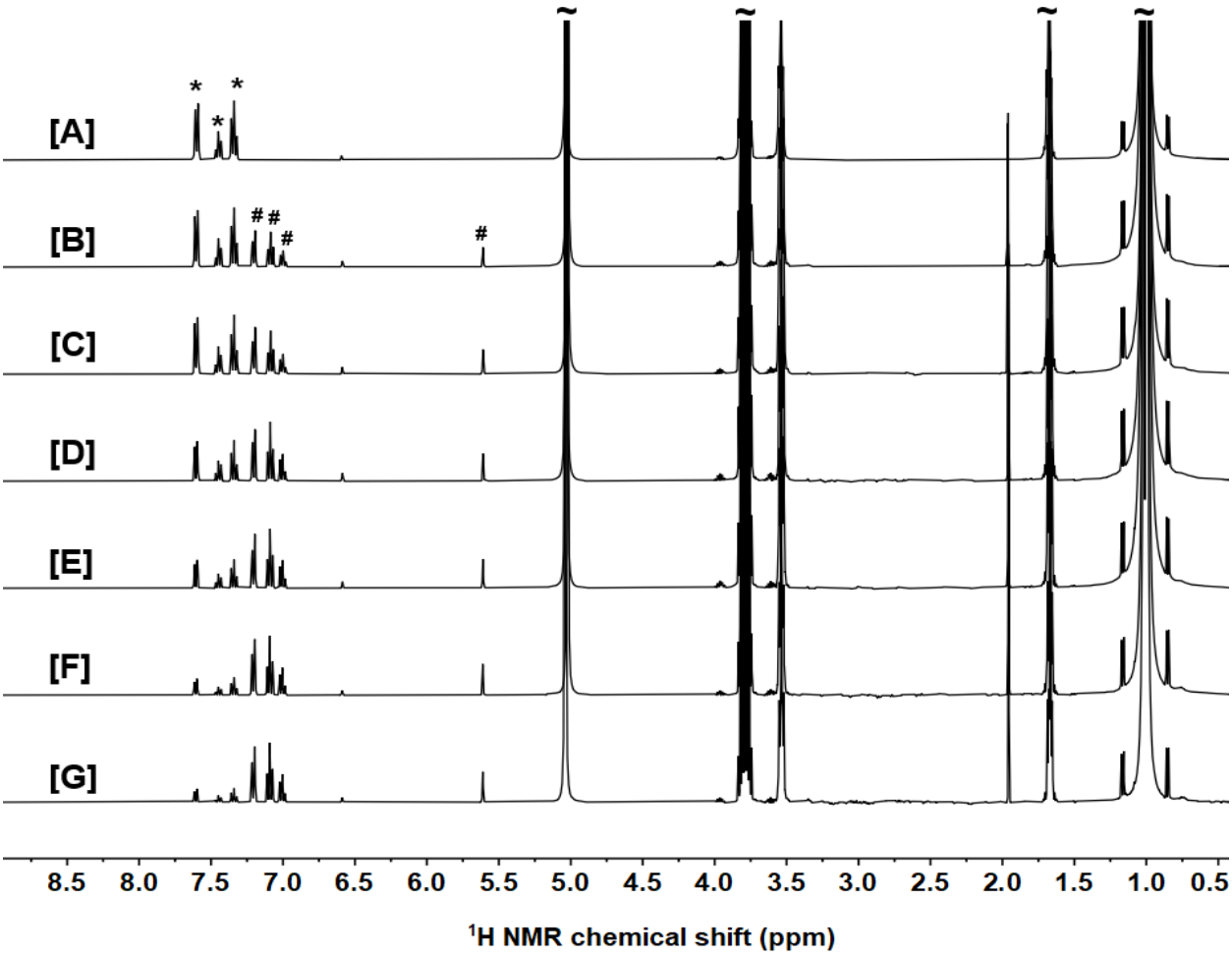

Figure S4. Representative ^{1}H NMR spectra to monitor the progress of the reaction between benzophenone (0.15 mmol) and iPrOH in presence of **2d** (0.1 mol% of Ru), and KOtBu (0.625 mol%). [A] after 0 h; [B] after 4 h; [C] after 8 h; [D] after 12 h; [E] 16 h; [F] after 20 h; [G] after 24 h. * = Benzophenone; # = diphenylmethanol. ~ = solvent signal cutoff.

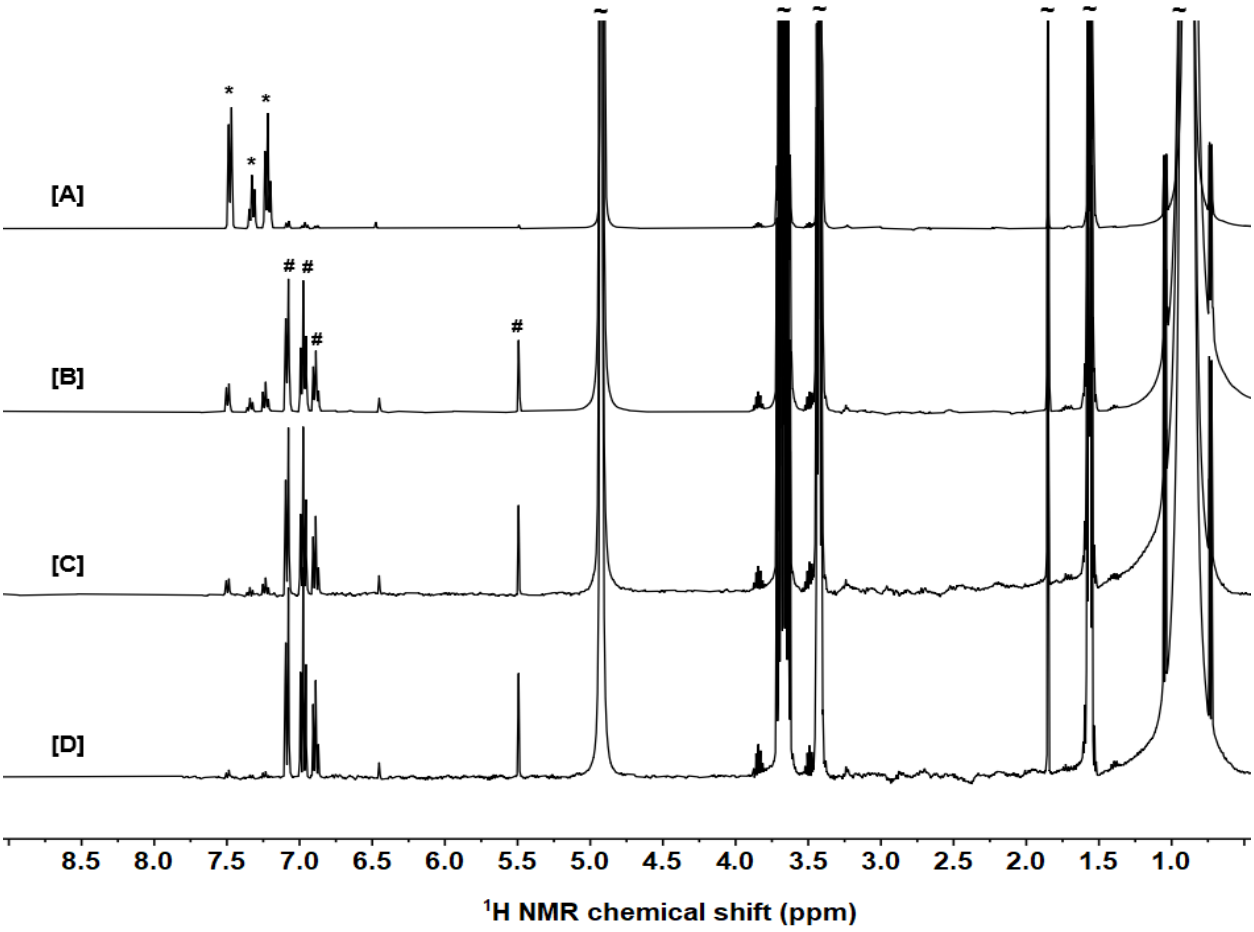

Figure S5. Representative ^{1}H NMR spectra to monitor the progress of the reaction between benzophenone (0.15 mmol) and iPrOH in presence of **3** (0.1 mol% of Ru), and KOtBu (0.625 mol%). [A] after 0 h; [B] after 0.5 h; [C] after 1 h; [D] after 1.5 h. * = Benzophenone; # = diphenylmethanol. ~ = solvent signal cutoff.

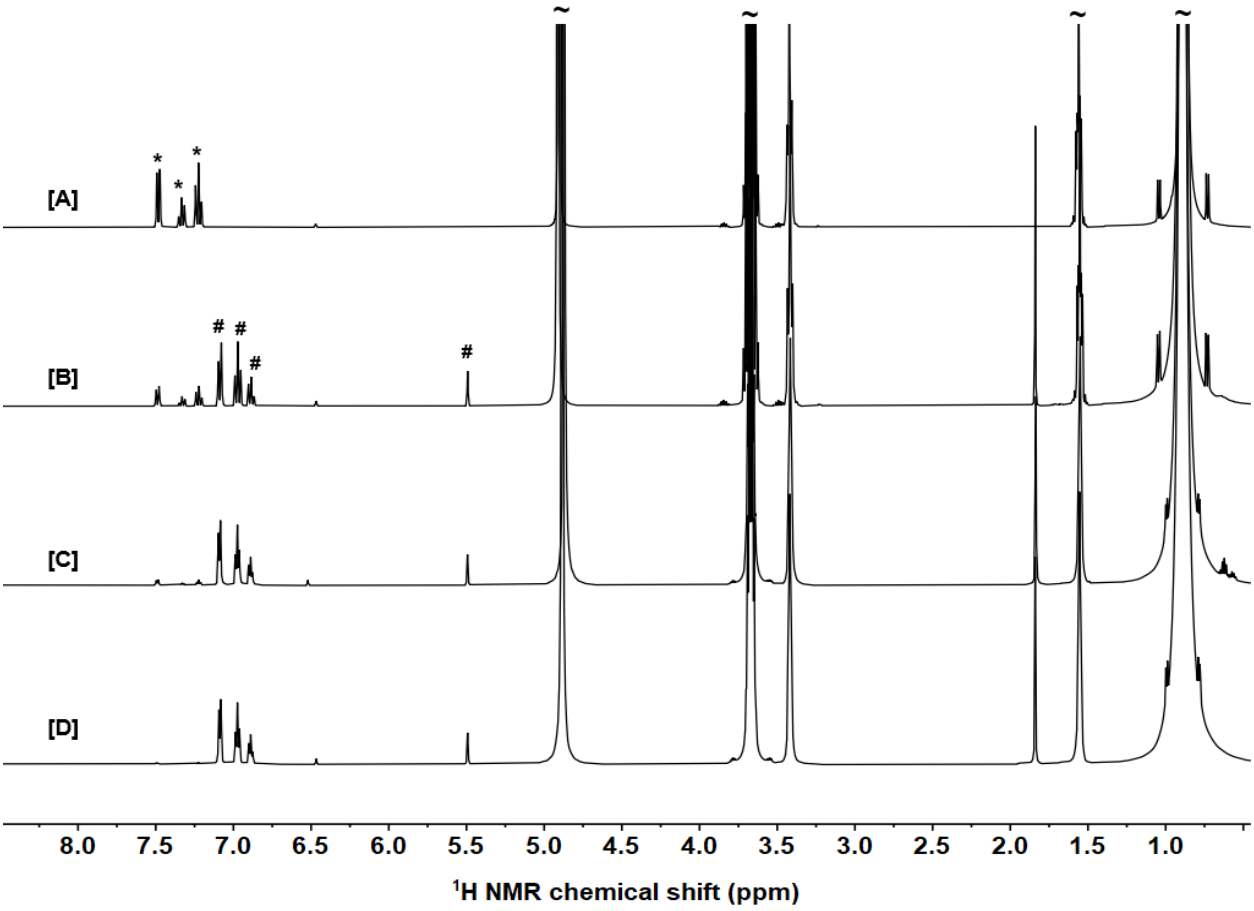

Figure S6. Representative ^{1}H NMR spectra to monitor the progress of the reaction between benzophenone (0.15 mmol) and iPrOH in presence of **4** (0.1 mol% of Ru), and KOtBu (0.625 mol%). [A] after 0 h; [B] after 0.5 h; [C] after 1 h; [D] after 1.5 h. * = Benzophenone; # = diphenylmethanol. ~ = solvent signal cutoff.

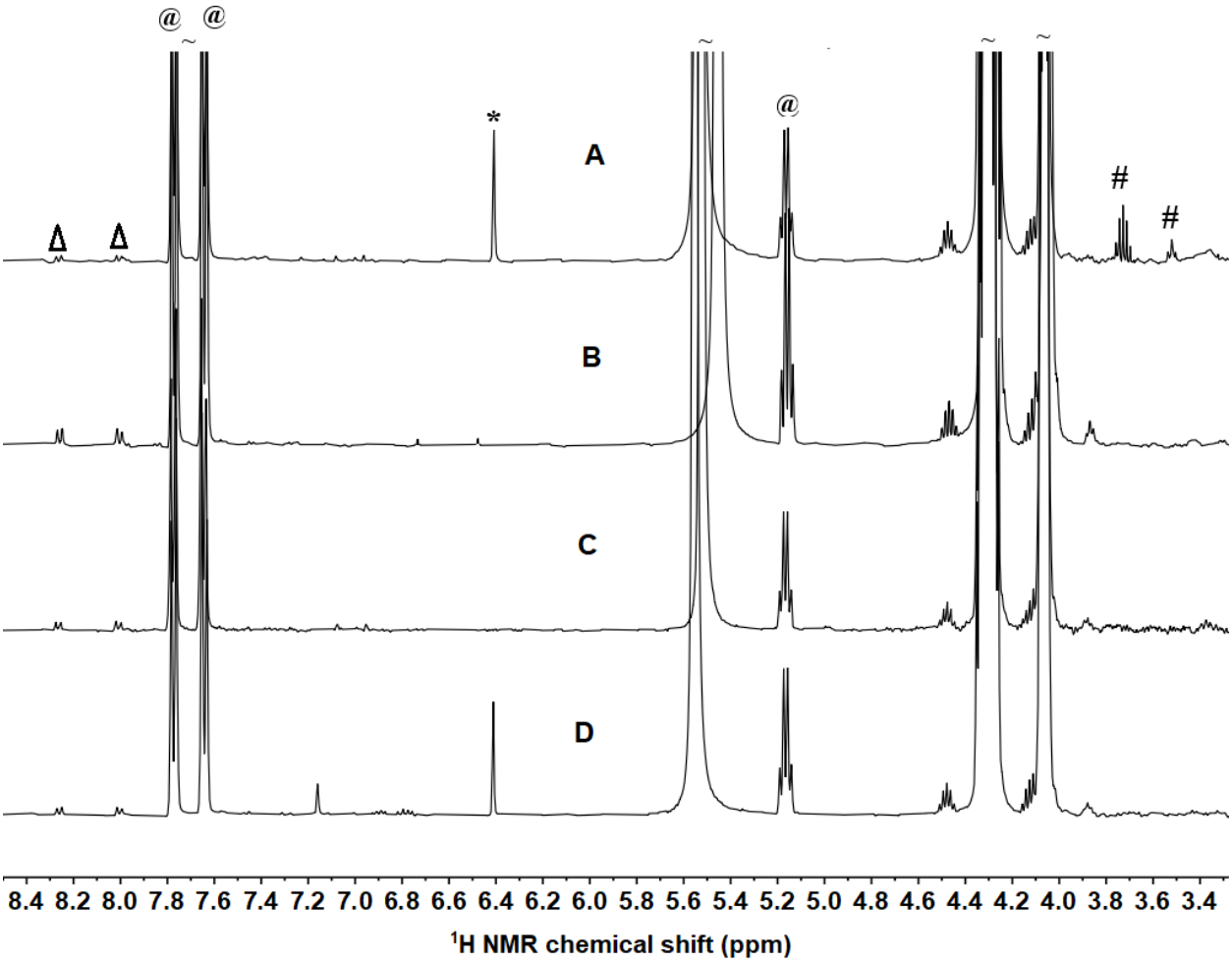

Figure S7. Representative ^{1}H NMR spectra for the transfer hydrogenation of 4-bromoacetophenone (0.15 mmol) with [A] **1** (0.1 mol%) after 2 h heating, [B] Catalyst **2a** (0.1 mol%) after 2 h heating, [C] Catalyst **3** (0.1 mol%) after 1 h heating, and [D] Catalyst **4** (0.1 mol%) after 1h heating at 80 °C in presence of KO^{t}Bu (0.625 mol%) and ^{i}PrOH (0.4 mL). Δ = starting material; @ = product peaks; * = Internal standard; # = unknown byproducts. Conditions B and C are before the addition of internal standard. ~ = solvent signal cutoff.

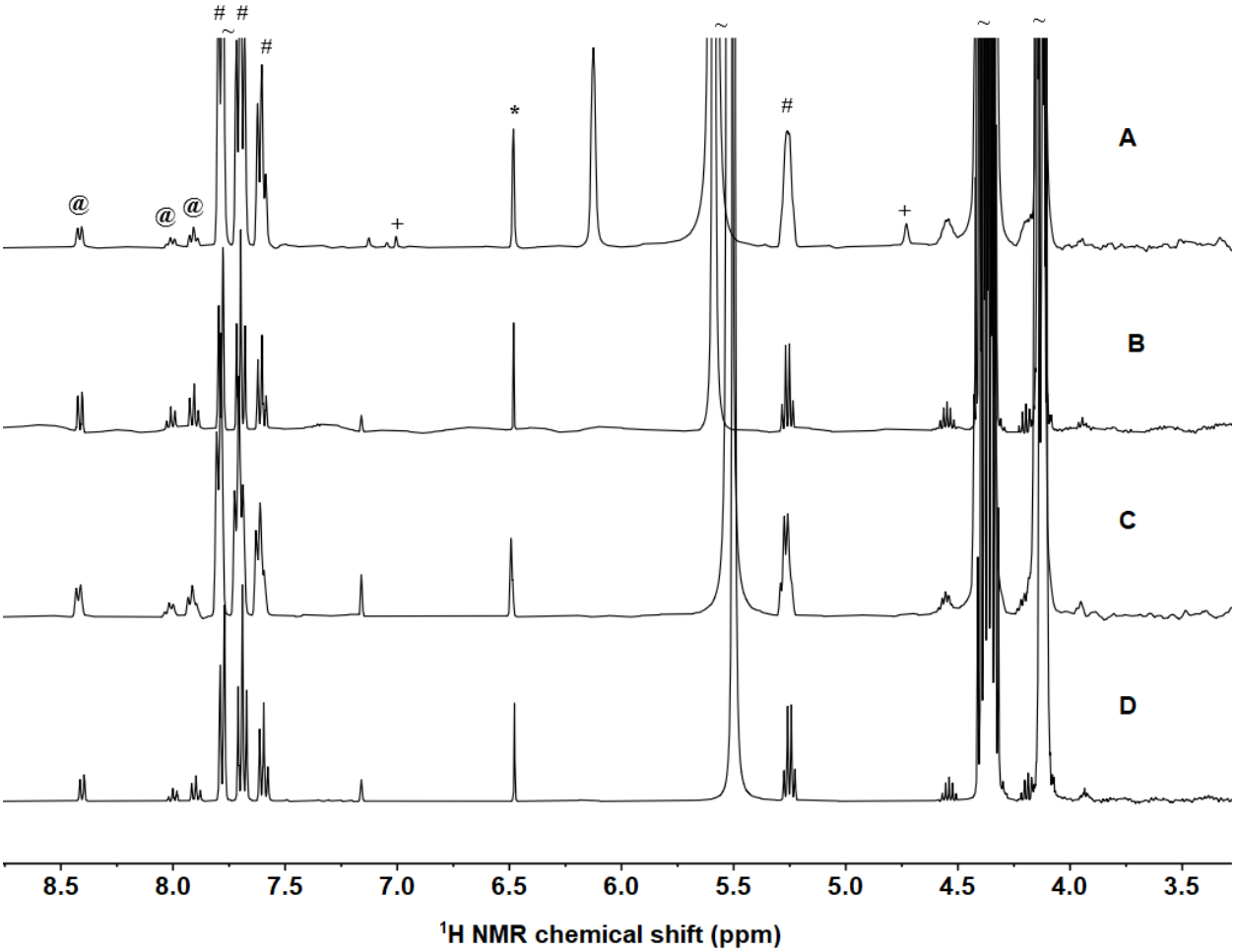

Figure S8. Representative ^{1}H NMR spectra for the transfer hydrogenation of acetophenone (0.15 mmol) with [A] **1** (0.1 mol%) after 2 h heating, [B] Catalyst **2a** (0.1 mol%) after 2 h heating, [C] Catalyst **3** (0.1 mol%) after 1 h heating, and [D] Catalyst **4** (0.1 mol%) after 1 h heating at 80 °C in presence of KO^{t}Bu (0.625 mol%) and ^{i}PrOH (0.4 mL). @ = starting material; # = product peaks; * = Internal standard; + = unknown byproducts. ~ = solvent signal cutoff.

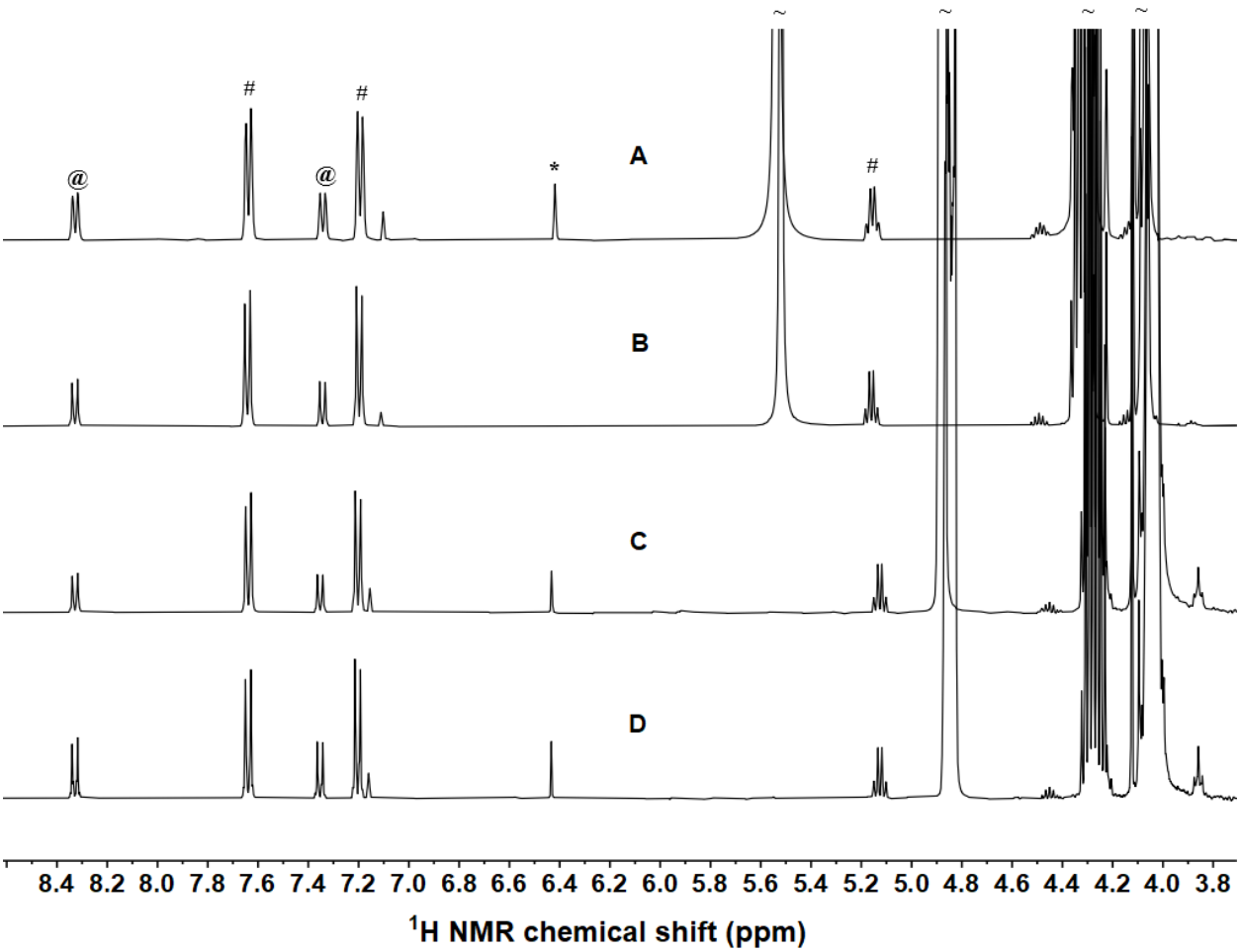

Figure S9. Representative ^{1}H NMR spectra for transfer hydrogenation of 4-methoxyacetophenone (0.15 mmol) with [A] **1** (0.1 mol%) after 2 h heating, [B] Catalyst **2a** (0.1 mol%) after 2 h heating, [C] Catalyst **3** (0.1 mol%) after 3 h heating, and [D] Catalyst **4** (0.1 mol%) after 3 h heating at 80 °C in presence of KO^{t}Bu (0.625 mol%) and ^{i}PrOH (0.4 mL). @ = starting material; # = product peaks; * = Internal standard; Conditions B is before the addition of internal standard. ~ = solvent signal cutoff.

Catalysis in the presence of excess ligand

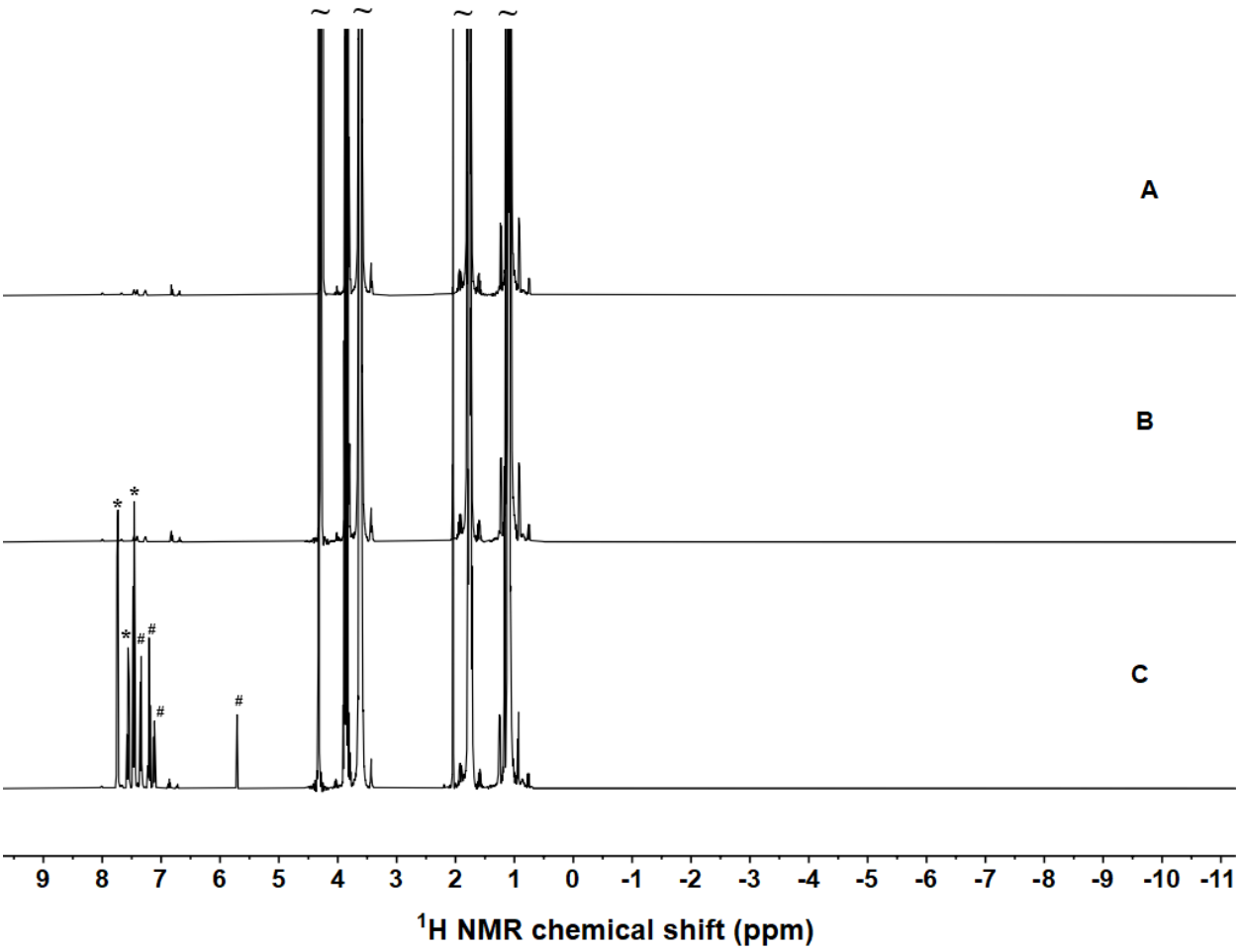

Figure S10. ^{1}H NMR spectra of **3** (3 μmol, 2 mol%), KO^{t}Bu (7.5 μmol, 5 mol%), ^{i}PrOH (0.4 mL), PMe_3 (3 μmol) and THF-d_8 (0.15 mL) [A] after 5 minutes sonication; [B] after 10 minutes heating at 80 °C; [C] after addition of benzophenone (0.15 mmol) followed by 0.5 h of heating at 80 °C. * = benzophenone; # = diphenylmethanol, ~ = solvent signal cutoff.

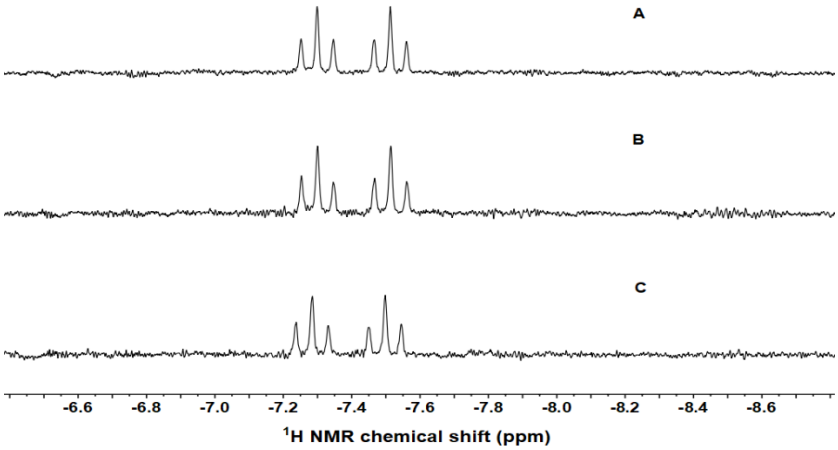

Figure S11. Expansion of the hydride region of the ^{1}H NMR spectra of **3** (3 µmol, 2 mol%), KO^{t}Bu (7.5 µmol, 5 mol%), ^{i}PrOH (0.4 mL), PMe_3 (3 µmol) and THF-d_8 (0.15 mL) [A] after 5 minutes sonication; [B] after 10 minutes heating at 80 °C; [C] after addition of benzophenone (0.15 mmol) followed by 0.5 h of heating at 80 °C.

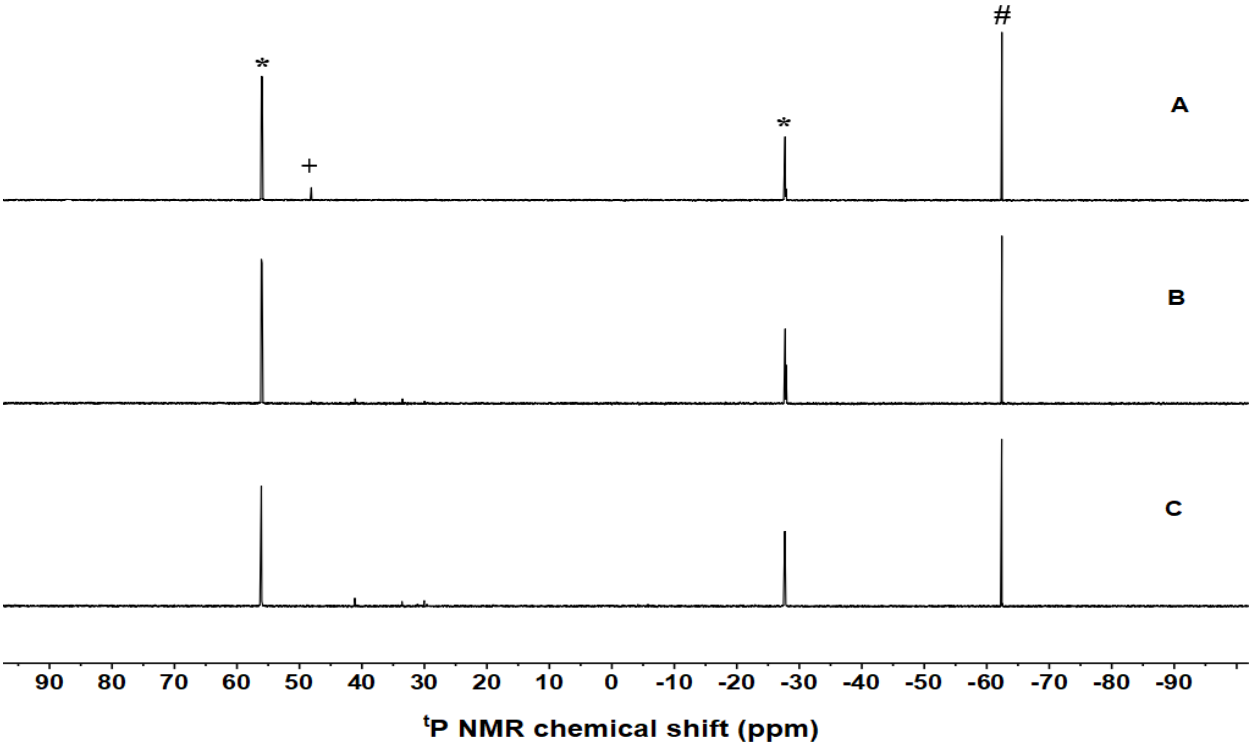

Figure S12. ^{31}P{^{1}H} NMR spectra of **3** (3 µmol, 2 mol%), KO^{t}Bu (7.5 µmol, 5 mol%), ^{i}PrOH (0.4 mL), PMe_3 (3 µmol) and THF-d_8 (0.15 mL) [A] after 5 minutes sonication; [B] after 10 minutes heating at 80 °C; [C] after addition of benzophenone (0.15 mmol) followed by 0.5 h of heating at 80 °C. * = Complex **3'**; # = PMe_3 ligand; + = unknown.

Complex speciation under catalysis conditions

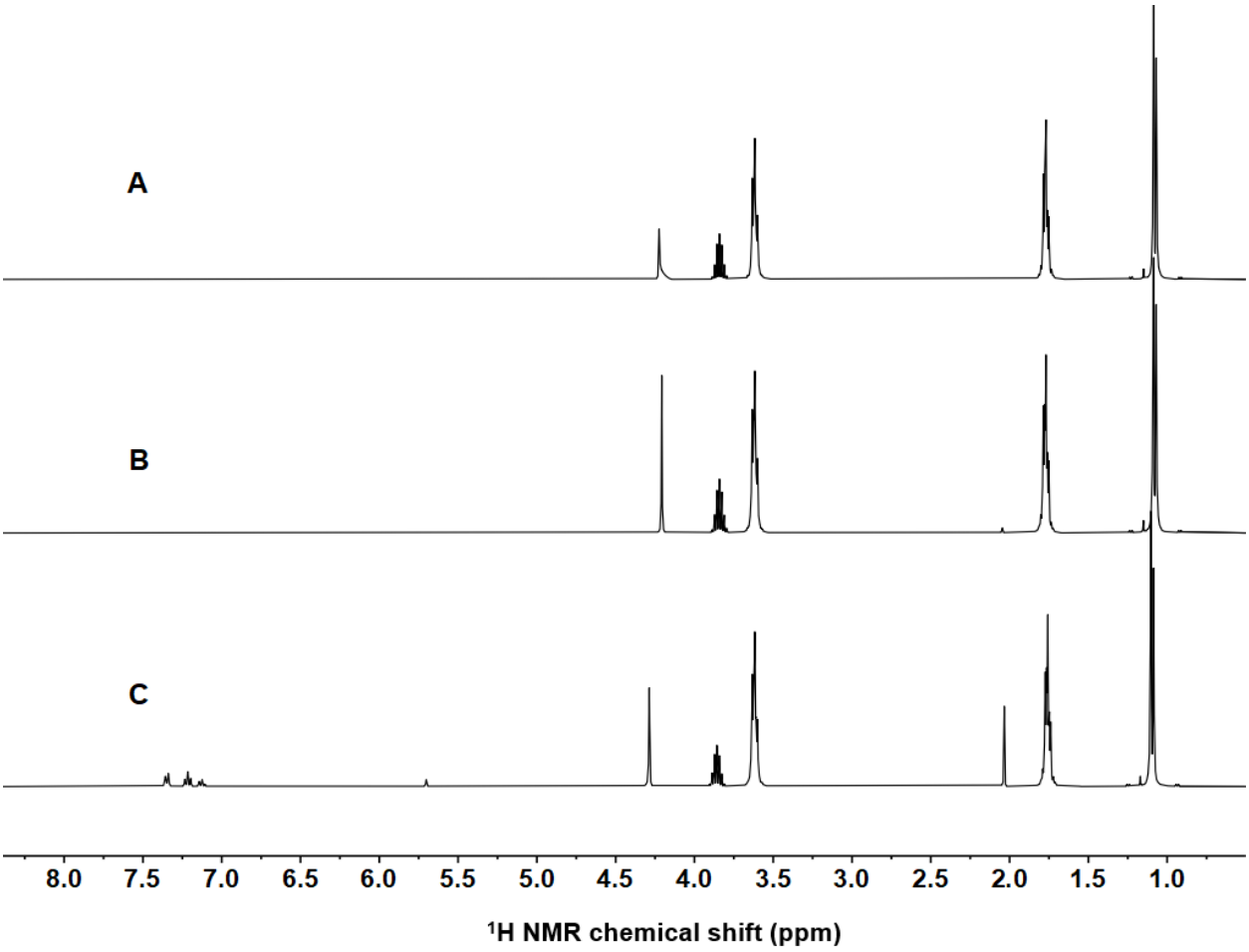

Figure S13. ^{1}H NMR spectra of **1** (3 μmol, 2 mol%), KO^{t}Bu (7.5 μmol, 5 mol%), ^{i}PrOH (0.4 mL) and THF-d_8 (0.15 m L) before (A) and after heating at 80 °C for 30 minutes (B); and after addition of benzophenone (0.15 mmol) followed by 30 minutes of heating at 80 °C (C).

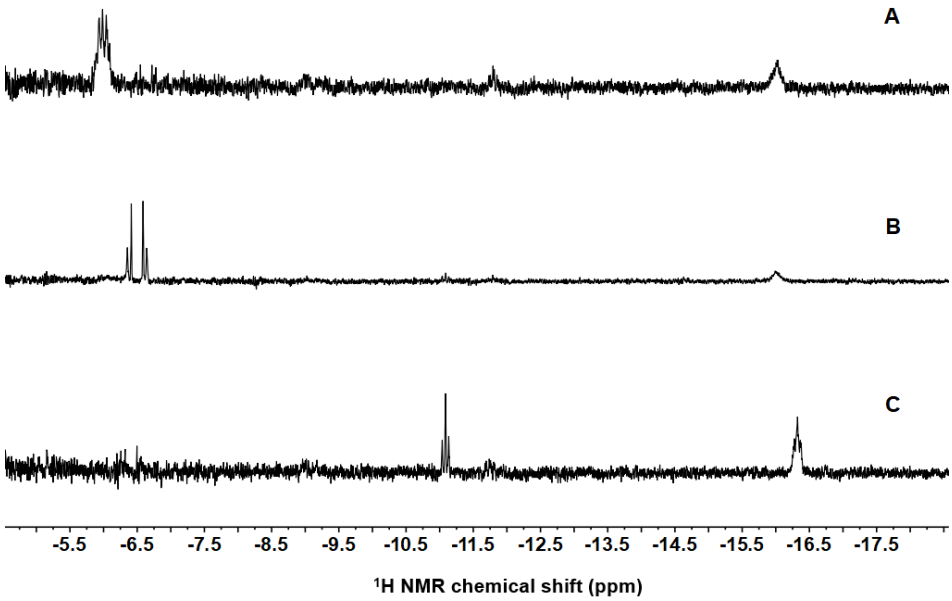

Figure S14. Expansion of the hydride region of the ^{1}H NMR spectra of **1** (3 μmol, 2 mol%), KO^{t}Bu (7.5 μmol, 5 mol%), ^{i}PrOH (0.4 mL) and THF-d_8 (0.15 mL) before (A) and after heating at 80 °C for 30 minutes (B); and after addition of benzophenone (0.15 mmol) followed by 30 minutes of heating at 80 °C (C).

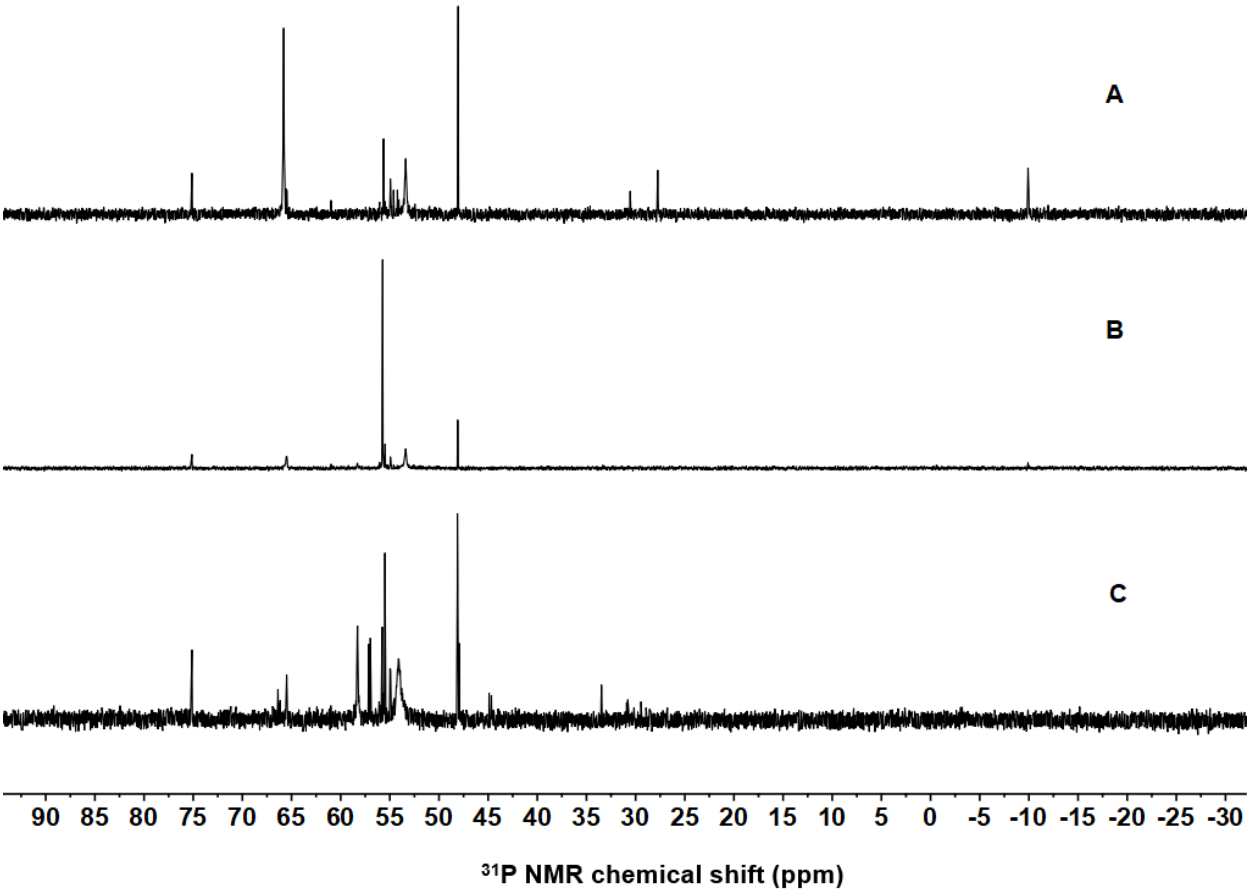

Figure S15. $^{31}P\{^{1}H\}$ NMR spectra of **1** (3 µmol, 2 mol%), KO^{t}Bu (7.5 µmol, 5 mol%), ^{i}PrOH (0.4 mL) and THF-d_8 (0.15 mL) before (A) and after heating at 80 °C for 30 minutes (B); and after addition of benzophenone (0.15 mmol) followed by 30 minutes of heating at 80 °C (C).

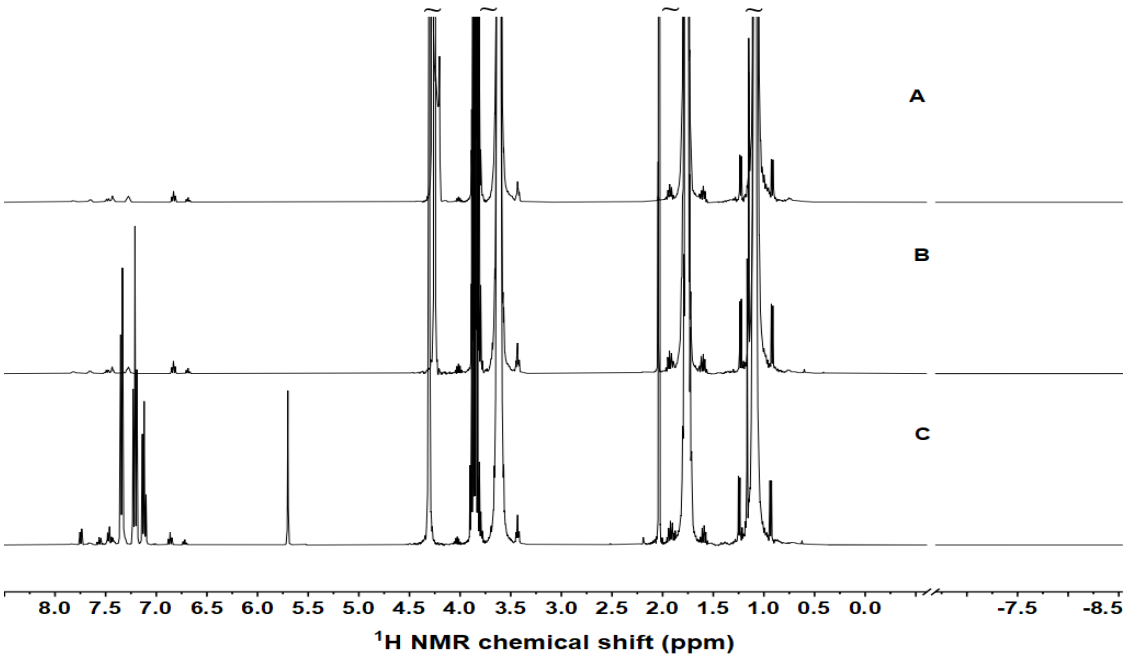

Figure S16. ^{1}H NMR spectra of **2b** (3 μmol, 2 mol%), KO^{t}Bu (7.5 μmol, 5 mol%), ^{i}PrOH (0.4 mL) and THF-d_8 (0.15 mL) before (A) and after heating at 80 °C for 30 minutes (B); and after addition of benzophenone (0.15 mmol) followed by 30 minutes of heating at 80 °C (C). ~ = signal cutoffs for isopropanol and THF-d_8.

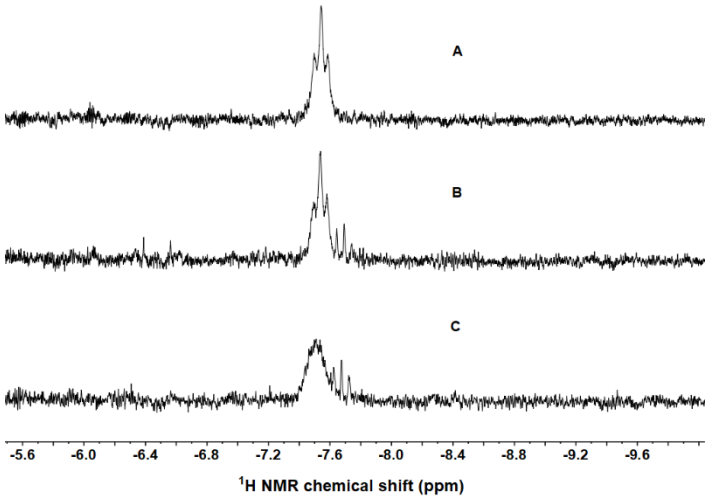

Figure S17. Expansion of the hydride region of the ^{1}H NMR spectra of **2b** (3 μmol, 2 mol%), KO^{t}Bu (7.5 μmol, 5 mol%), ^{i}PrOH (0.4 mL) and THF-d_8 (0.15 mL) before (A) and after heating at 80 °C for 30 minutes (B); and after addition of benzophenone (0.15 mmol) followed by 30 minutes of heating at 80 °C (C).

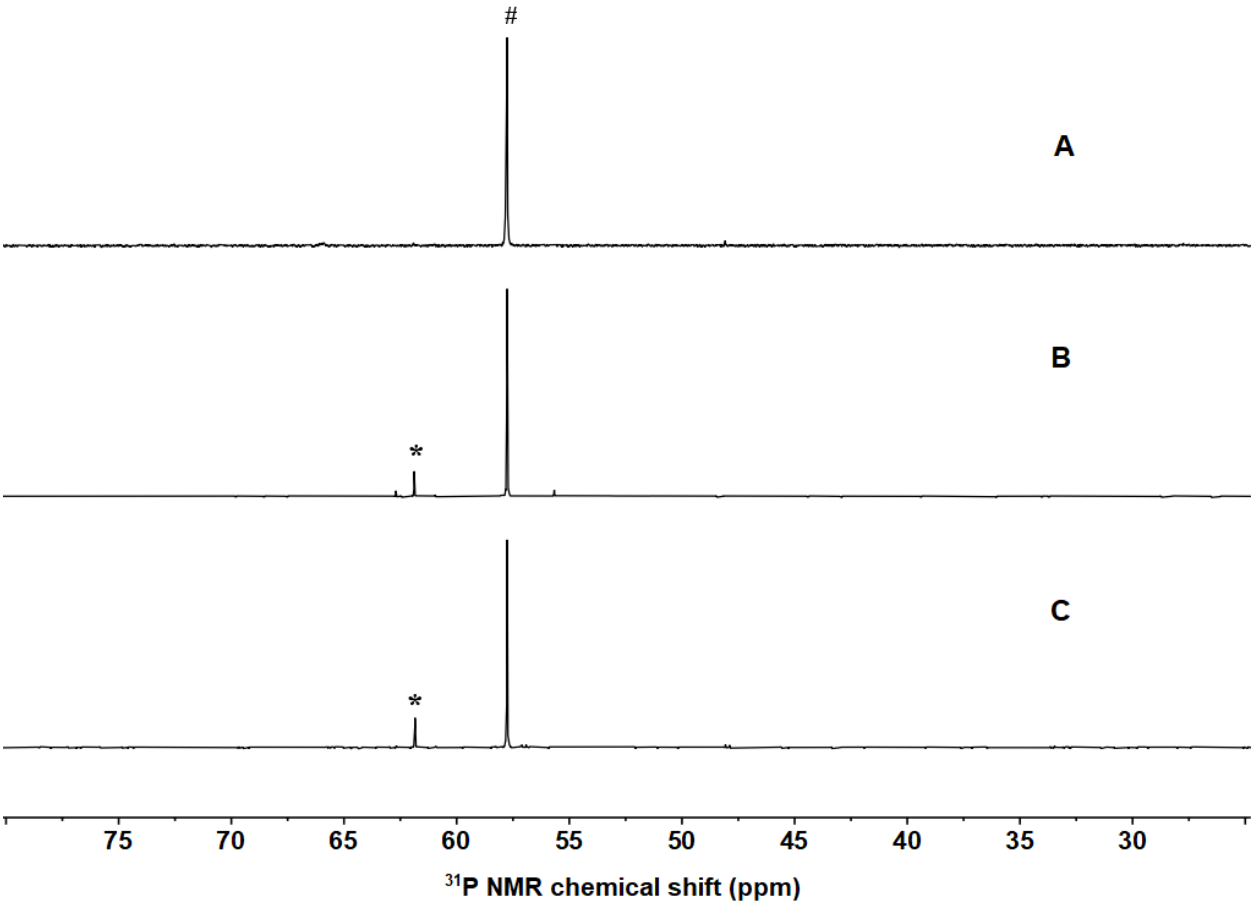

Figure S18. $^{31}P\{^{1}H\}$ NMR spectra of **2b** (3 µmol, 2 mol%), KO^{t}Bu (7.5 µmol, 5 mol%), ^{i}PrOH (0.4 mL) and THF-d_8 (0.15 mL) before (A) and after heating at 80 °C for 30 minutes (B); and after addition of benzophenone (0.15 mmol) followed by 30 minutes of heating at 80 °C (C). # denotes **2b'** and * is an unknown species.

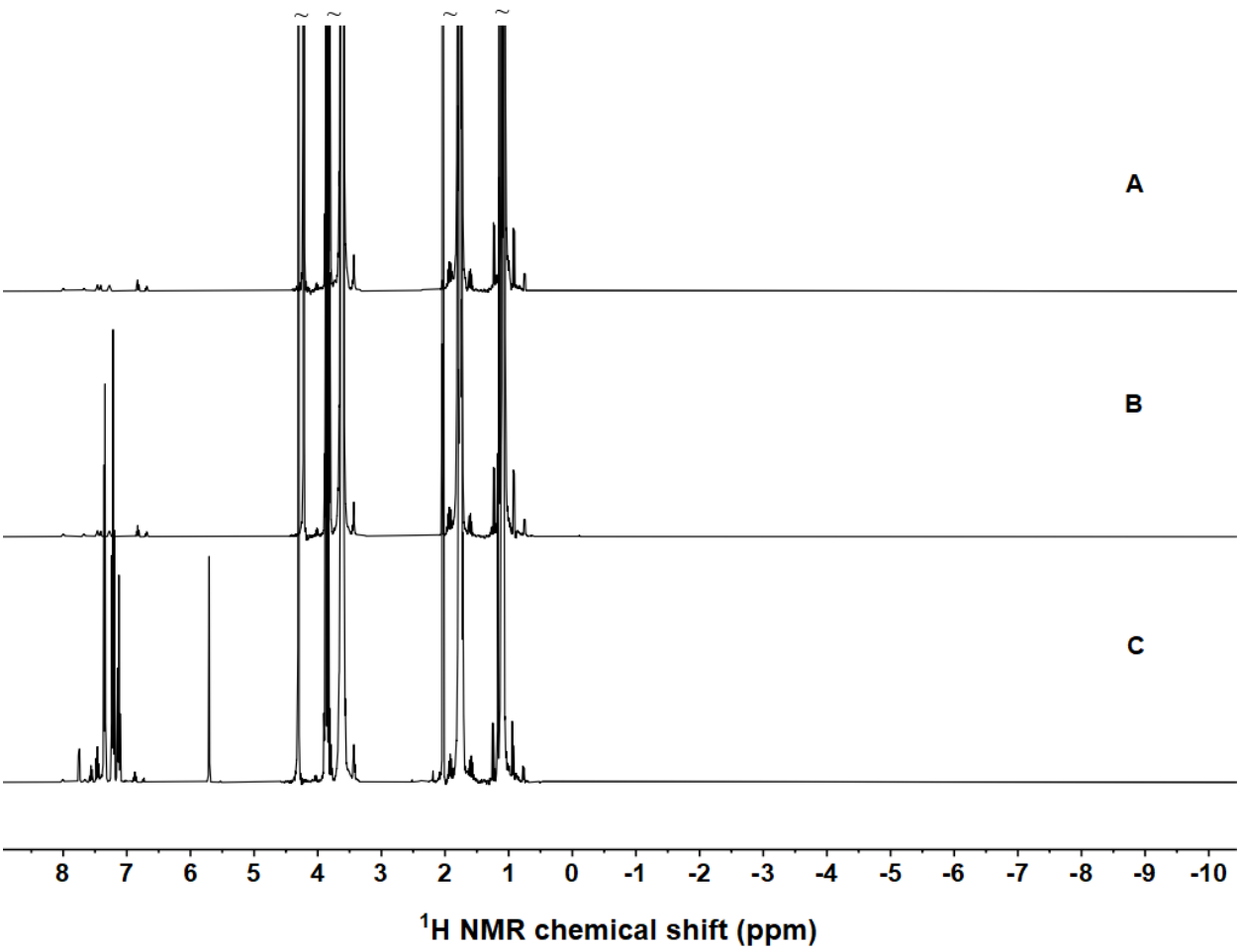

Figure S19. ^{1}H NMR spectra of **3** (3 μmol, 2 mol%), KO^{t}Bu (7.5 μmol, 5 mol%), ^{i}PrOH (0.4 mL) and THF-d_8 (0.15 mL) before (A) and after heating at 80 °C for 30 minutes (B); and after addition of benzophenone (0.15 mmol) followed by 30 minutes of heating at 80 °C (C). ~ = signal cutoffs for isopropanol and THF-d_8.

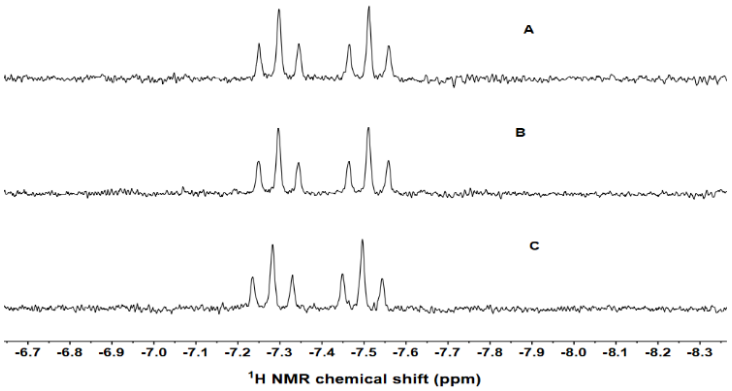

Figure S20. Expansion of hydride region in the ^{1}H NMR spectra of **3** (3 μmol, 2 mol%), KO^{t}Bu (7.5 μmol, 5 mol%), ^{i}PrOH (0.4 mL) and THF-d_8 (0.15 mL) before (A) and after heating at 80 °C for 30 minutes (B); and after addition of benzophenone (0.15 mmol) followed by 30 minutes of heating at 80 °C (C).

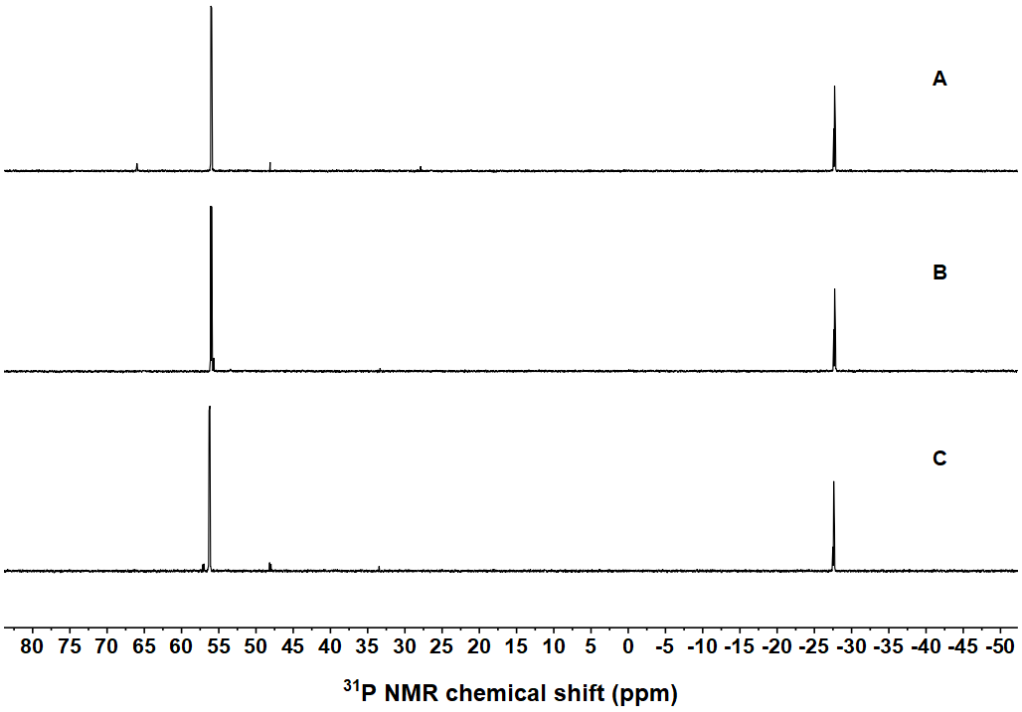

Figure S21. ^{31}P {^{1}H} NMR spectra of **3** (3 μmol, 2 mol%), KO^{t}Bu (7.5 μmol, 5 mol%), ^{i}PrOH (0.4 mL) and THF-d_8 (0.15 mL) before (A) and after heating at 80 °C for 30 minutes (B); and after addition of benzophenone (0.15 mmol) followed by 30 minutes of heating at 80 °C (C).

SCXRD structures and data

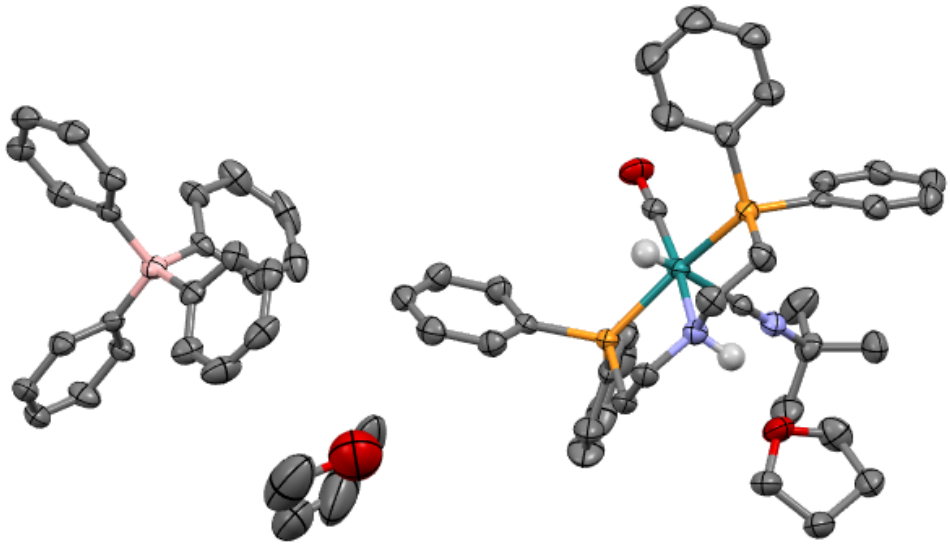

Figure S22. SCXRD for **2b,** thermal ellipsoids are drawn at 50% probability, and most hydrogens are omitted for clarity.

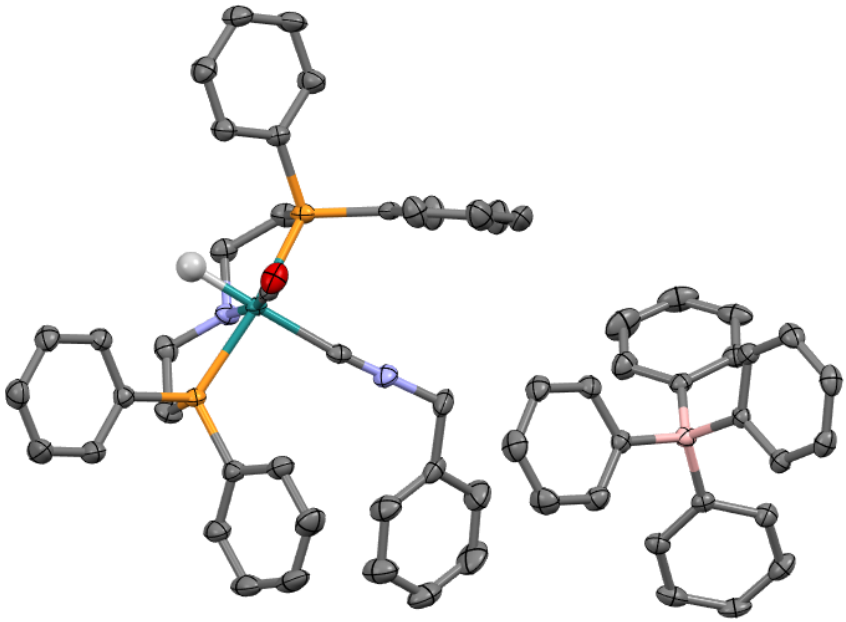

Figure S23. SCXRD for **2d**, thermal ellipsoids are drawn at 50% probability, and most hydrogens are omitted for clarity.

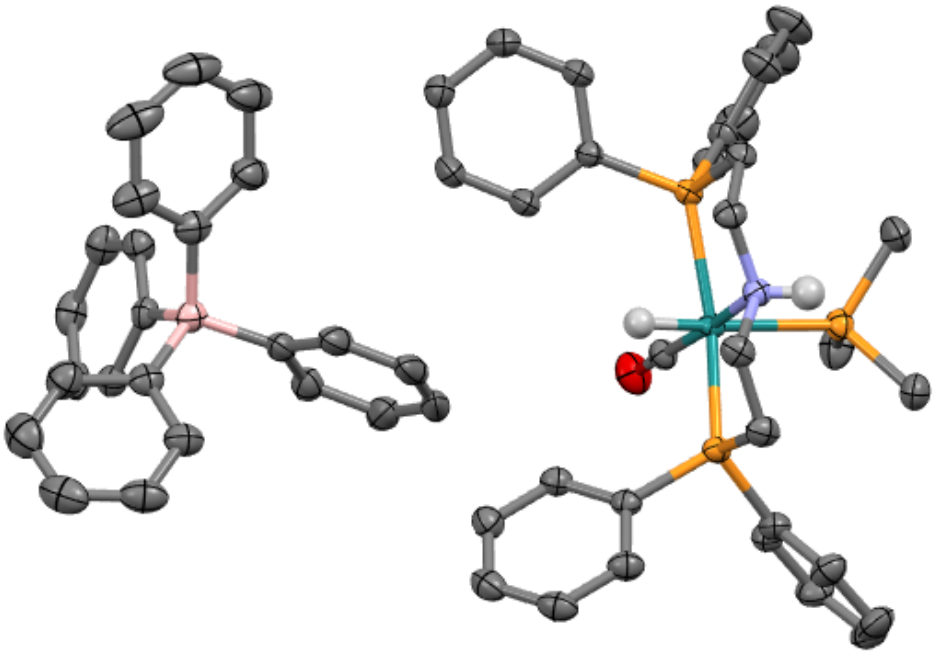

Figure S24. SCXRD for **3**, thermal ellipsoids are drawn at 50 % probability, and most hydrogens are omitted for clarity.

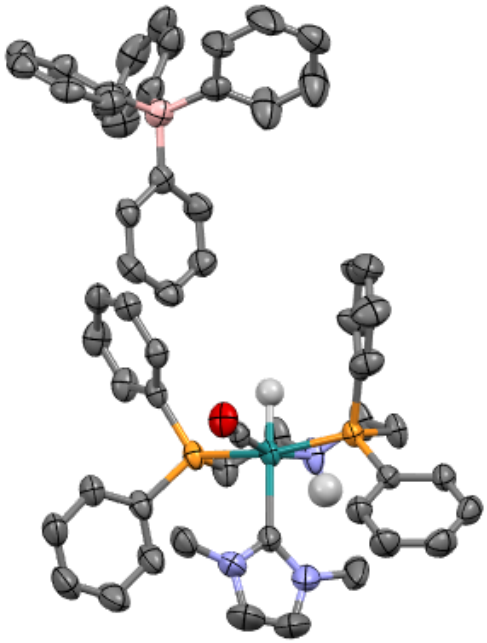

Figure S25. SCXRD for **4**, thermal ellipsoids are drawn at 50 % probability, and most hydrogens are omitted for clarity.

Table S2. Summary of relevant bond lengths and angles for the SCXRD structures of **2b**, **2d**, **3** and **4**.[a]

Complex	Bond length (Å)				Bond angles			
	Ru-C/P (ligand *trans* to hydride)	Ru-C (CO)	Ru-P (Ph**P**N^{H}**P**)	Ru-N (PhP**N**^{H}P)	P-Ru-P	X-Ru-H	N-Ru-CO	Ru-C-N (isonitrile)
2b	2.048(6)	1.841(6)	2.3258(14)/ 2.3199(14)	2.180(4)	164.11	175.09	169.93	173.60
2d	2.043(3)	1.856(3)	2.3145(7)/ 2.3237(7)	2.189(2)	165.7	173.5	170.45	172.23
3	2.4358(6)	1.847(2)	2.3160(5)/ 2.3248(5)	2.2027(17)	159.61	176.94	174.01	NA
4	2.168(4)	1.819(4)	2.2885(9)/ 2.3450(9)	2.224(3)	161.74	179.68	166.26	NA

a. Errors are indicated in the parantheses. NA = not applicable.

Table S3. Crystallographic data and refinement parameters for **2b** and **2d**.

Parameter	**2b**	**2d**
Empirical formula	$C_{58}H_{59}BN_2OP_2Ru$	$C_{61}H_{57}BN_2OP_2Ru$
Formula weight	973.95	1006.89
Temperature/K	173(2) K	173(2) K
Crystal system	triclinic	monoclinic
Space group	P-1	P 1 21/c 1
a/Å	12.7846(8)	13.1411(5)
b/Å	13.8907(11)	12.9946(5)
c/Å	17.4106(13)	29.4189(11)
α/°	101.625(3)	90
β/°	105.684(2)	90.2580(10)
γ/°	94.257(3)	90
Volume/Å^3	2888.4(4)	5023.6(3)
Z	2	4
ρ_{calc} g/cm^3	1.286	1.331
μ/mm^{-1}	0.375	0.420
F(000)	1176.0	2092.0
Crystal size/mm^3	0.25 × 0.24 × 0.1	0.42 × 0.38 × 0.12
Radiation	MoKα (λ = 0.71073)	MoKα (λ = 0.71073)
2Θ range for data collection/°	2.29 to 23.17	2.09 to 27.50
Index ranges	-14 ≤ h ≤ 14, -15 ≤ k ≤ 15, -19 ≤ l ≤ 19	-16 ≤ h ≤ 16, -15 ≤ k ≤ 15, -36 ≤ l ≤ 36

Reflections collected	93094	226272
Independent reflections	8193 (Rint = 0.1290, Rsig = 0.0566)	11499
Data/restraints/parameters	8193 / 0 / 679	11499 / 0 / 617
Goodness-of-fit on F^2	1.023	1.038
Final R indexes [I>=2σ (I)]	R1 = 0.0562, wR2 = 0.1387	R1 = 0.0395, wR2 = 0.0896
Final R indexes [all data]	R1 = 0.0768, wR2 = 0.1531	R1 = 0.0515, wR2 = 0.0979
Largest diff. peak/hole /e $Å^{-3}$	2.404/-0.771	0.753/ -0.585

Table S4. Crystallographic data and refinement parameters for **3** and **4**.

Parameter	**3**	**4**
Empirical formula	$C_{56}H_{59}BNOP_3Ru$	$C_{58}H_{58}BN_3OP_2Ru$
Formula weight	966.90	986.95
Temperature/K	273 K	173 K
Crystal system	monoclinic	monoclinic
Space group	P 1 21/n 1	P 1 21/n 1
a/Å	9.9730(3)	11.4158(5)
b/Å	22.1902(7)	34.6443(15)
c/Å	22.4709(7)	12.7068(5)
α/°	90	90
β/°	97.363(10)	99.007(10)
γ/°	90	90

Volume/Å^3	4931.9(3)	4963.5(4)
Z	4	4
ρ_{calc}g/cm^3	1.302	1.321
μ/mm^{-1}	0.455	0.424
F(000)	2016	2056.0
Crystal size/mm^3	0.29 × 0.14 × 0.11	0.34 × 0.30 × 0.08
Radiation	MoKα (λ = 0.71073)	MoKα (λ = 0.71073)
2Θ range for data collection/°	2.33 to 28.71	2.15 to 25.68
Index ranges	-12 ≤ h ≤ 13, -29 ≤ k ≤ 29, -30 ≤ l ≤ 30	-13 ≤ h ≤ 13, -42 ≤ k ≤ 42, -15 ≤ l ≤ 15
Reflections collected	126831	167482
Independent reflections	12745 (Rint = 0.0532, Rsig = 0.0263)	9416 (R_{int} = 0.1034, R_{sig} = 0.0380)
Data/restraints/parameters	12745 / 0 / 578	9416 / 0 / 604
Goodness-of-fit on F^2	1.040	1.044
Final R indexes [I>=2σ (I)]	R1 = 0.0367, wR2 = 0.0946	R1 = 0.0450, wR2 = 0.0951
Final R indexes [all data]	R1 = 0.0459, wR2 = 0.1023	R1 = 0.0698, wR2 = 0.1082
Largest diff. peak/hole /e Å^{-3}	1.002/ -0.717	0.569/ -0.449

NMR and FTIR spectra of **2a-d**, **3** and **4**

2a

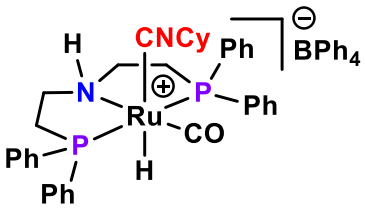

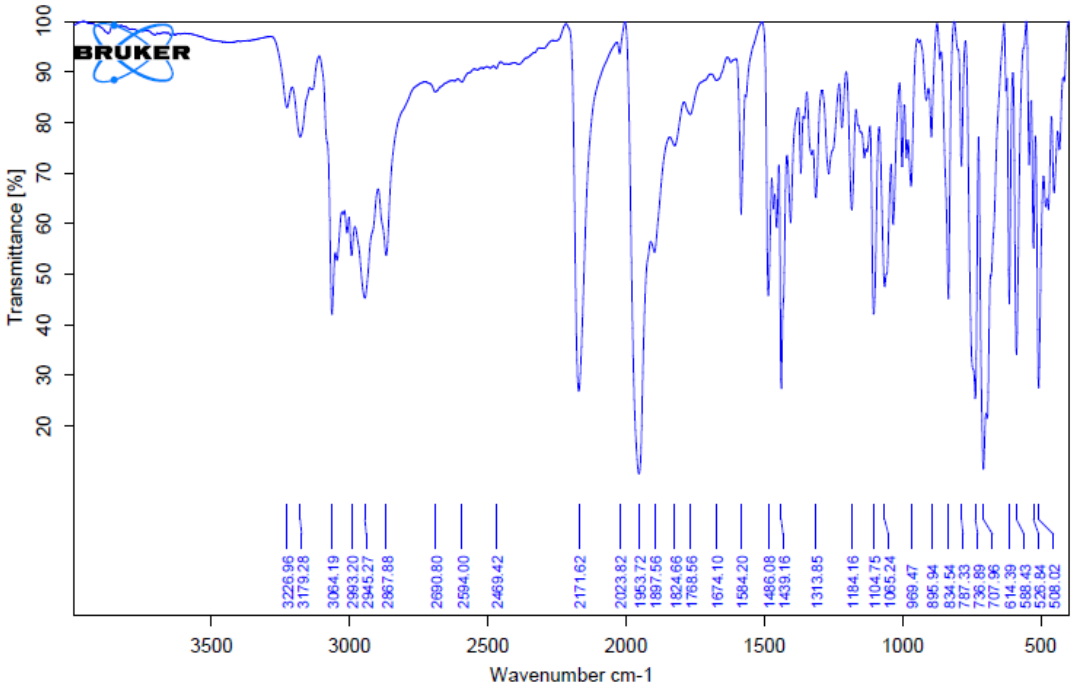

Figure S26. FTIR spectrum of **2a**.

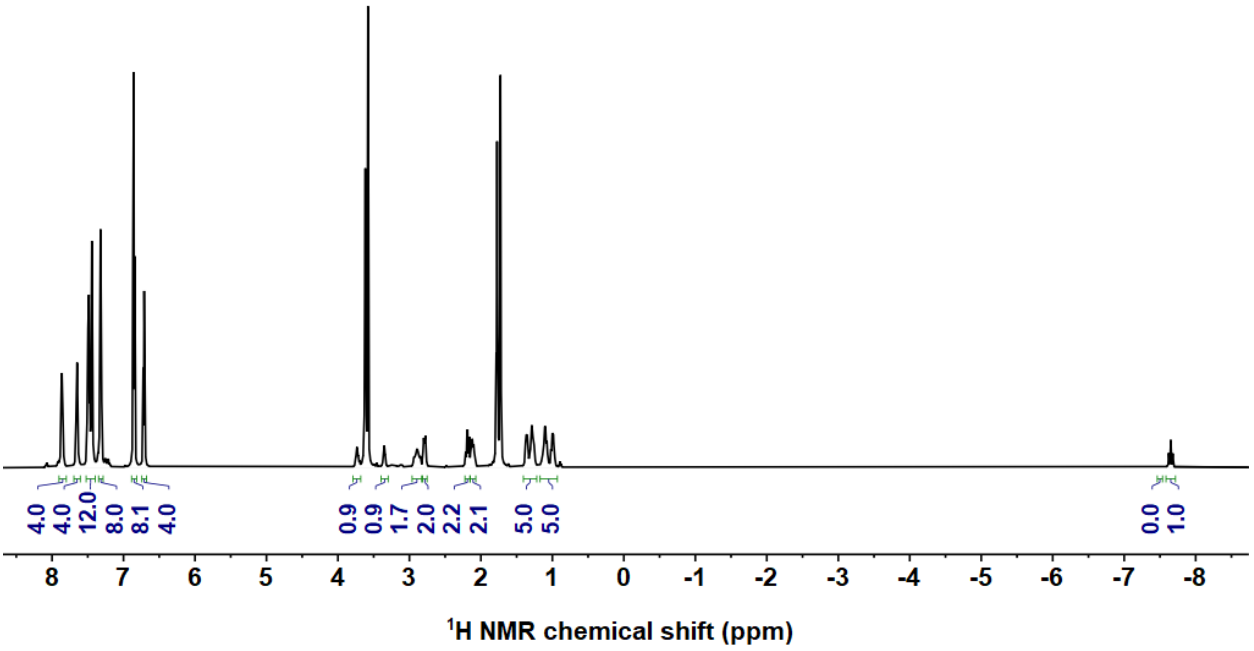

Figure S27. ^{1}H NMR spectrum of **2a** in THF-d_8.

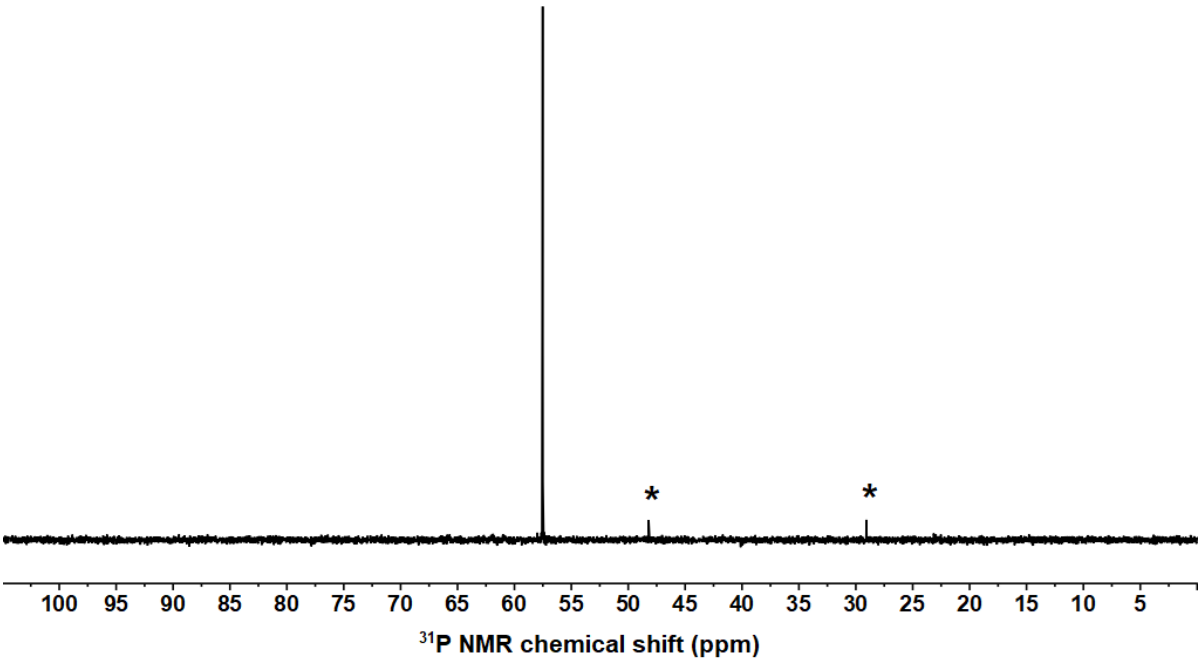

Figure S28. ^{31}P{^{1}H} NMR spectrum of **2a** in THF-d_8; [*]: residual impurities.

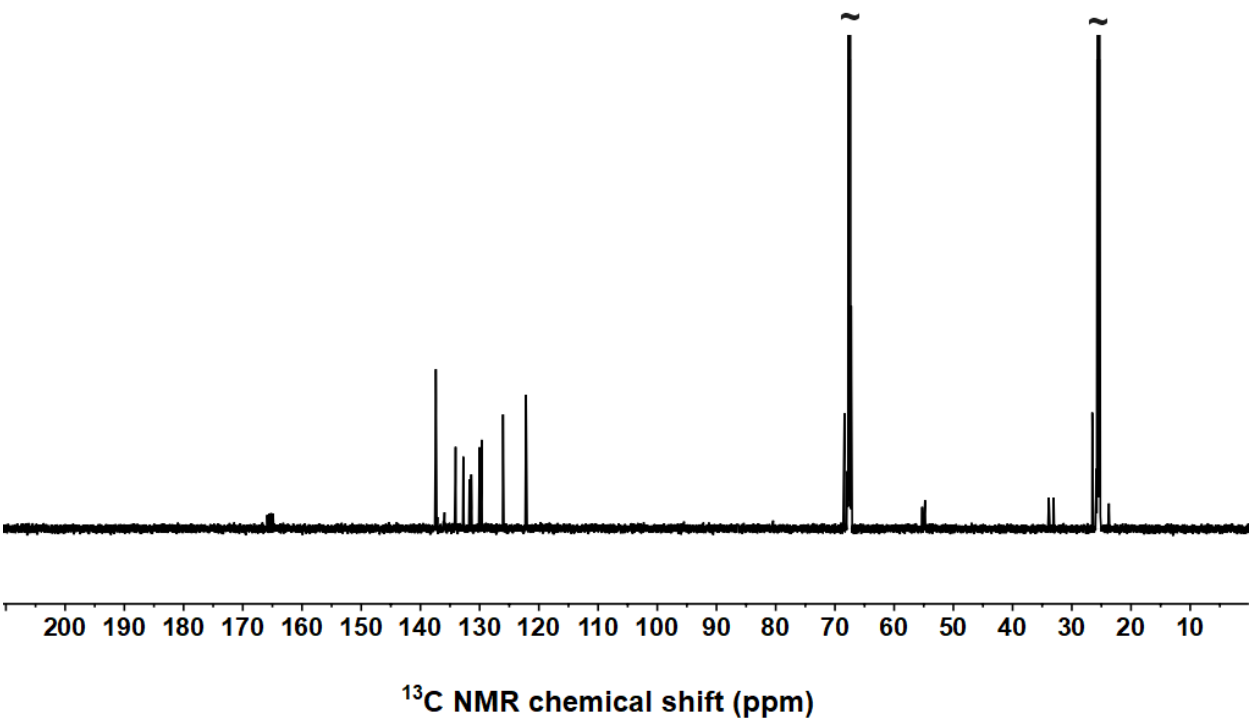

Figure S29. $^{13}C\{^{1}H\}$ NMR spectrum of **2a** in THF-d_8. ~ = solvent signal cutoff.

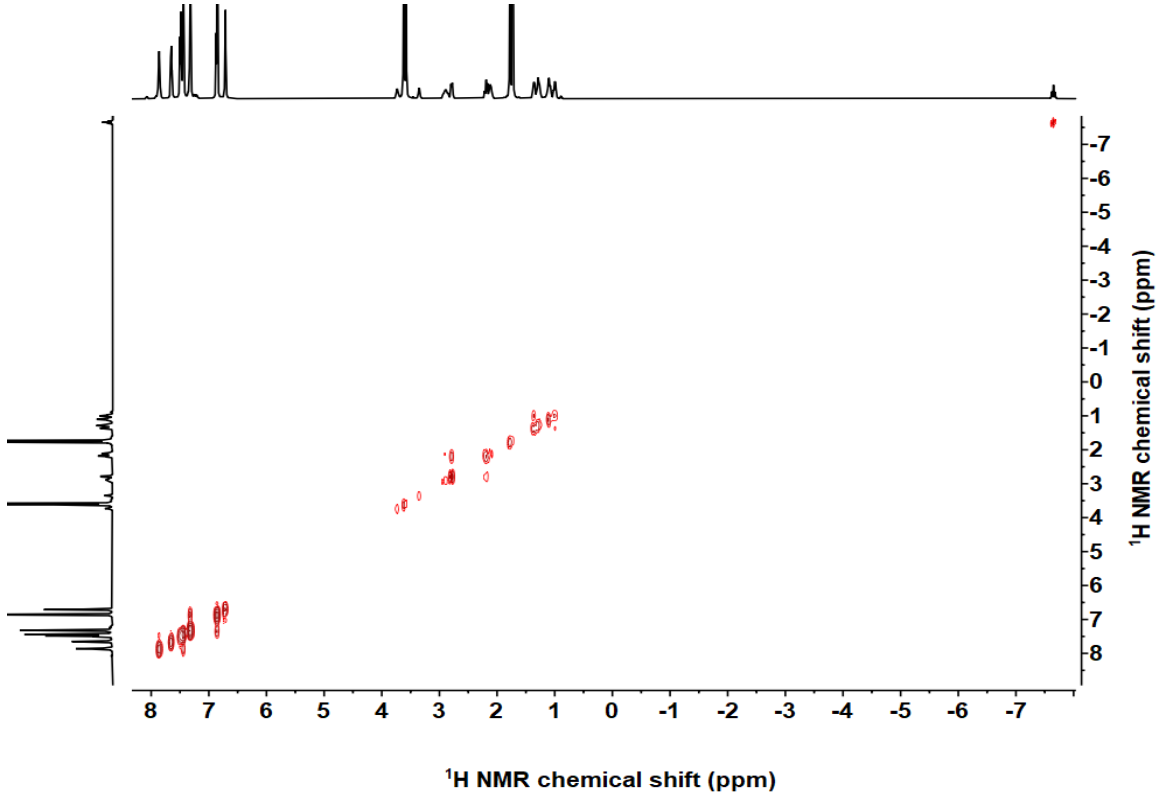

Figure S30. ^{1}H-^{1}H COSY NMR spectrum of **2a** in THF-d_8.

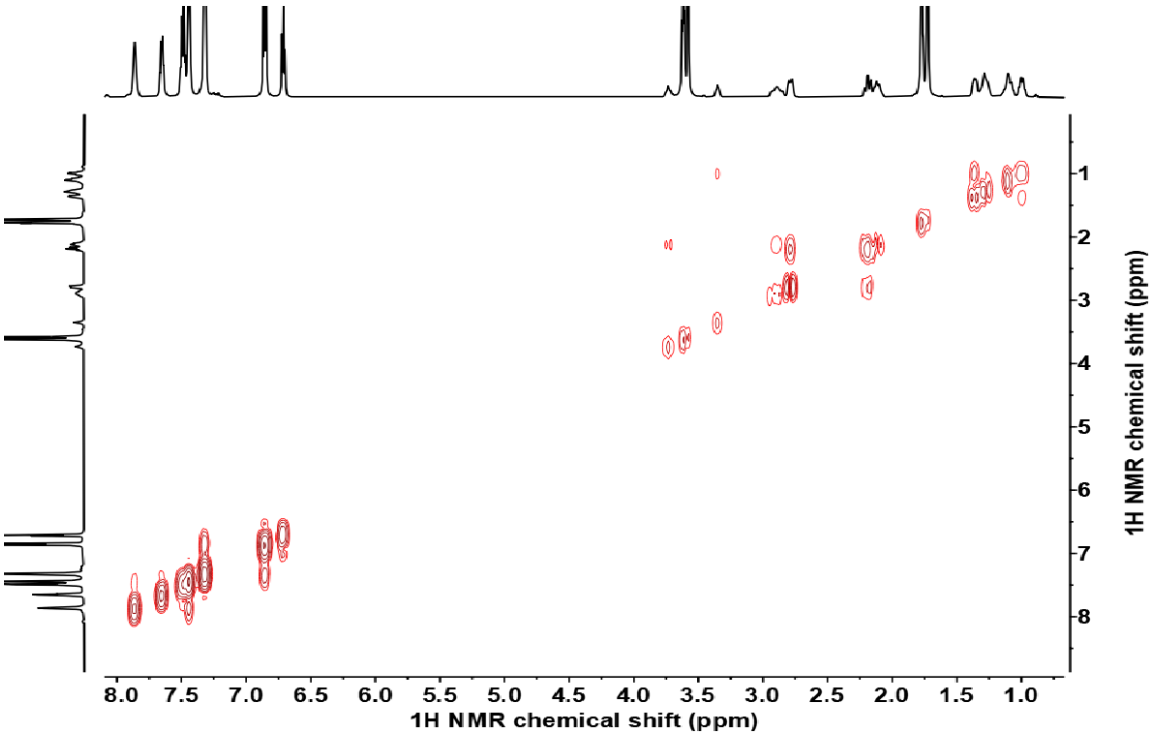

Figure S31. Expansions of the aromatic and aliphatic regions of the ^{1}H-^{1}H COSY NMR spectrum of **2a** in THF-d_8.

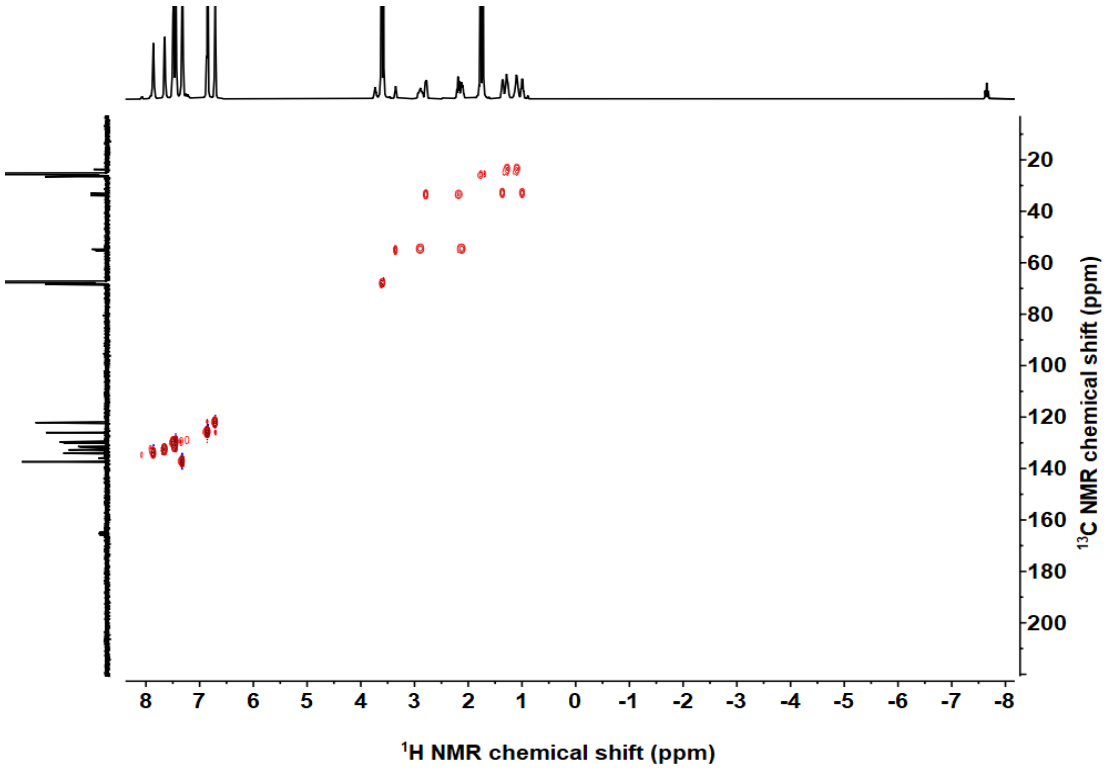

Figure S32. ^{1}H-^{13}C HSQC NMR spectrum of **2a** in THF-d_8.

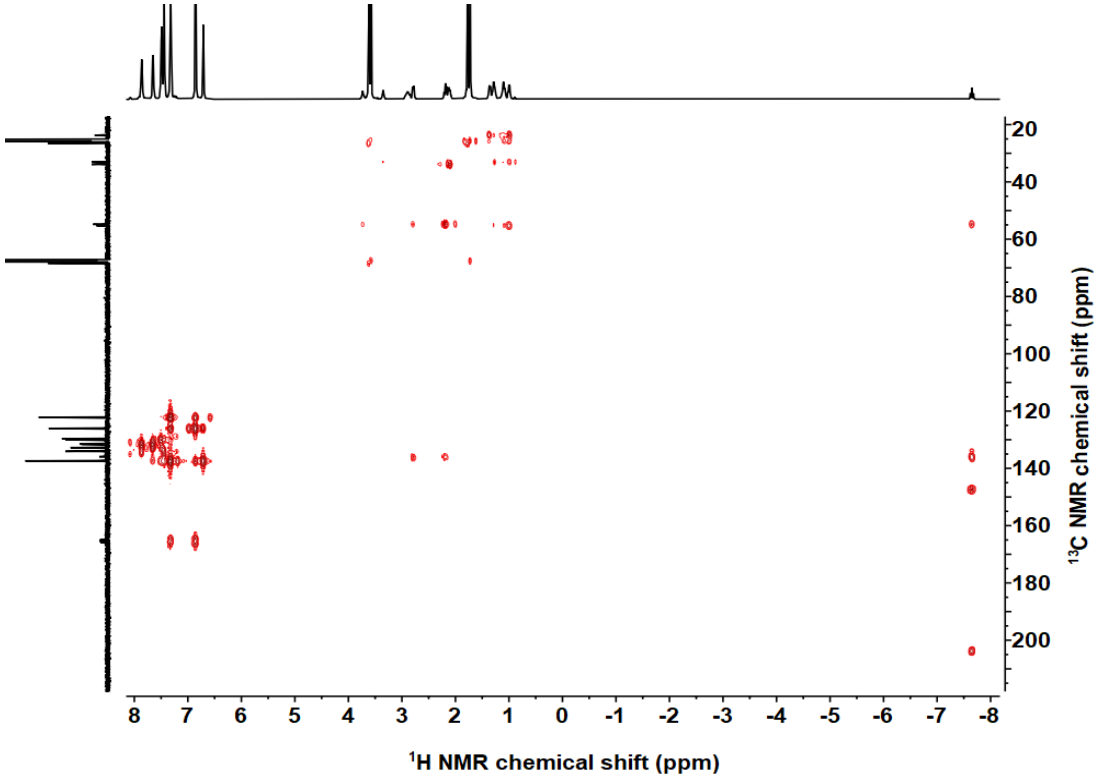

Figure S33. ^{1}H-^{13}C HMBC NMR spectrum of **2a** in THF-d_8.

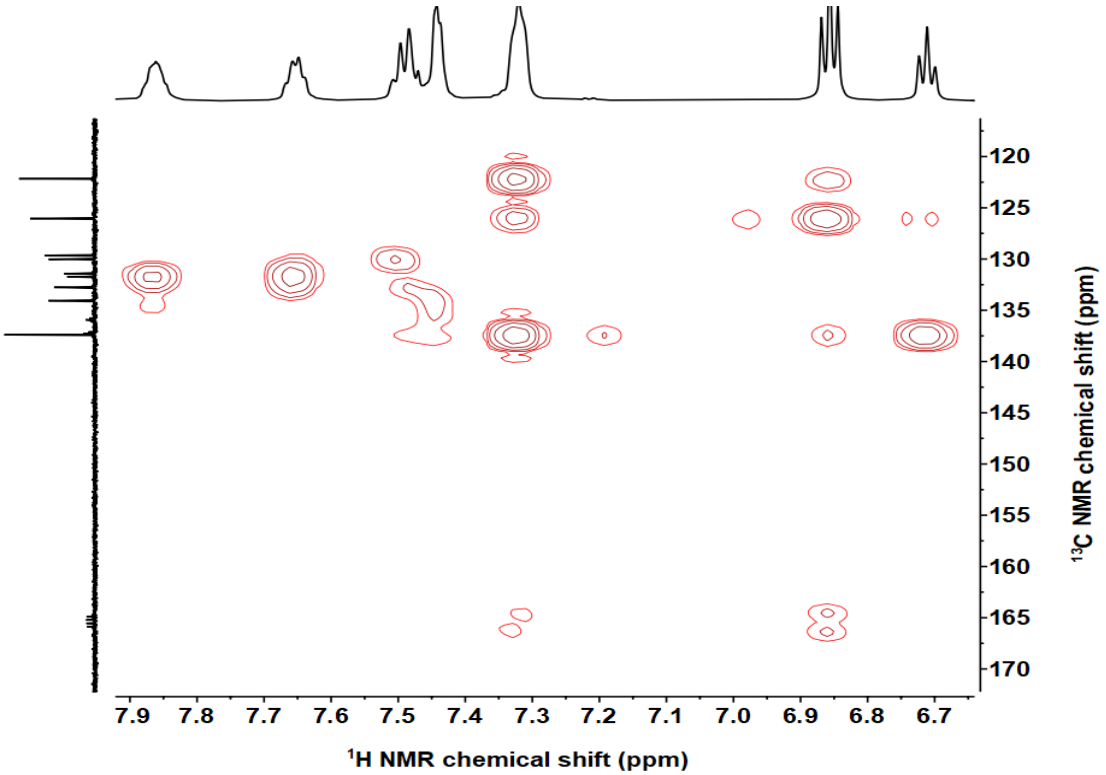

Figure S34. Expansions of the aliphatic regions of the ^{1}H-^{13}C HMBC NMR spectrum of **2a** in THF-d_8.

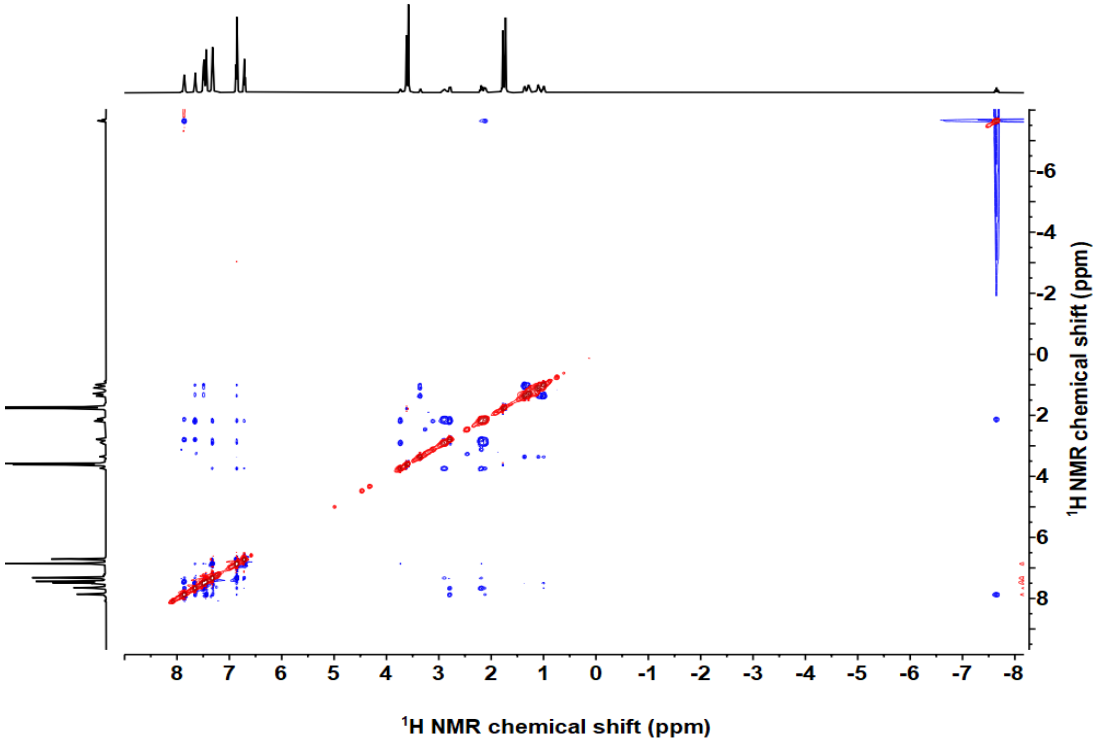

Figure S35. ^{1}H-^{1}H NOSY NMR spectrum of **2a** in THF-d_8.

2b

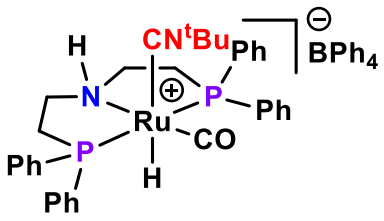

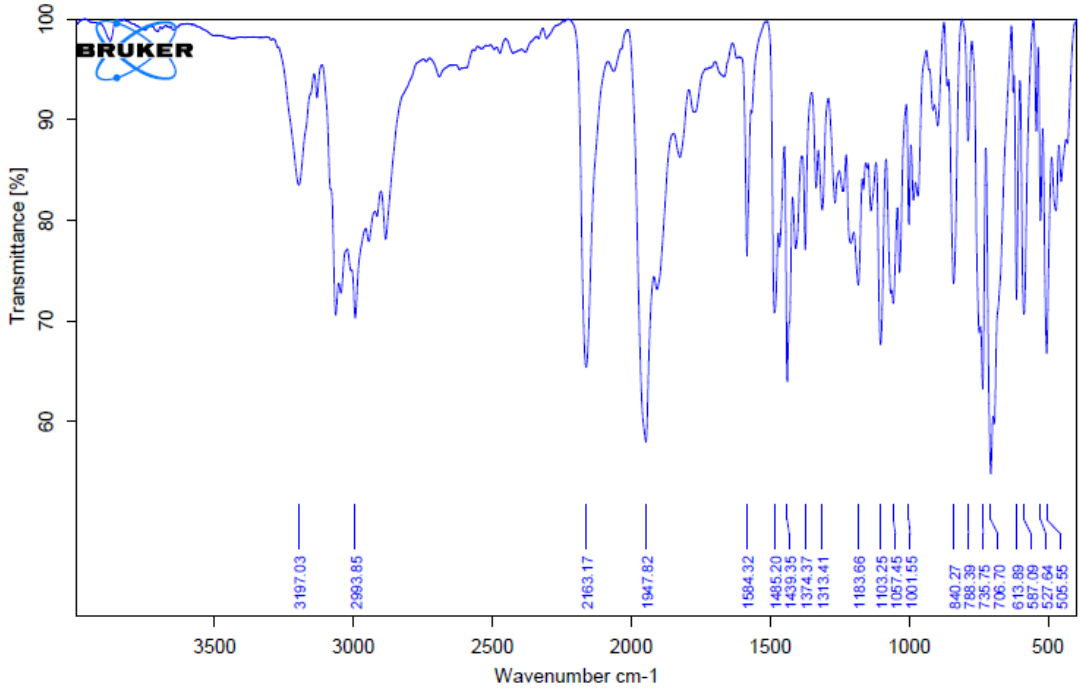

Figure S36. FTIR spectrum of **2b**.

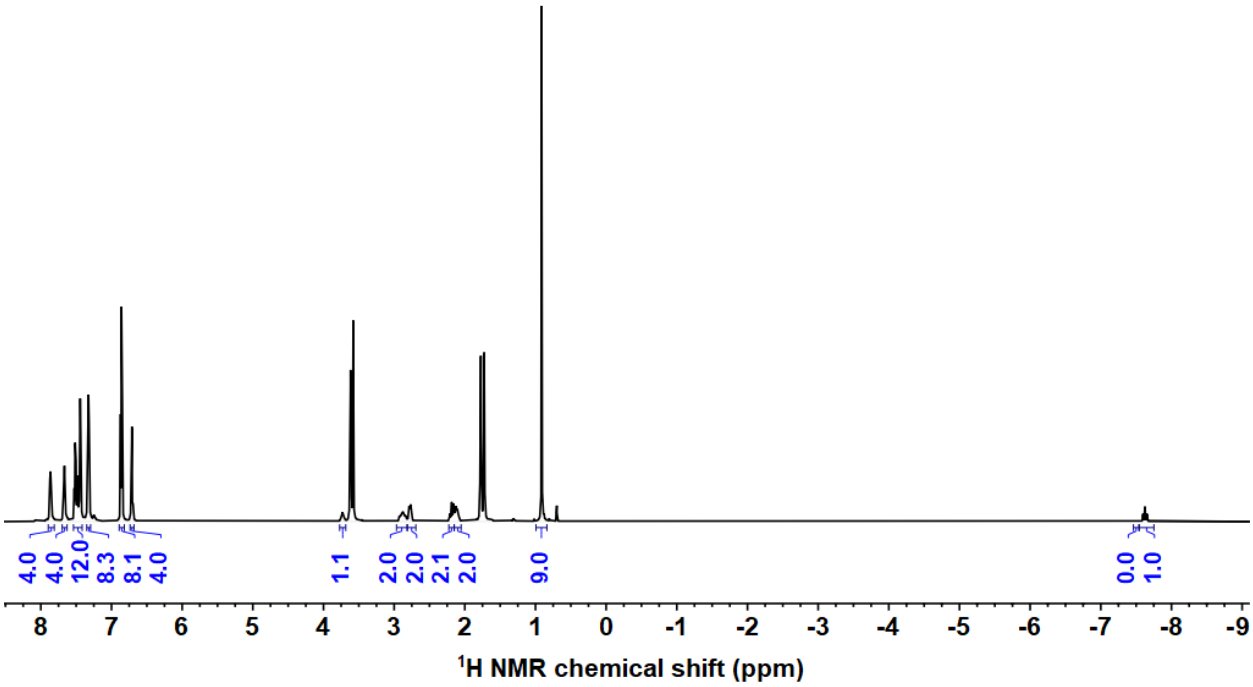

Figure S37. ^{1}H NMR spectrum of **2b** in THF-d_8.

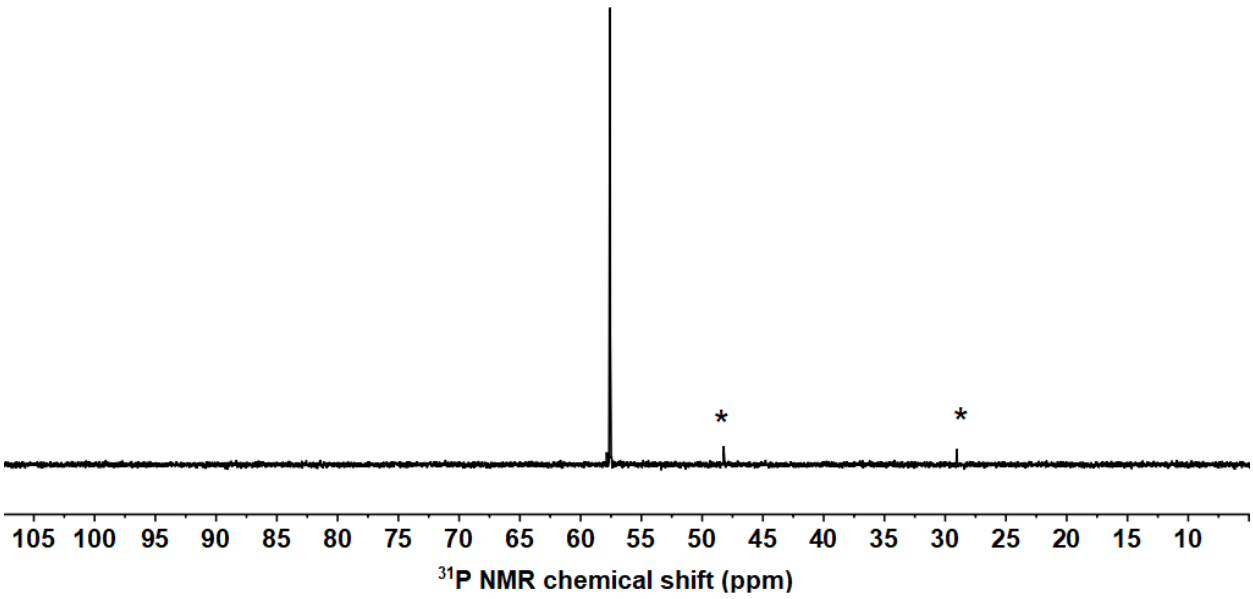

Figure S38. ^{31}P{^{1}H} NMR spectrum of **2b** in THF-d_8; [*]: residual impurities.

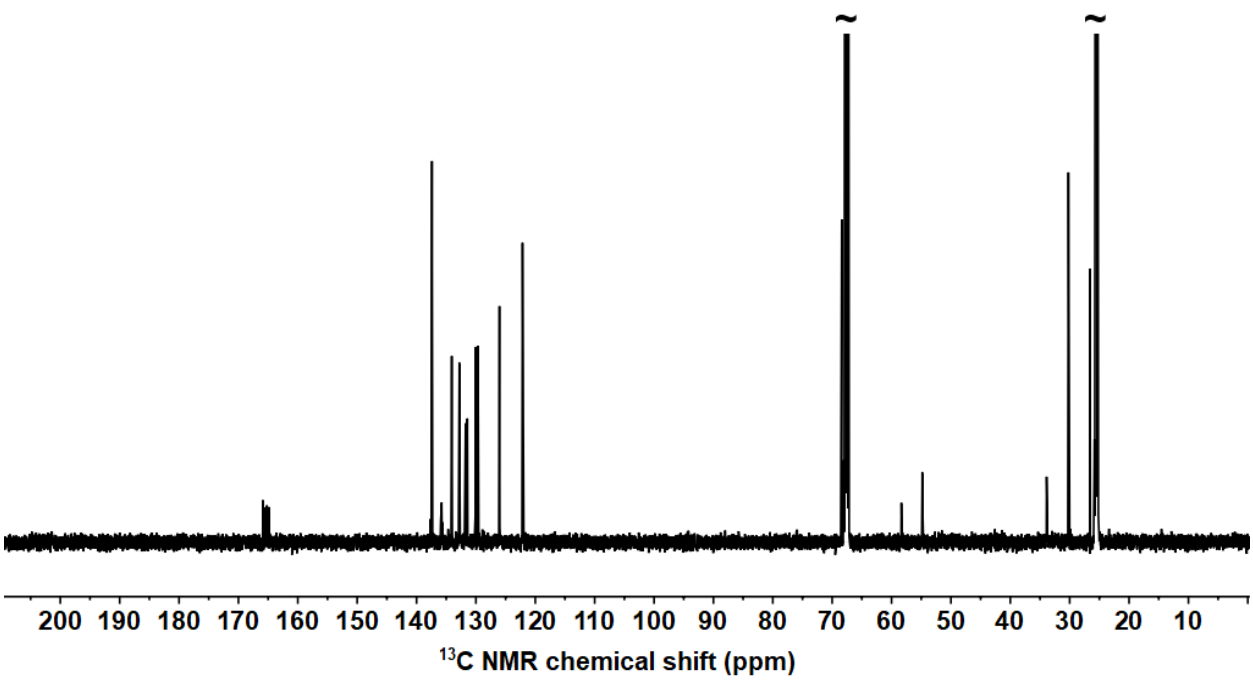

Figure S39. $^{13}C\{^{1}H\}$ NMR spectrum of **2b** in THF-d_8. ~ = solvent signal cutoff.

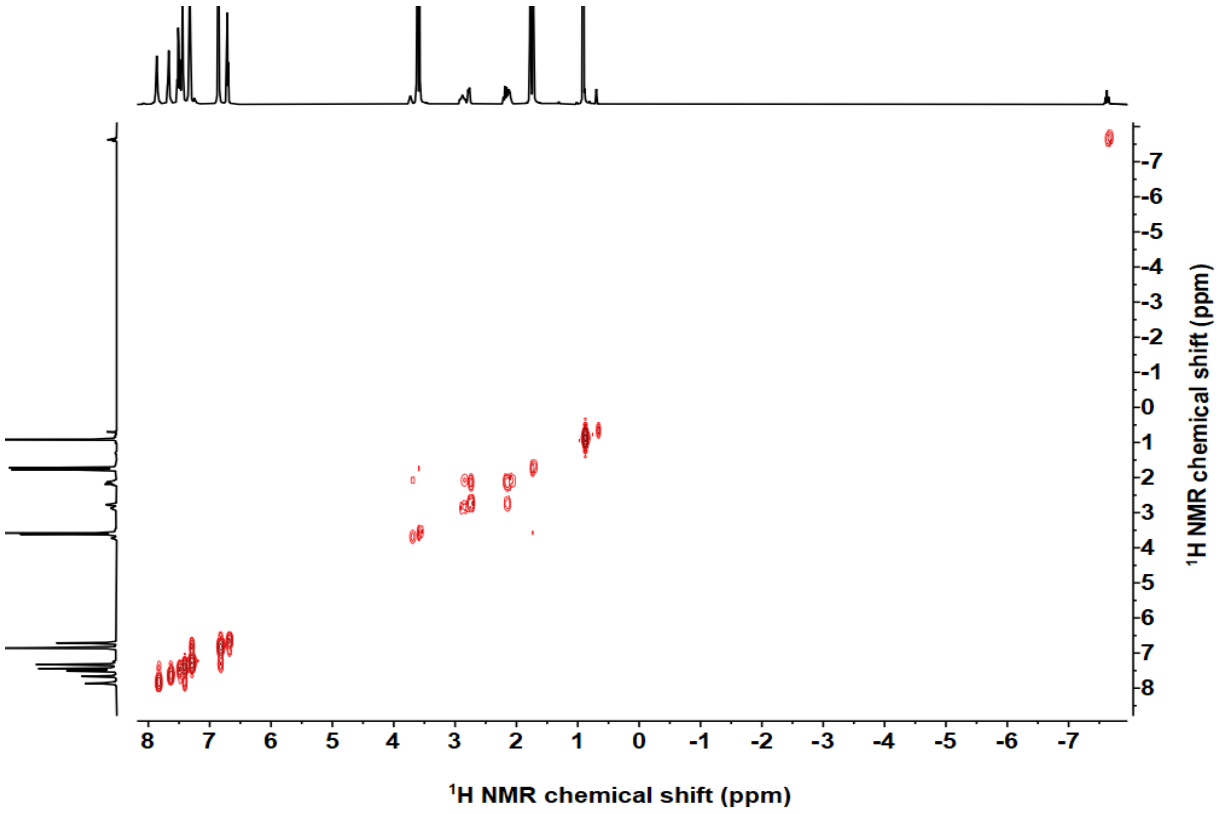

Figure S40. ^{1}H-^{1}H COSY NMR spectrum of **2b** in THF-d_8.

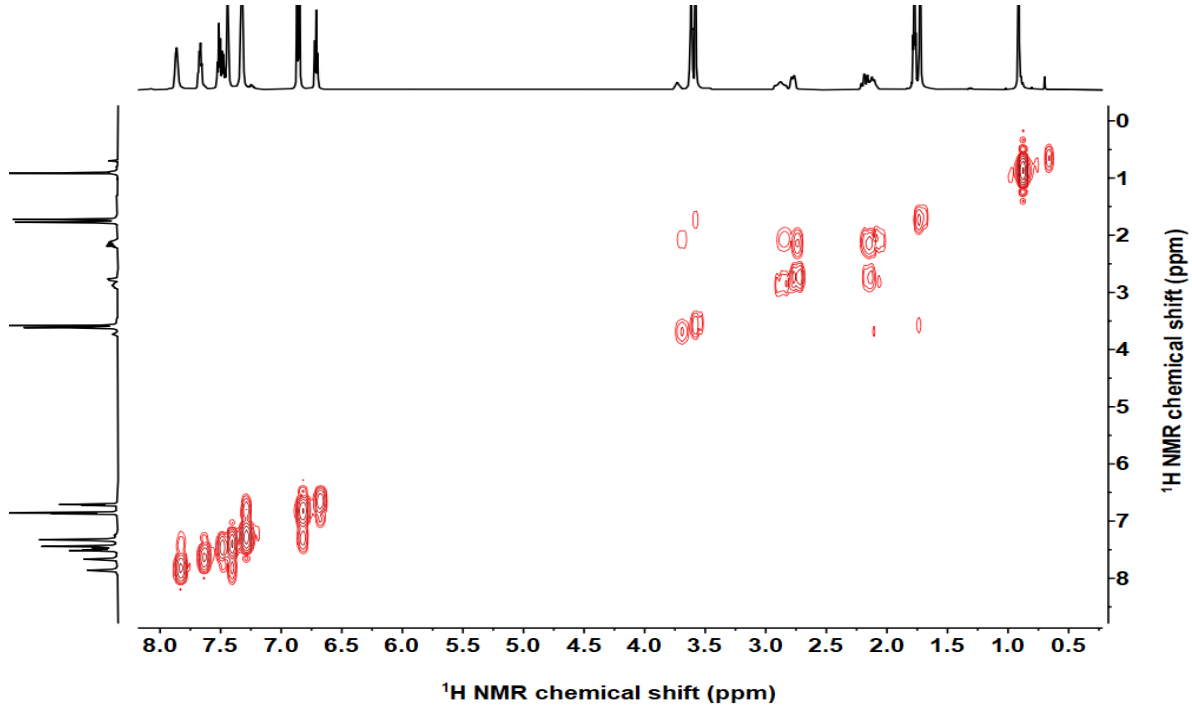

Figure S41. Expansions of the aromatic and aliphatic regions of the ^{1}H-^{1}H COSY NMR spectrum of **2b** in THF-d_8.

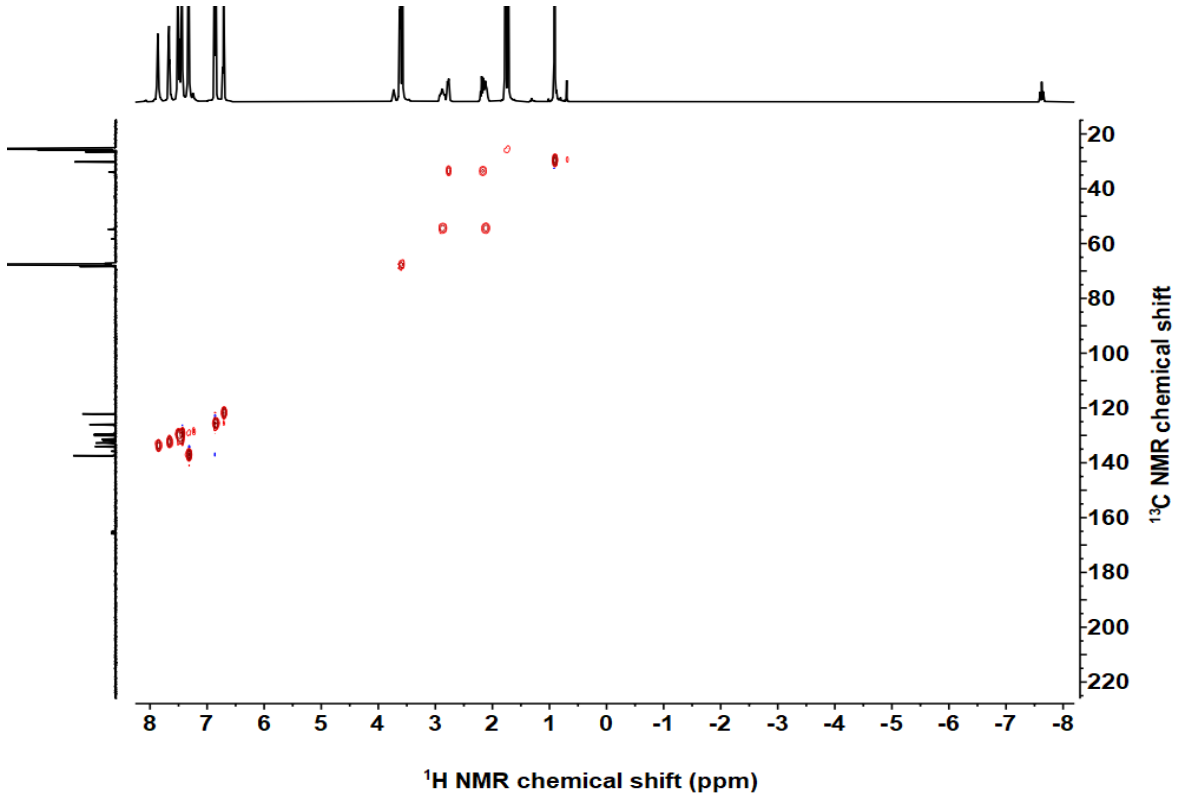

Figure S42. ^{1}H-^{13}C HSQC NMR spectrum of **2b** in THF-d_8.

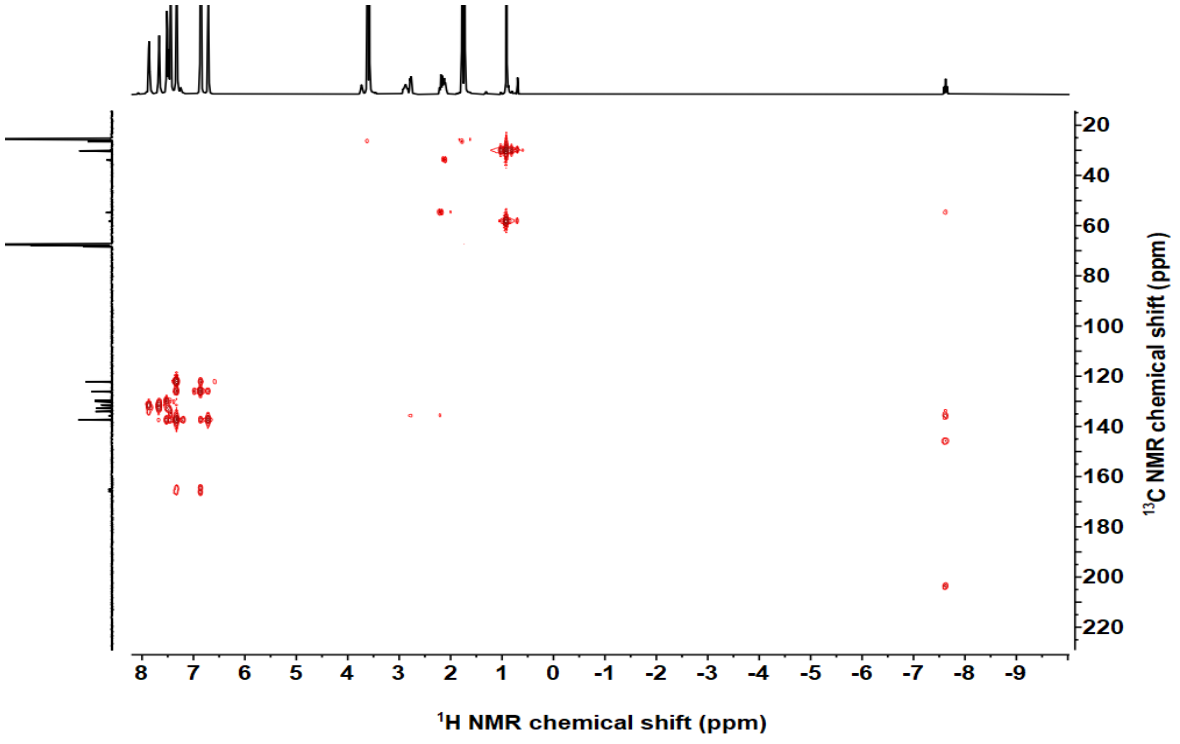

Figure S43. ^{1}H-^{13}C HMBC NMR spectrum of **2b** in THF-d_8.

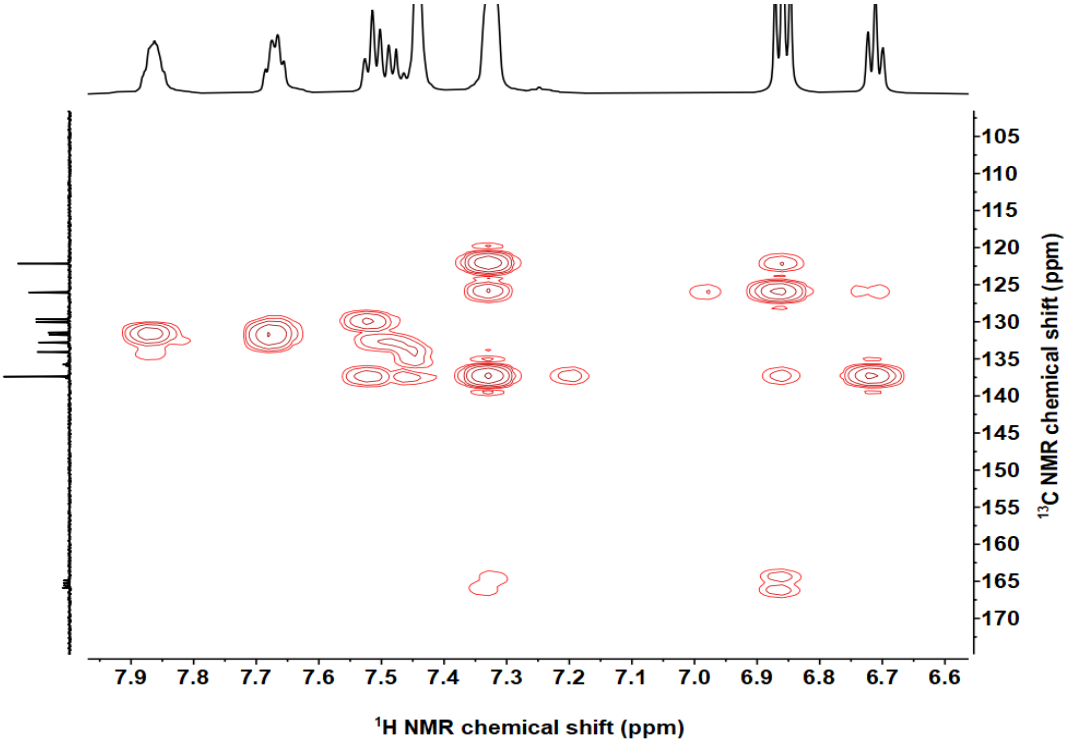

Figure S44. Expansions of the aromatic regions of the ^{1}H-^{13}C HMBC NMR spectrum of **2b** in THF-d_8.

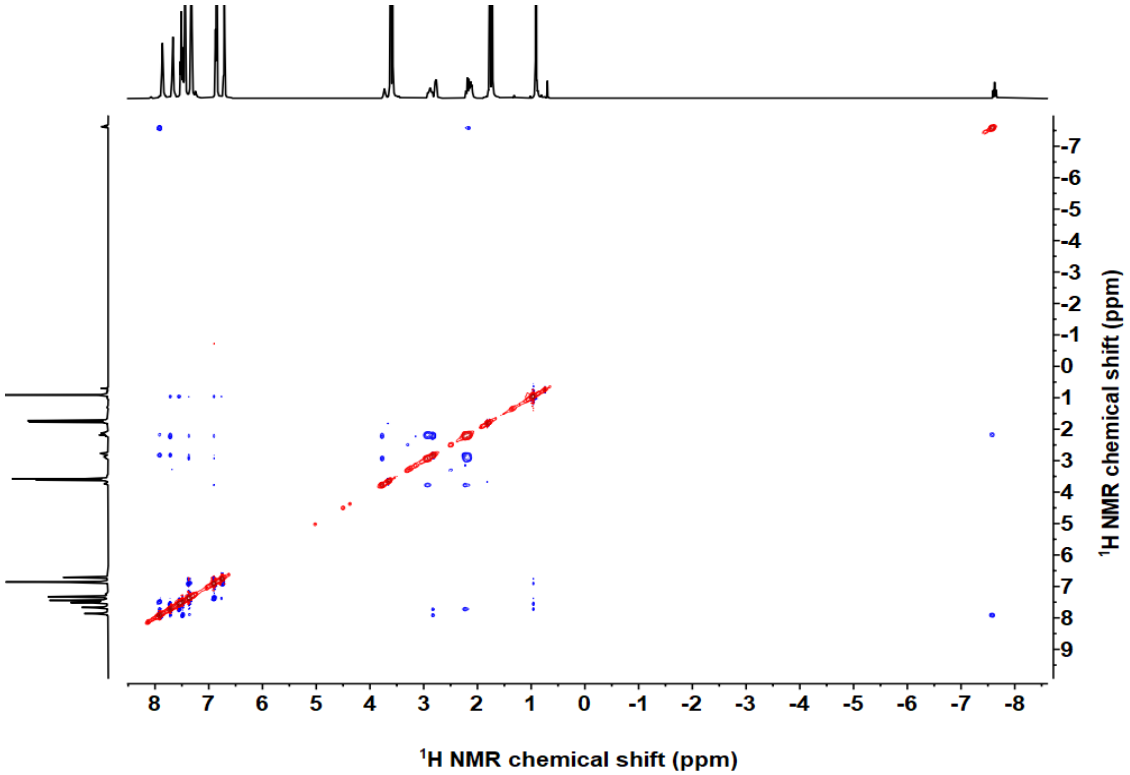

Figure S45. ^{1}H-^{1}H NOSY NMR spectrum of **2b** in THF-d_8.

2c

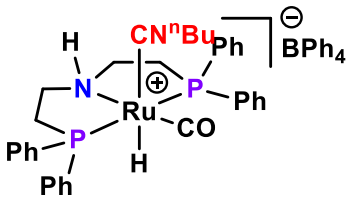

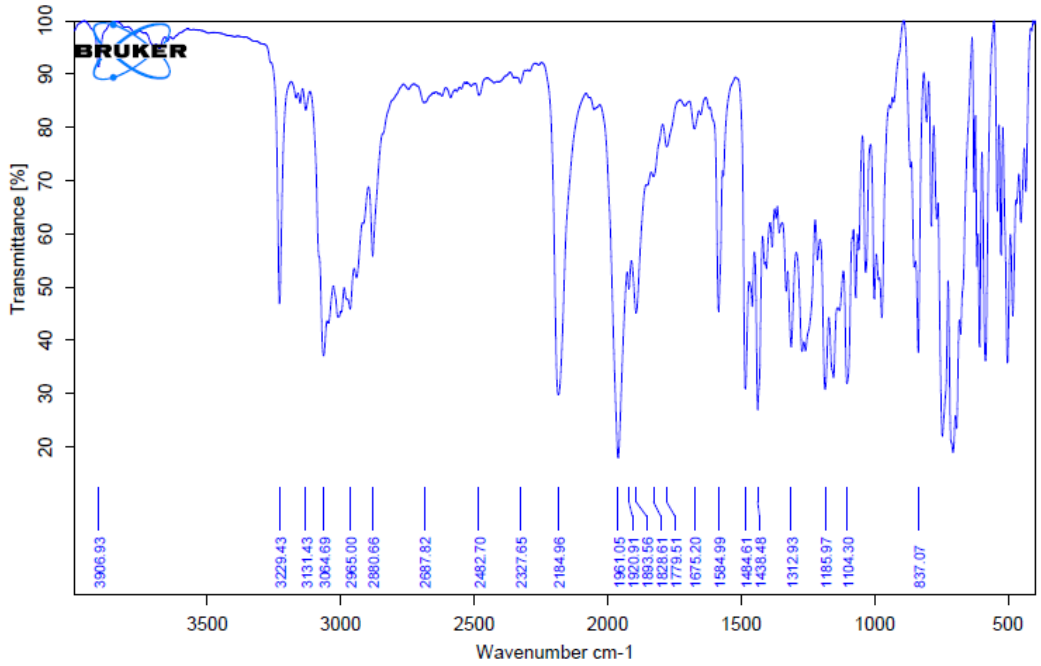

Figure S46. FTIR spectrum of **2b**.

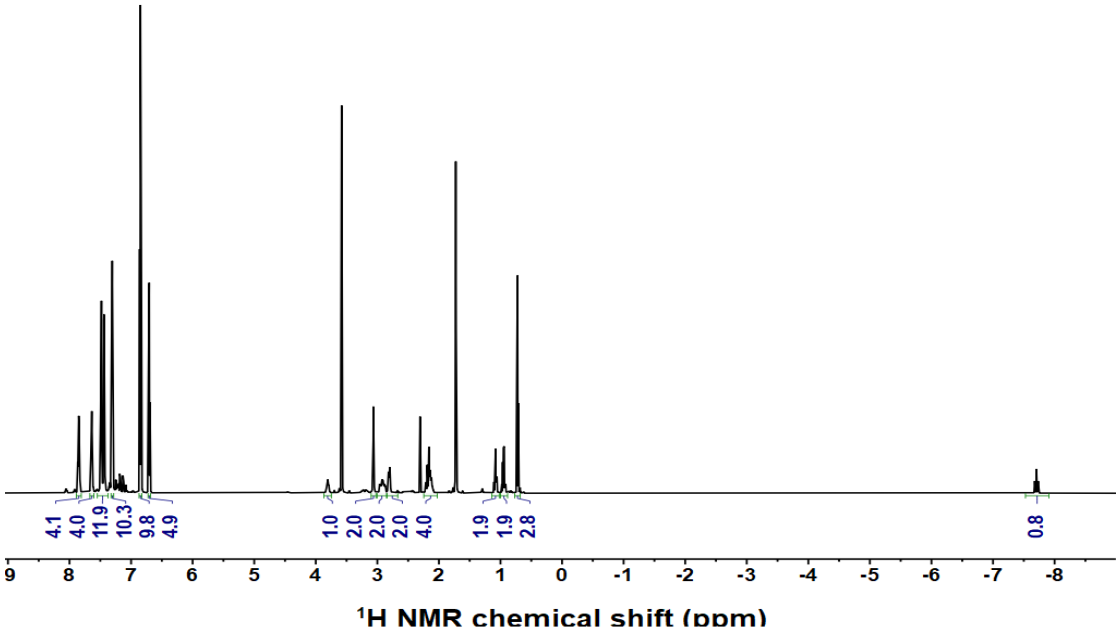

Figure S47. ^{1}H NMR spectrum of **2c** in THF-d_8.

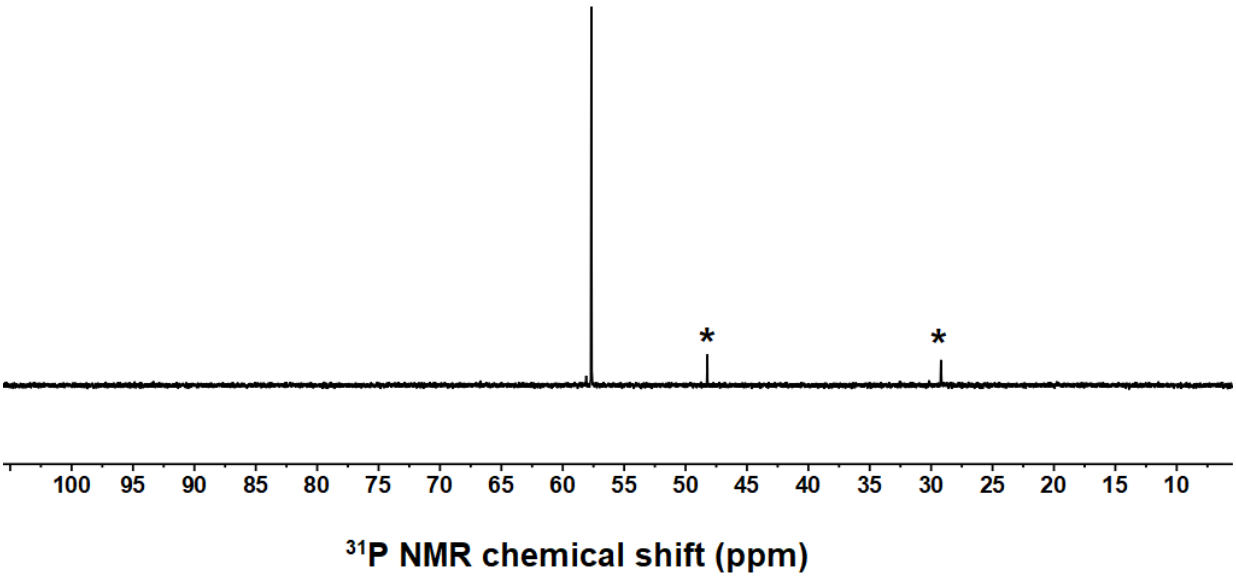

Figure S48. ^{31}P{^{1}H} NMR spectrum of **2c** in THF-d_8; [*]: residual impurities.

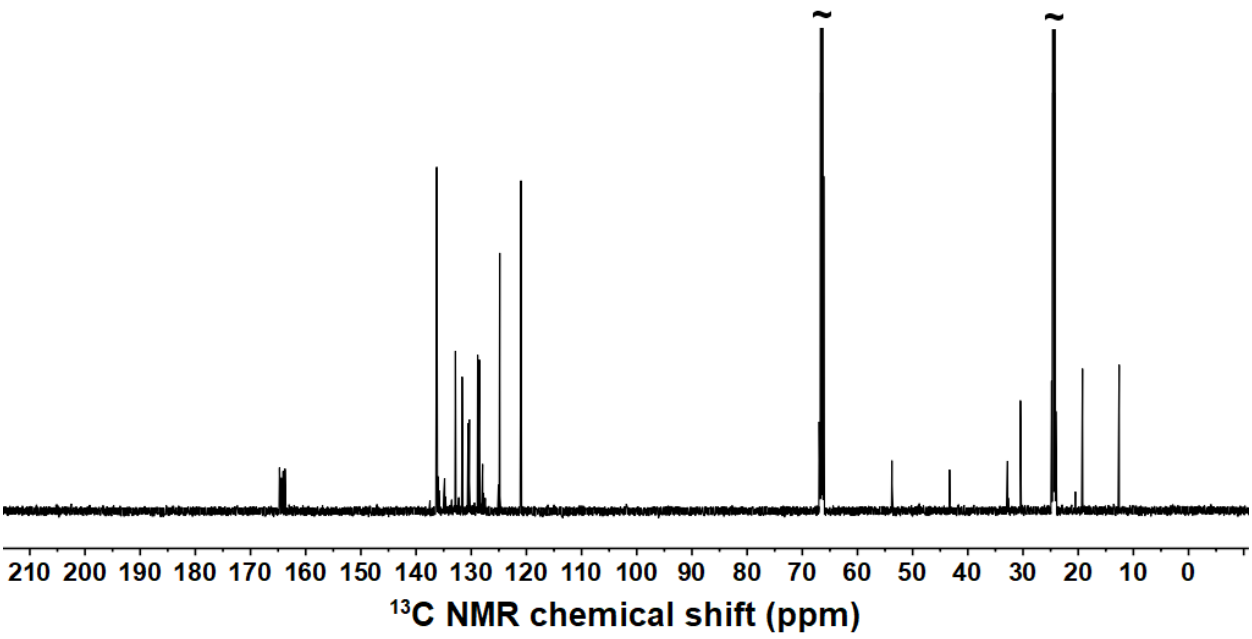

Figure S49. $^{13}C\{^{1}H\}$ NMR spectrum of **2c** in THF-d_8. ~ = solvent signal cutoff.

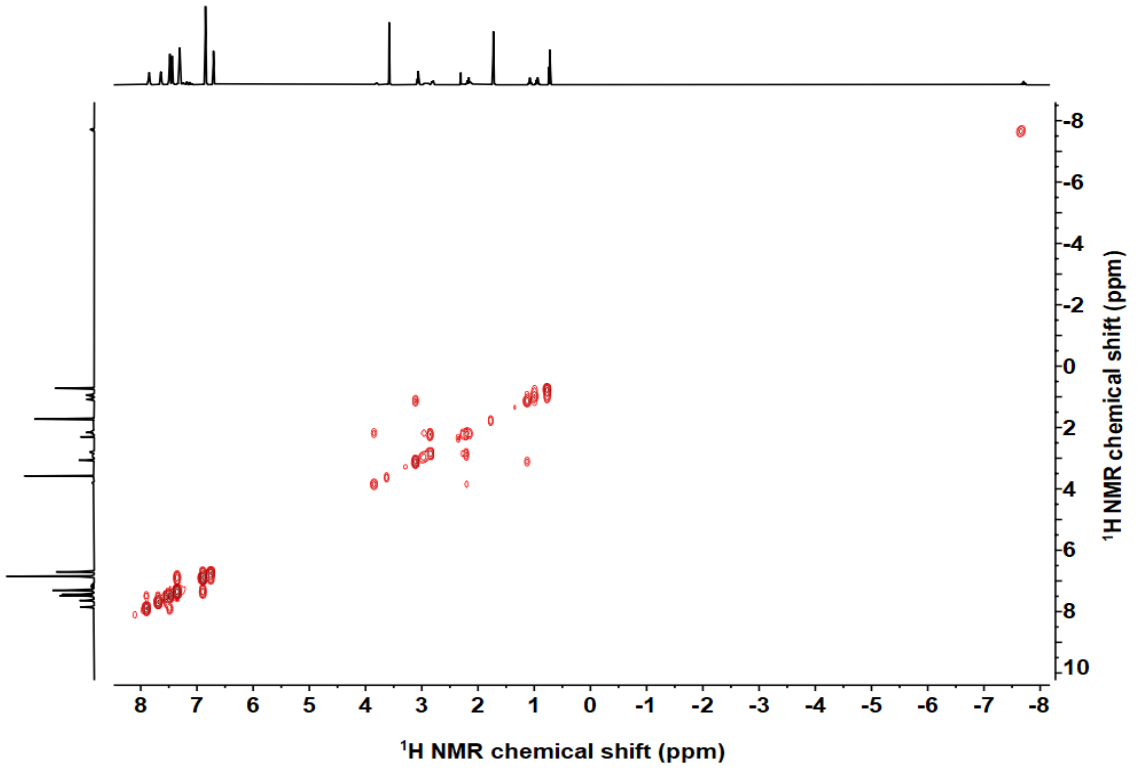

Figure S50. ^{1}H-^{1}H COSY NMR spectrum of **2c** in THF-d_8.

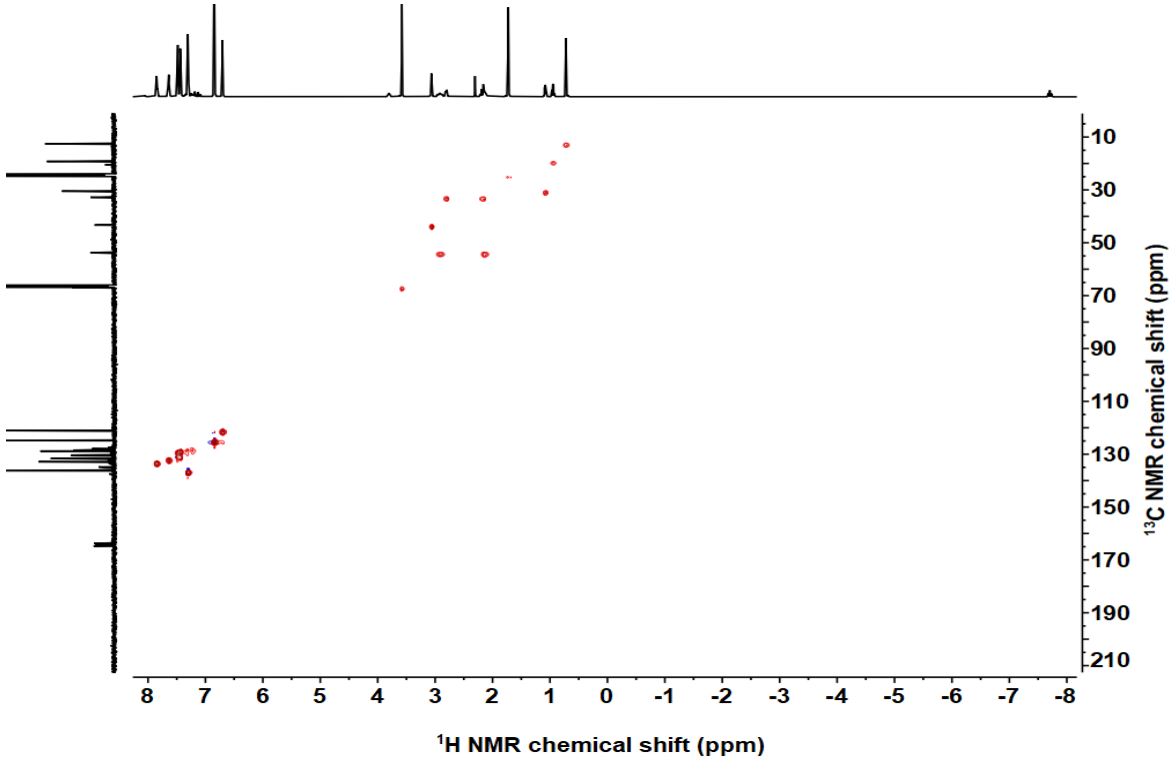

Figure S51. ^{1}H-^{13}C HSQC NMR spectrum of **2c** in THF-d_8.

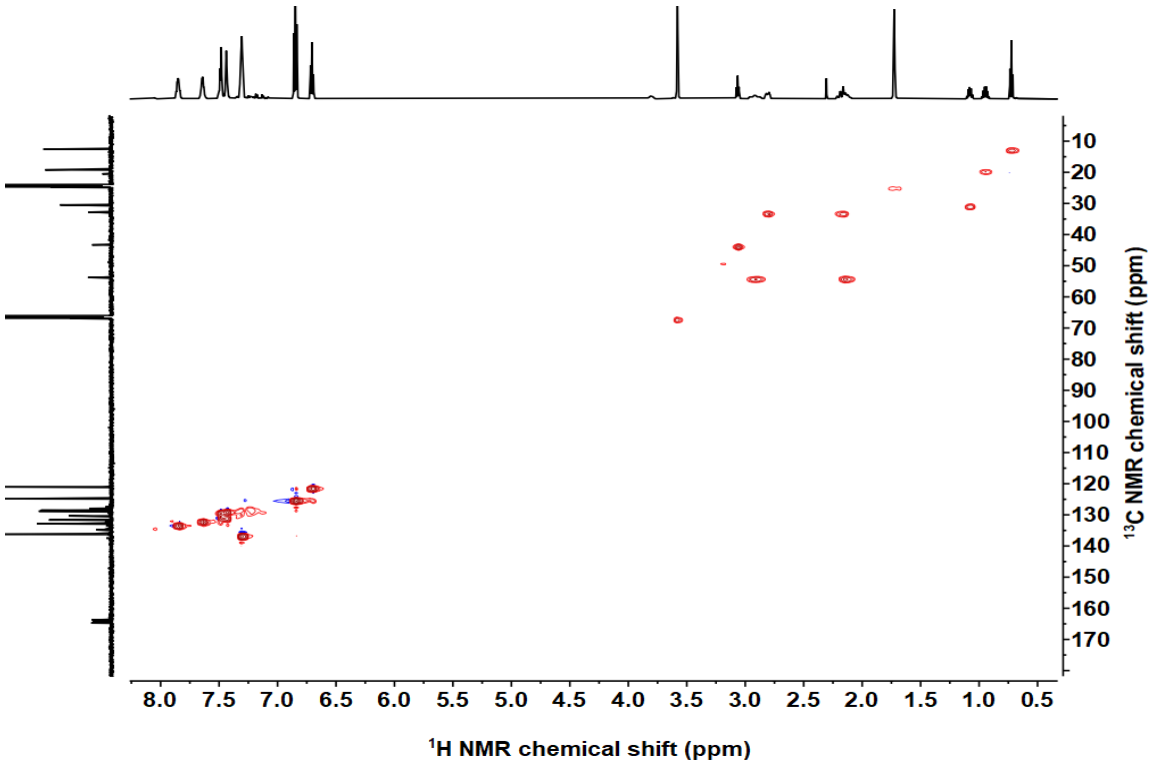

Figure S52. Expansions of the aromatic and aliphatic regions of the ^{1}H-^{13}C HSQC NMR spectrum of **2c** in THF-d_8.

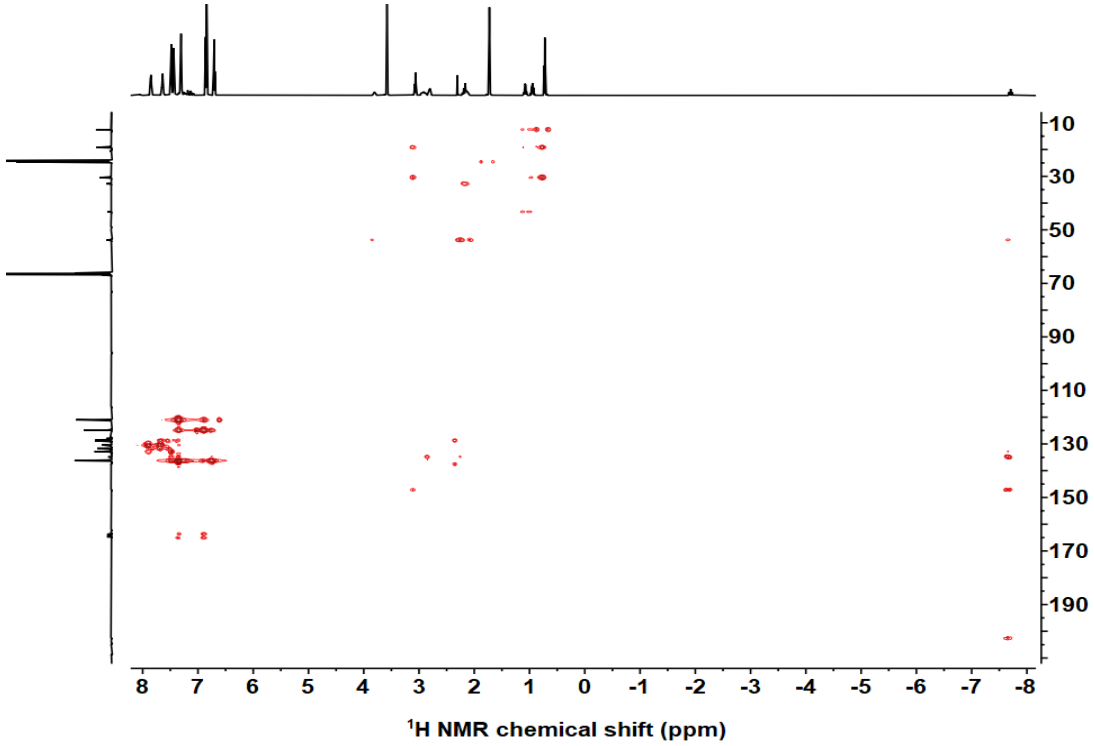

Figure S53. ^{1}H-^{13}C HMBC NMR spectrum of **2c** in THF-d_8.

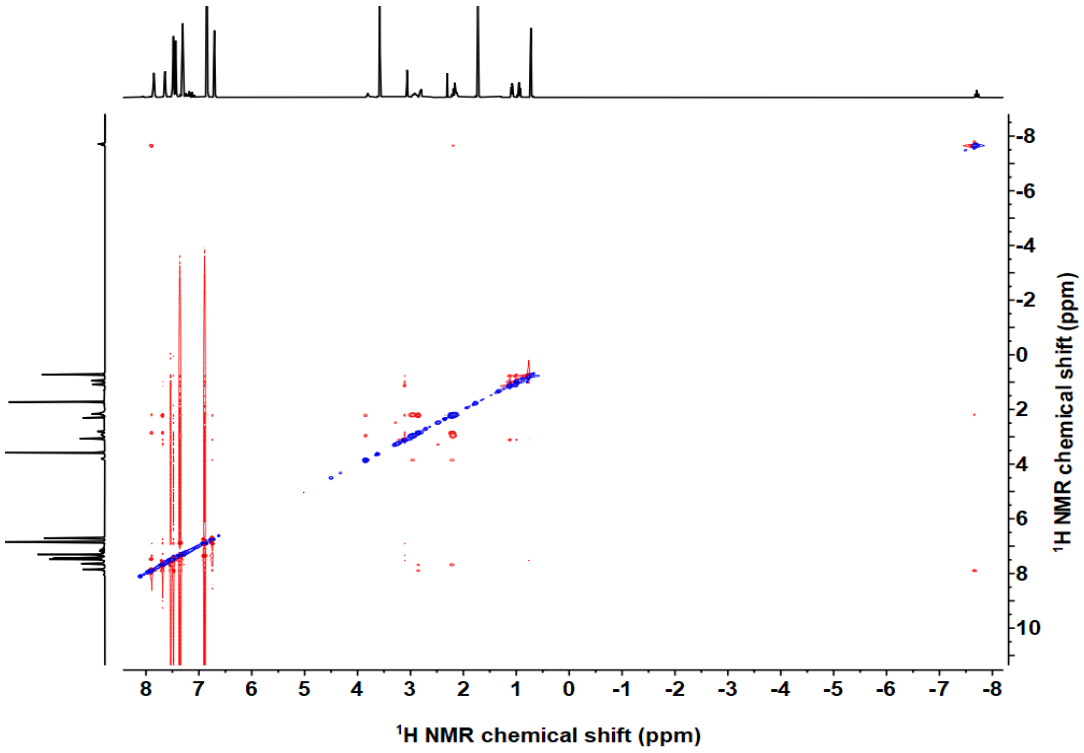

Figure S54. ^{1}H-^{1}H NOSY NMR spectrum of **2c** in THF-d_8.

2d

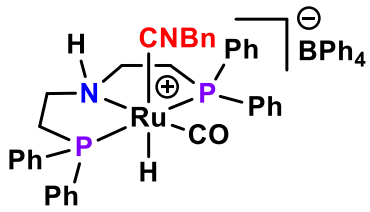

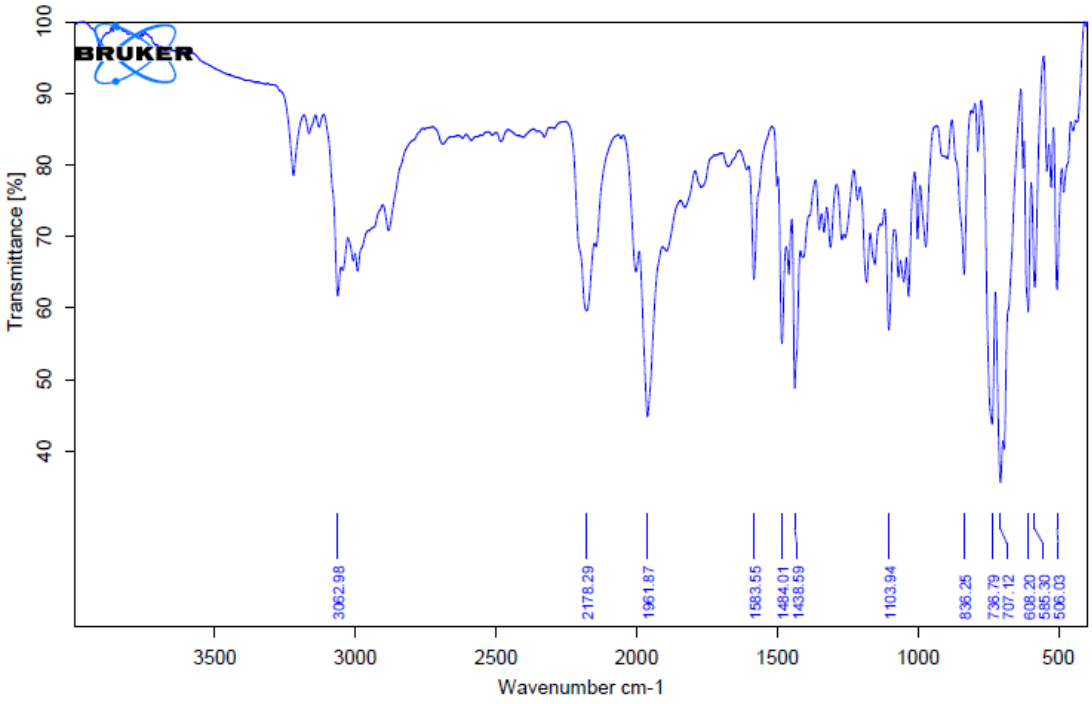

Figure S55. FTIR spectrum of **2d**.

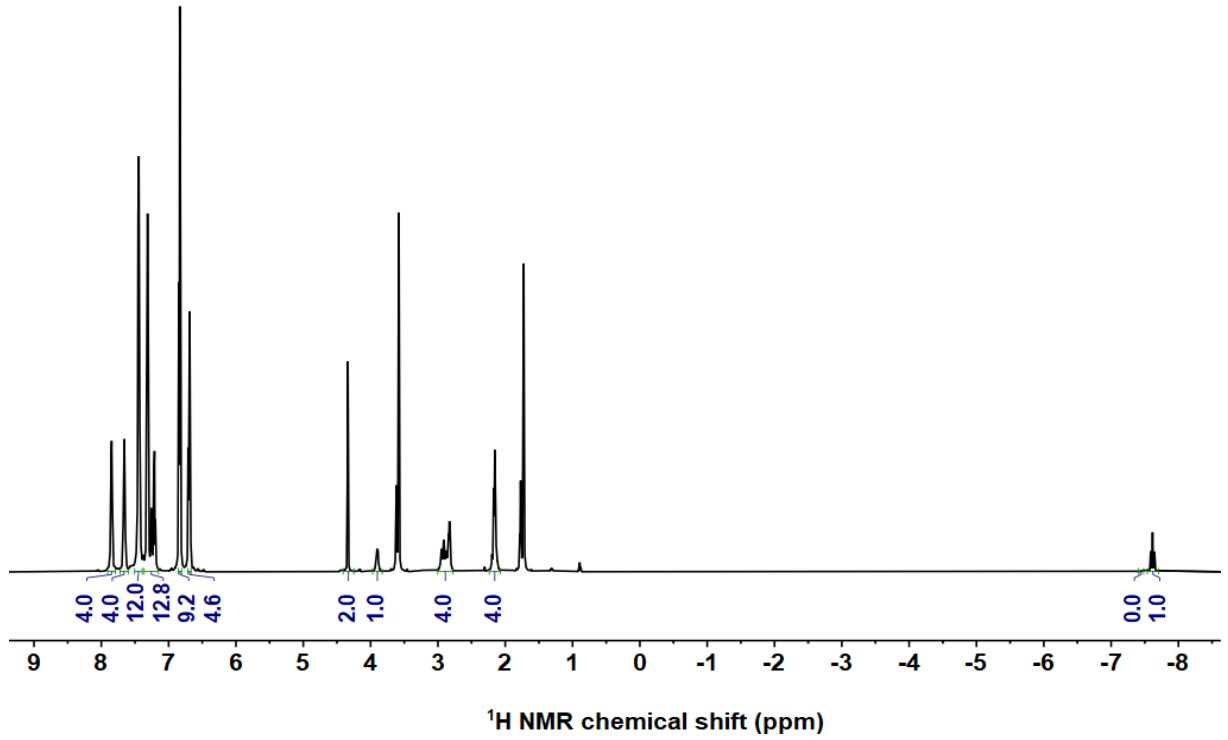

Figure S56. ^{1}H NMR spectrum of **2d** in THF-d_8.

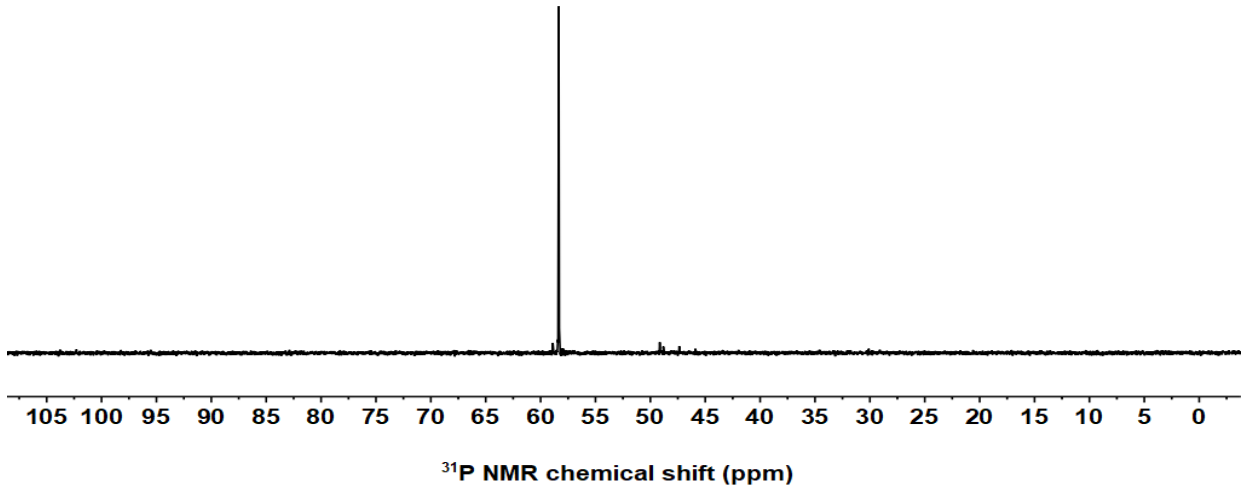

Figure S57. ^{31}P{^{1}H} NMR spectrum of **2d** in THF-d_8.

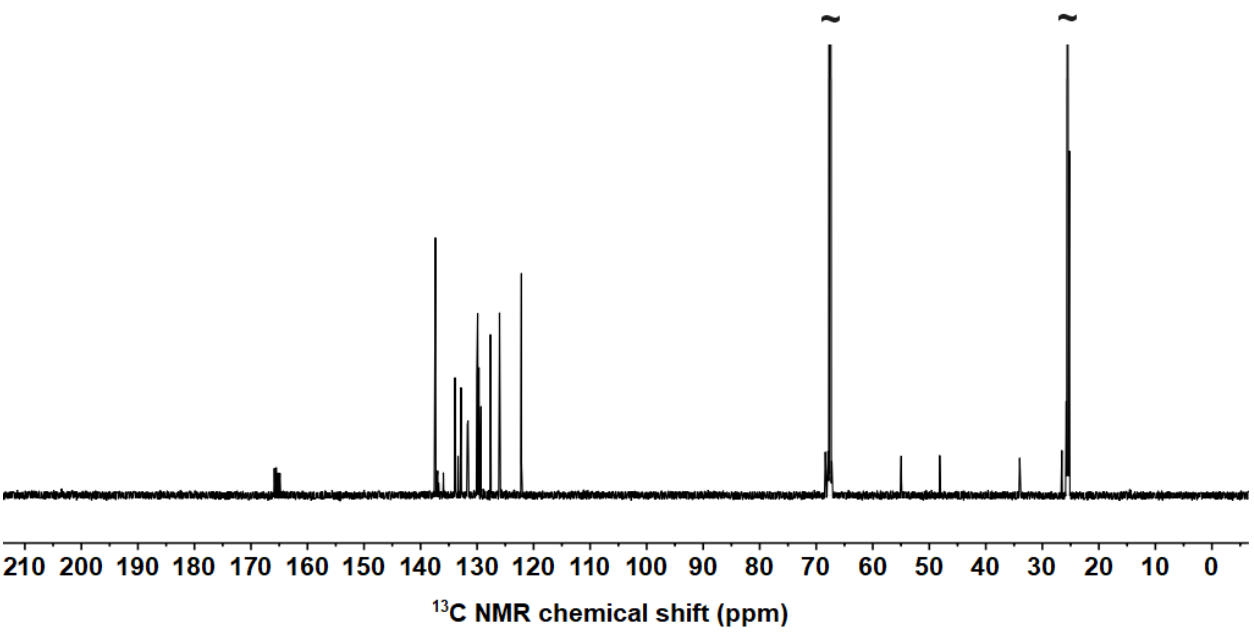

Figure S58. $^{13}C\{^{1}H\}$ NMR spectrum of **2d** in THF-d_8. ~ = solvent signal cutoff.

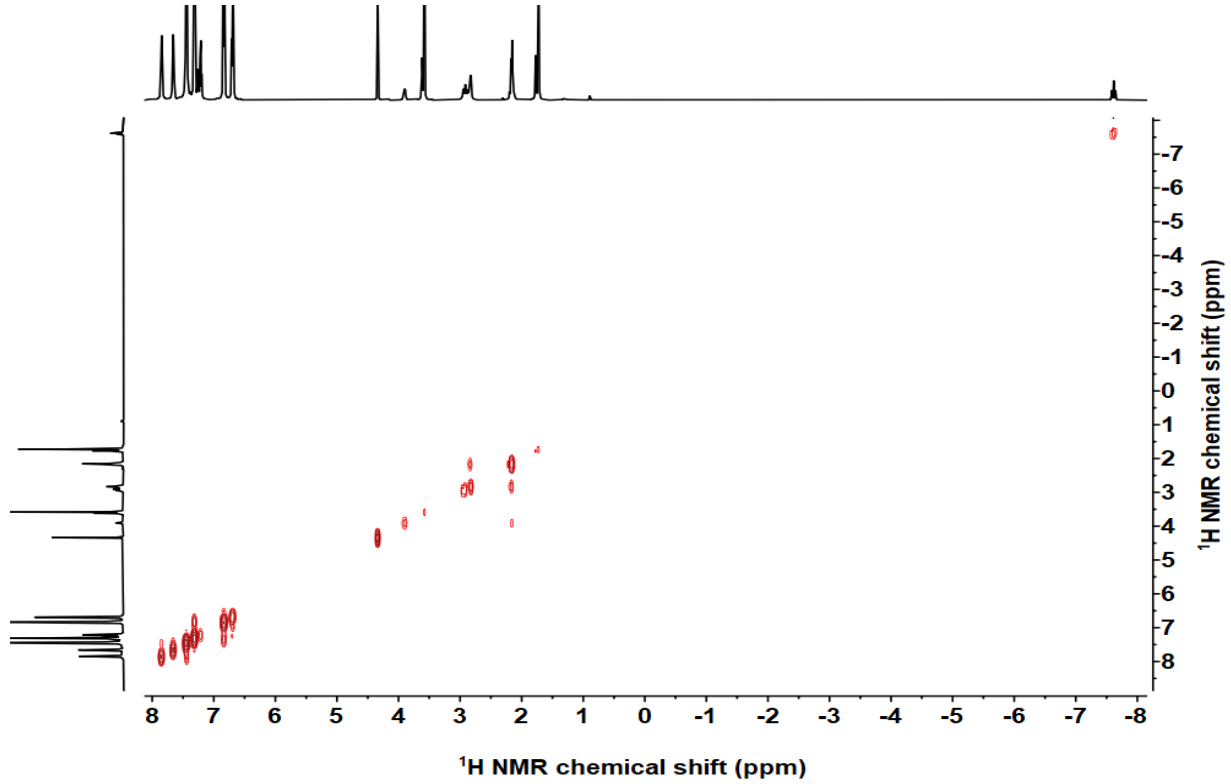

Figure S59. ^{1}H-^{1}H COSY NMR spectrum of **2d** in THF-d_8.

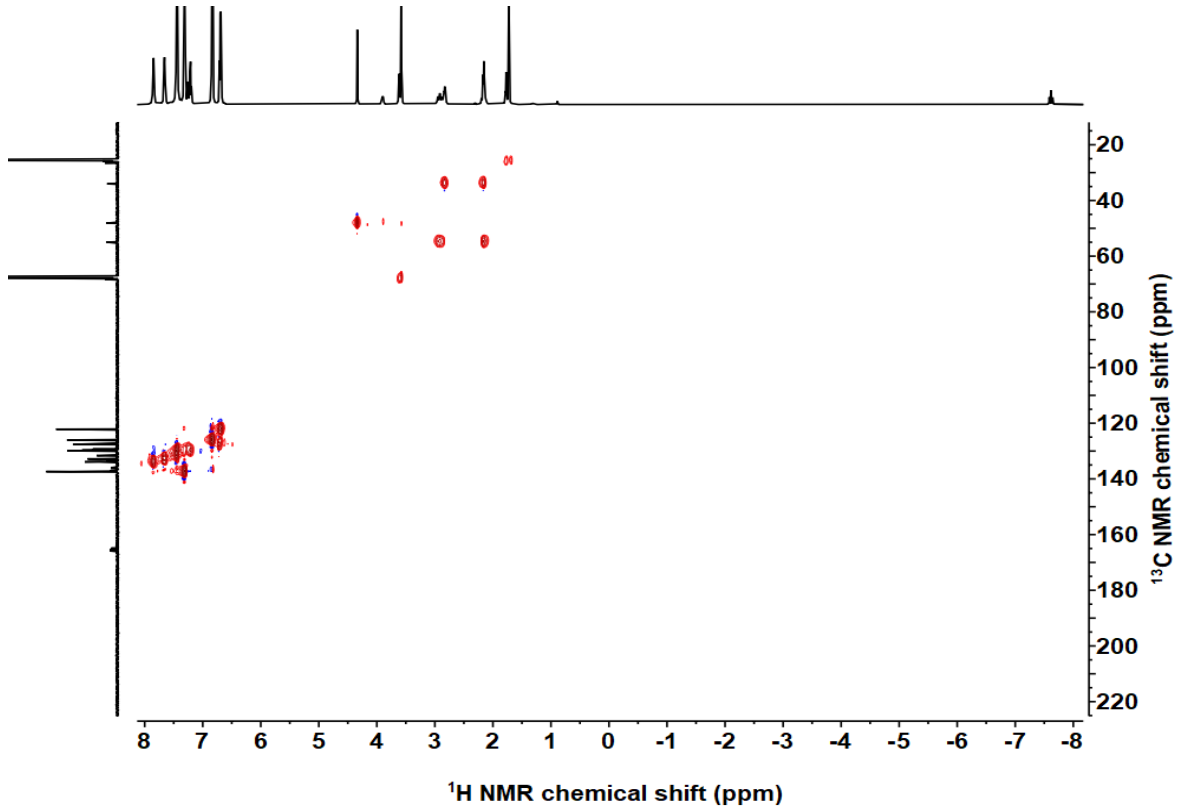

Figure S60. ^{1}H-^{13}C HSQC NMR spectrum of **2d** in THF-d_8.

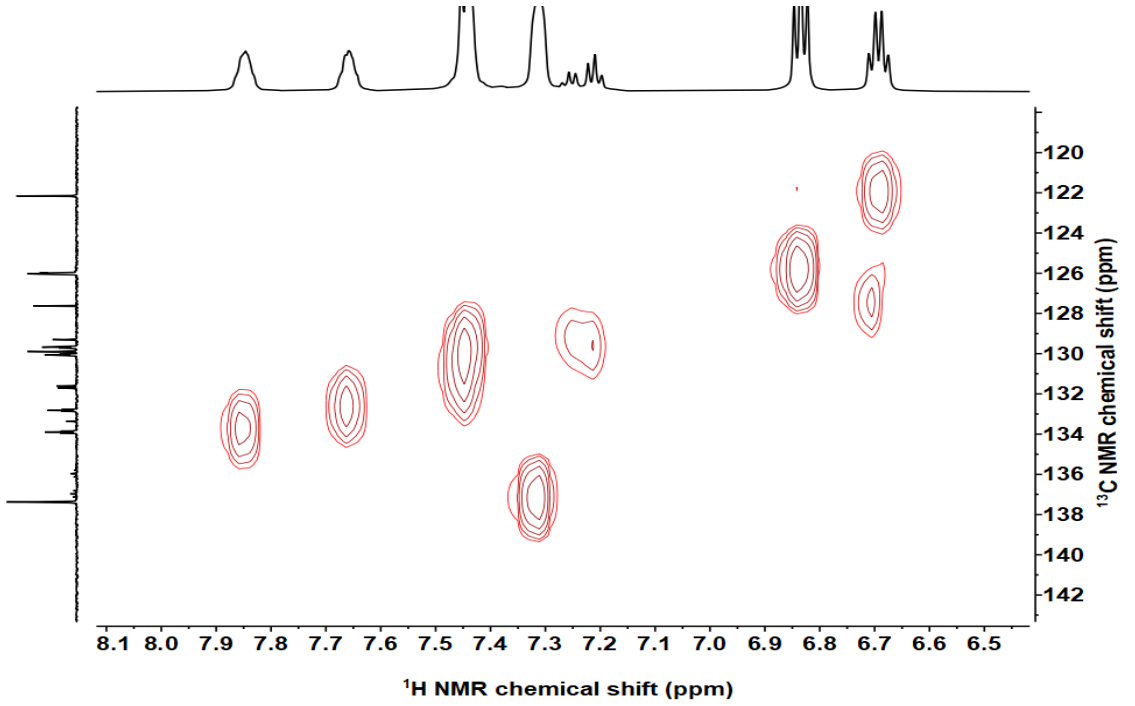

Figure S61. Expansion of the aliphatic regions of the ^{1}H-^{13}C HSQC NMR spectrum of **2d** in THF-d_8.

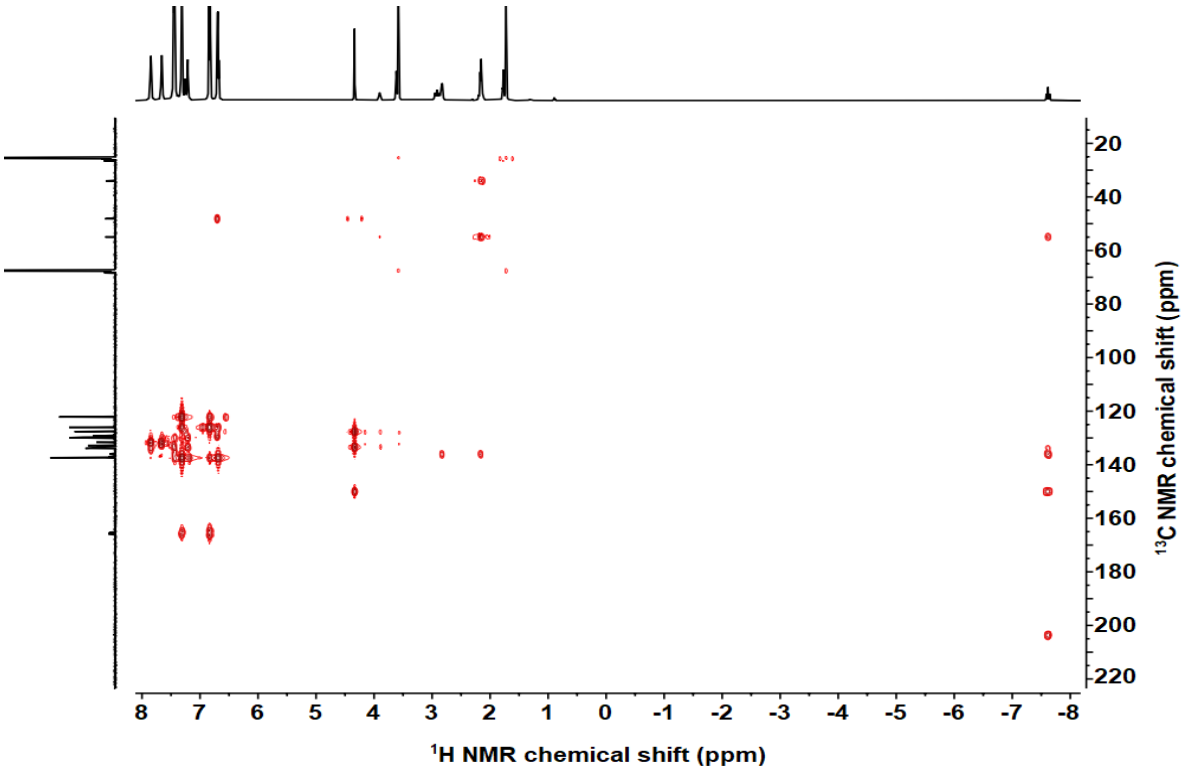

Figure S62. ^{1}H-^{13}C HMBC NMR spectrum of **2d** in THF-d_8.

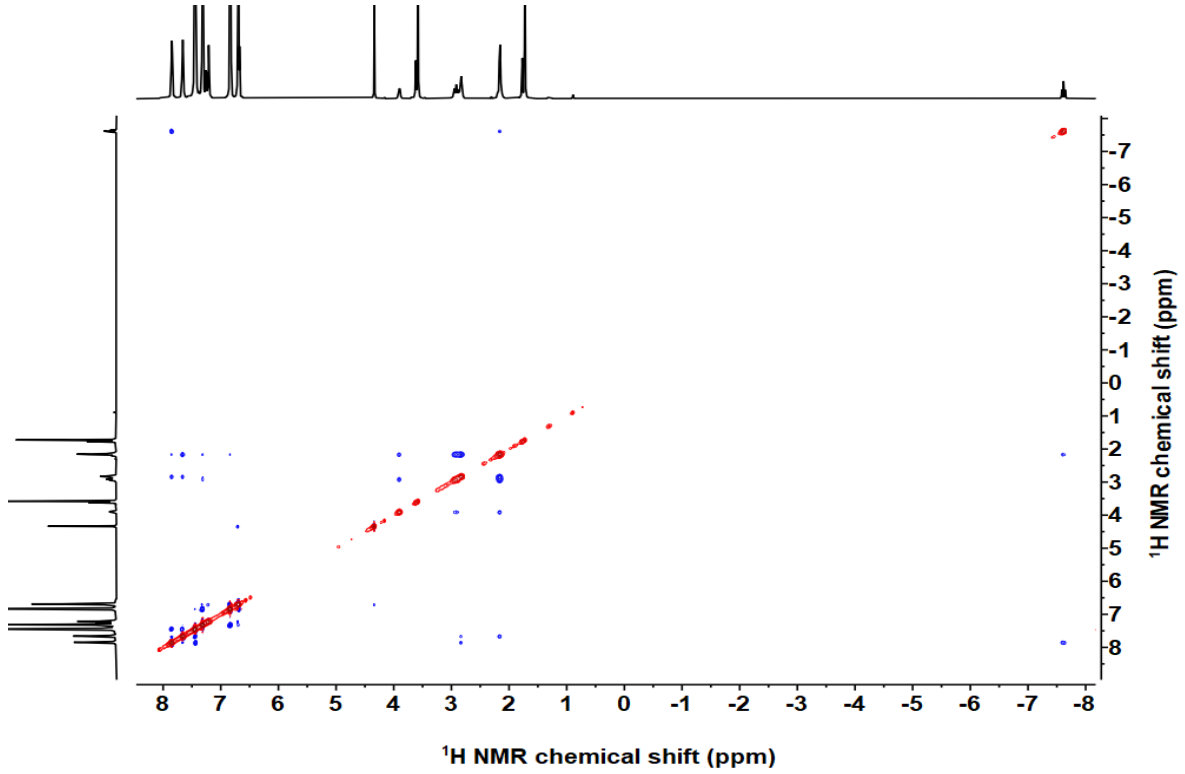

Figure S63. ^{1}H-^{1}H NOSY NMR spectrum of **2d** in THF-d_8.

3

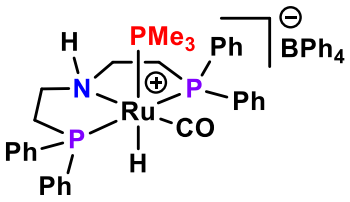

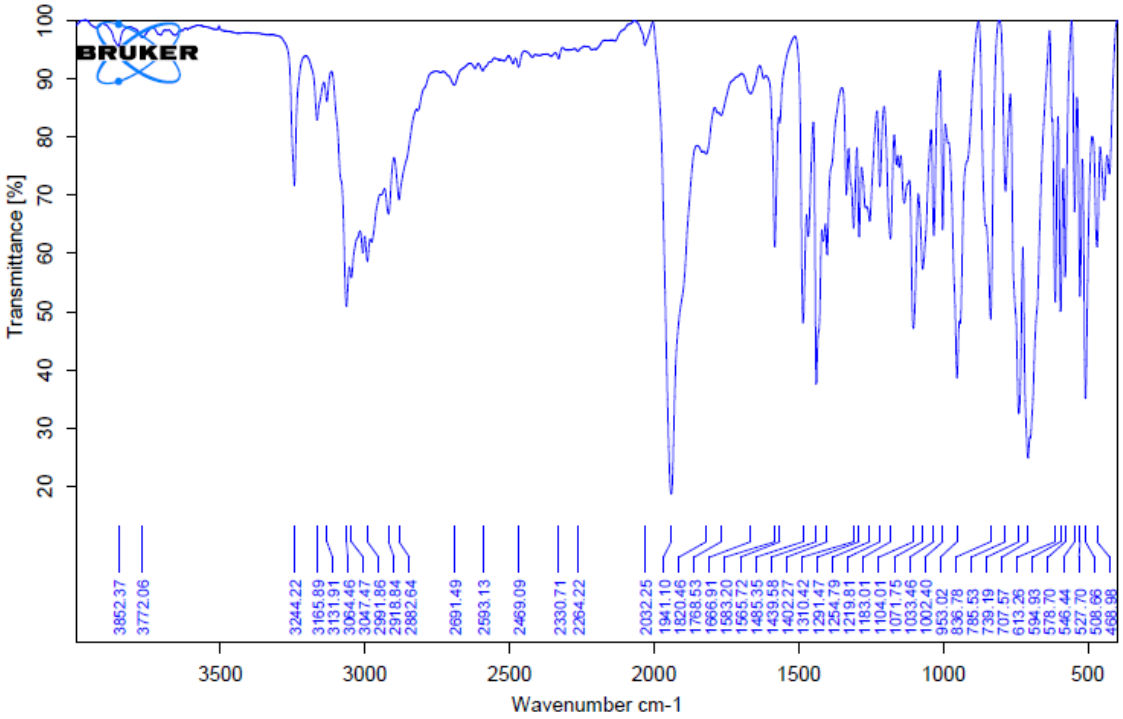

Figure S64. FTIR spectrum of **3**.

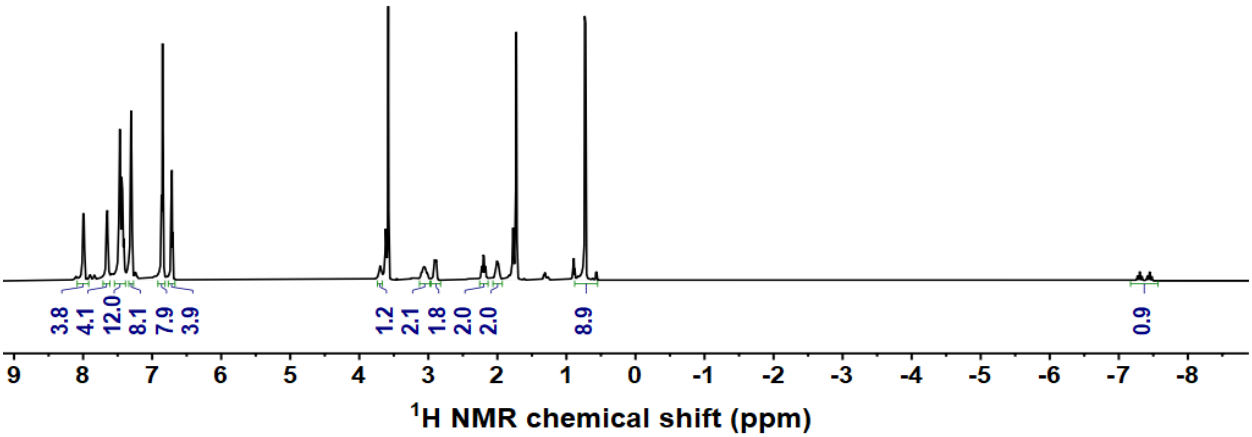

Figure S65. ^{1}H NMR spectrum of **3** in THF-d_8.

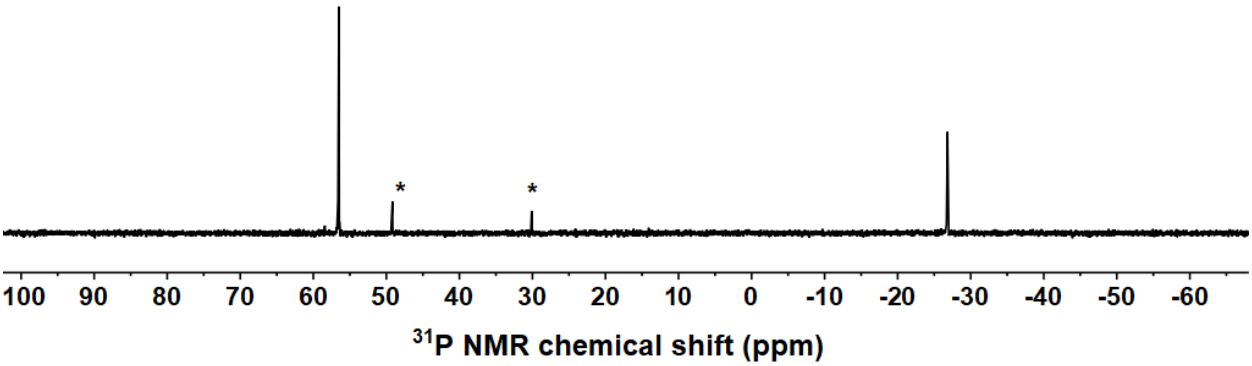

Figure S66. ^{31}P{^{1}H} NMR spectrum of **3** in THF-d_8; [*]: residual impurities.

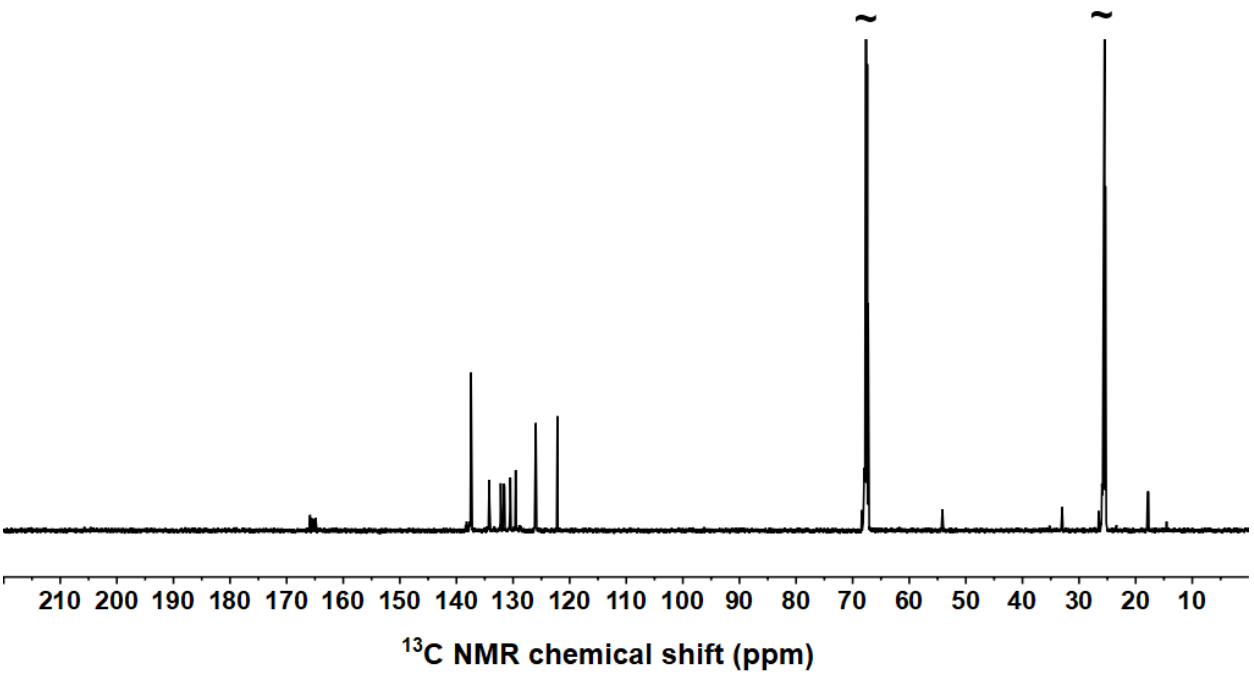

Figure S67. $^{13}C\{^{1}H\}$ NMR spectrum of **3** in THF-d_8.

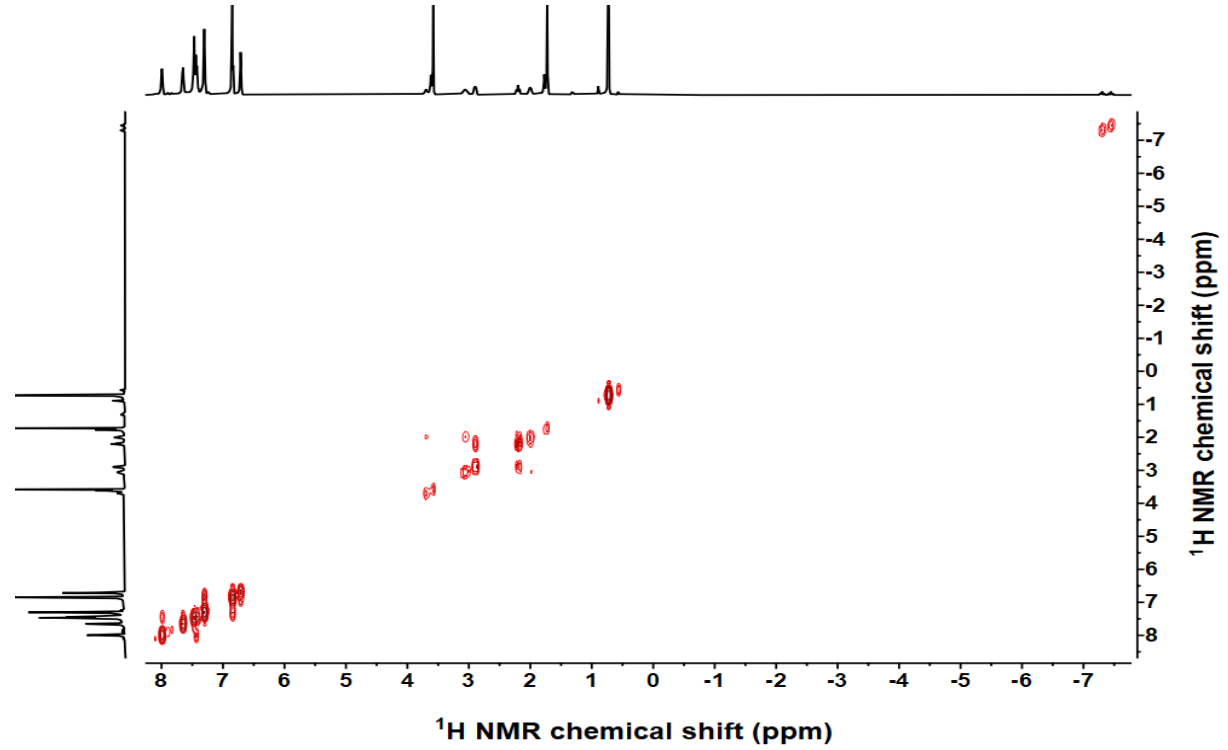

Figure S68. ^{1}H-^{1}H COSY NMR spectrum of **3** in THF-d_8.

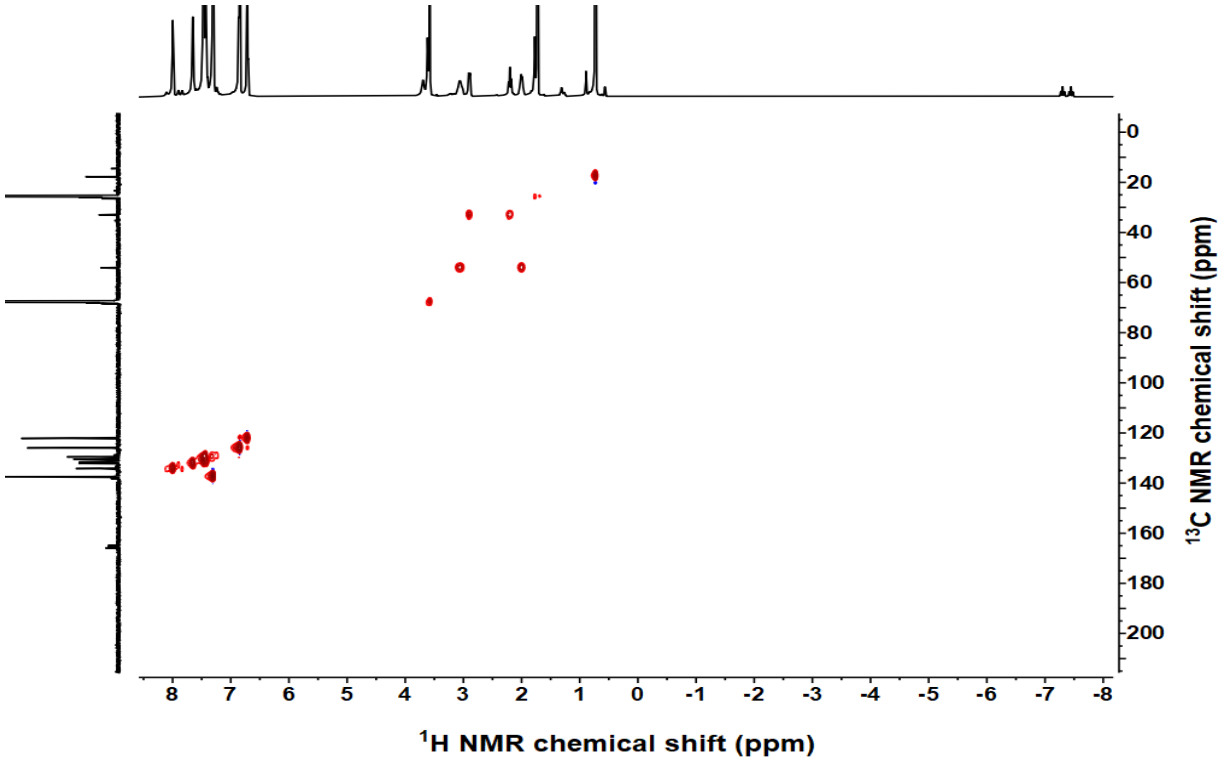

Figure S69. ^{1}H-^{13}C HSQC NMR spectrum of **3** in THF-d_8.

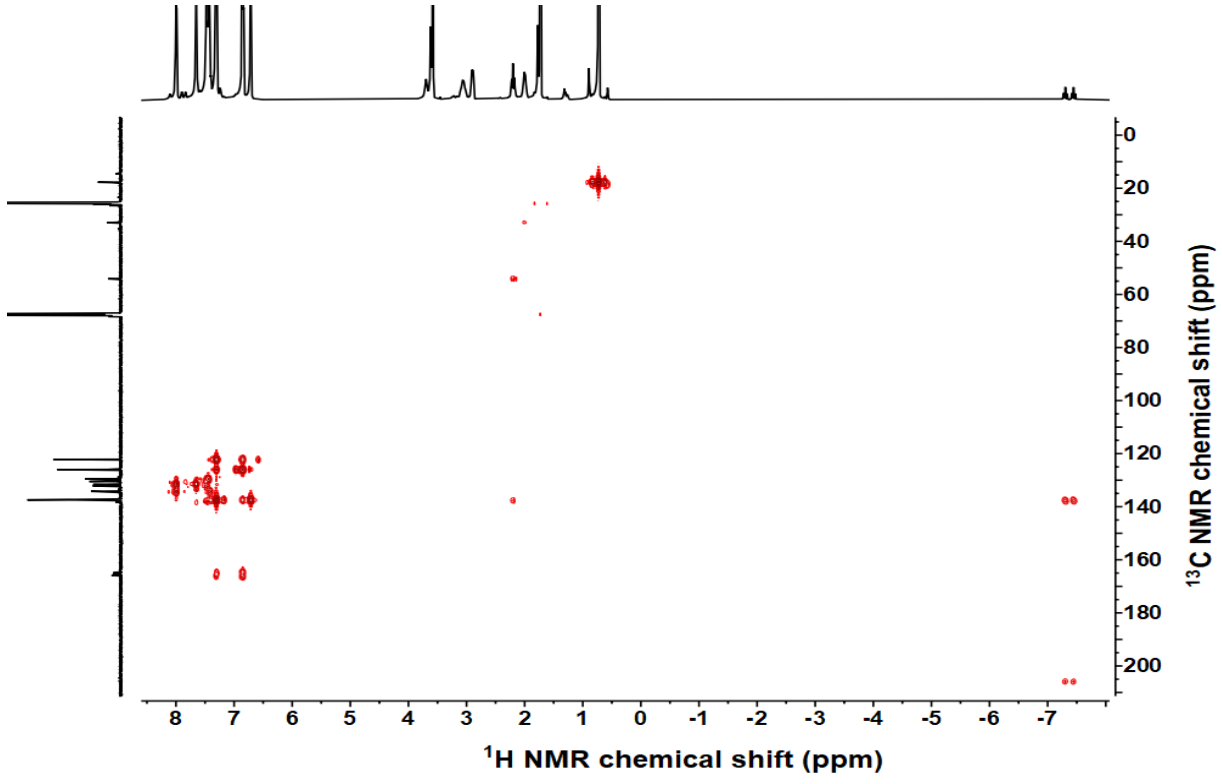

Figure S70. ^{1}H-^{13}C HMBC NMR spectrum of **3** in THF-d_8.

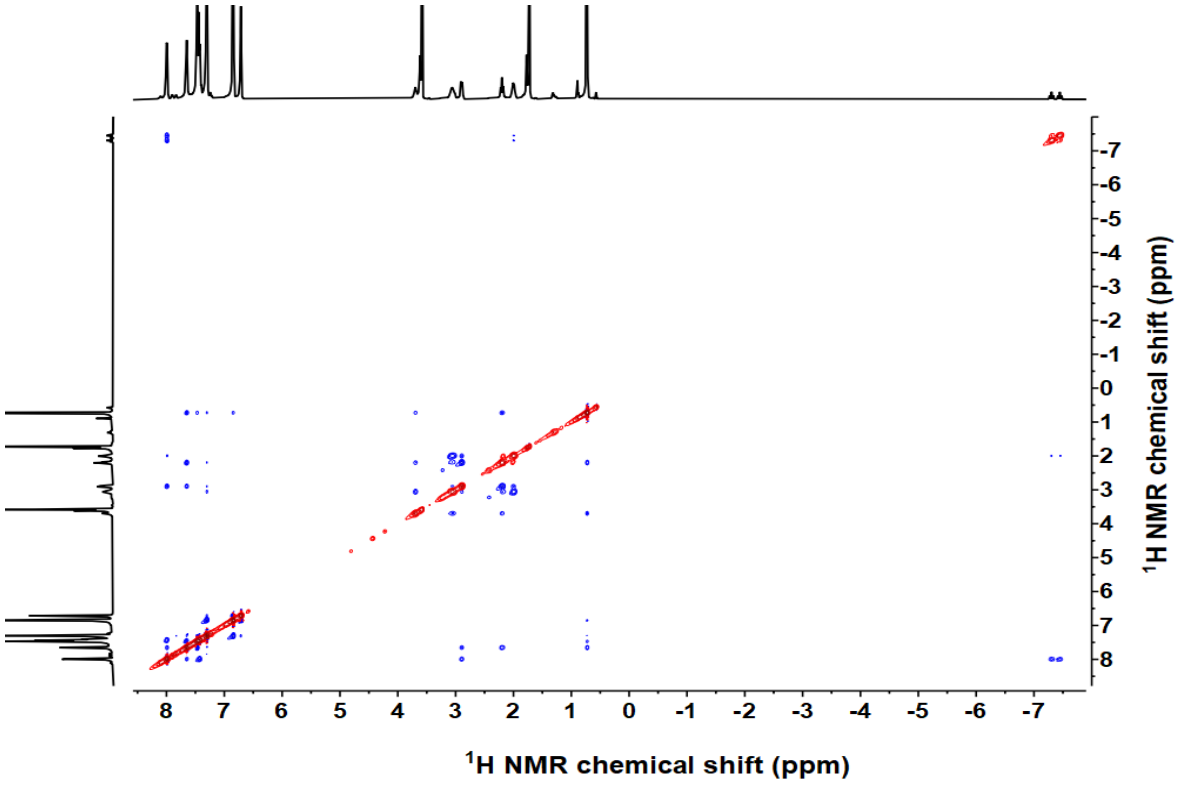

Figure S71. ^{1}H-^{1}H NOSY NMR spectrum of **3** in THF-d_8.

4

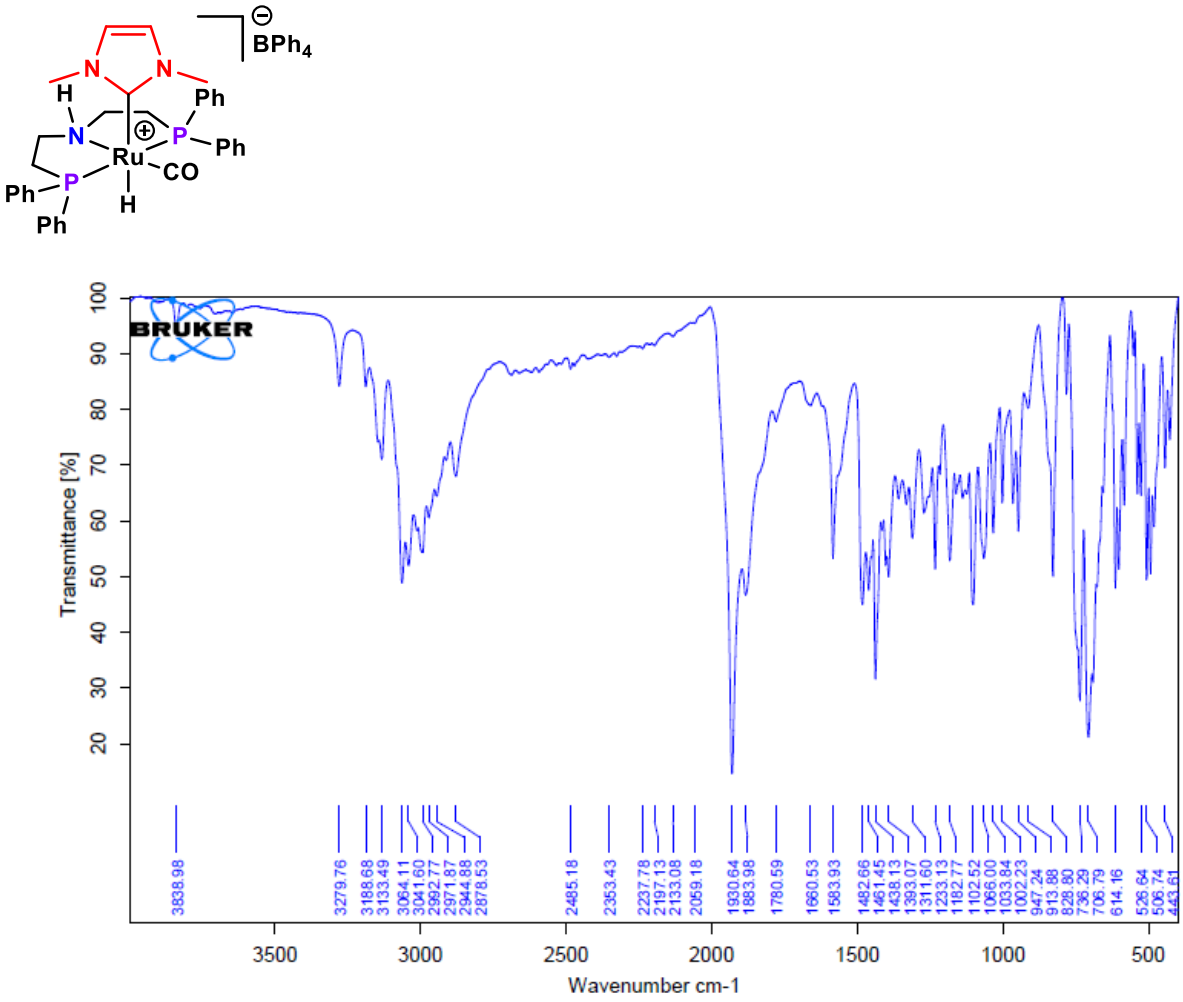

Figure S72. FTIR spectrum of **4**.

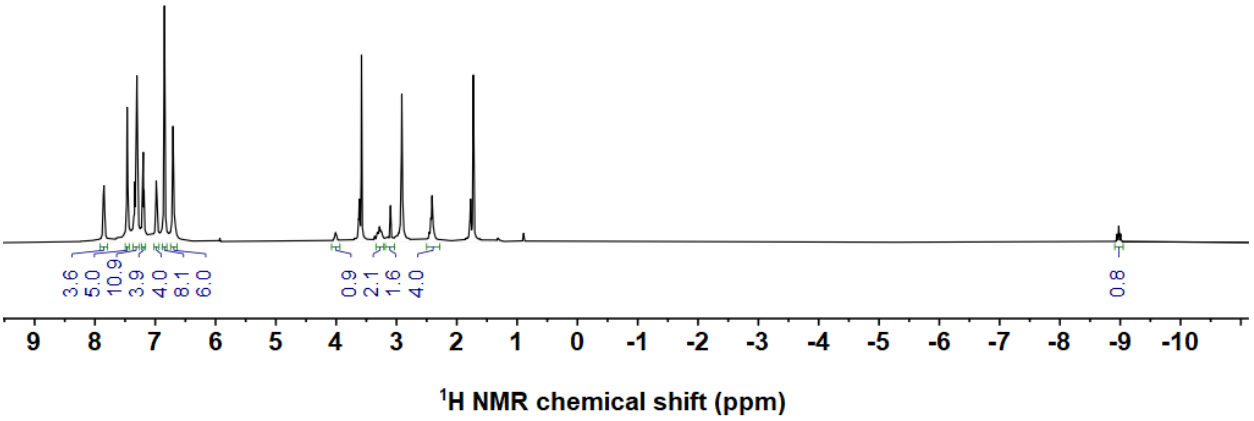

Figure S73. ^{1}H NMR spectrum of **4** in THF-d_8.

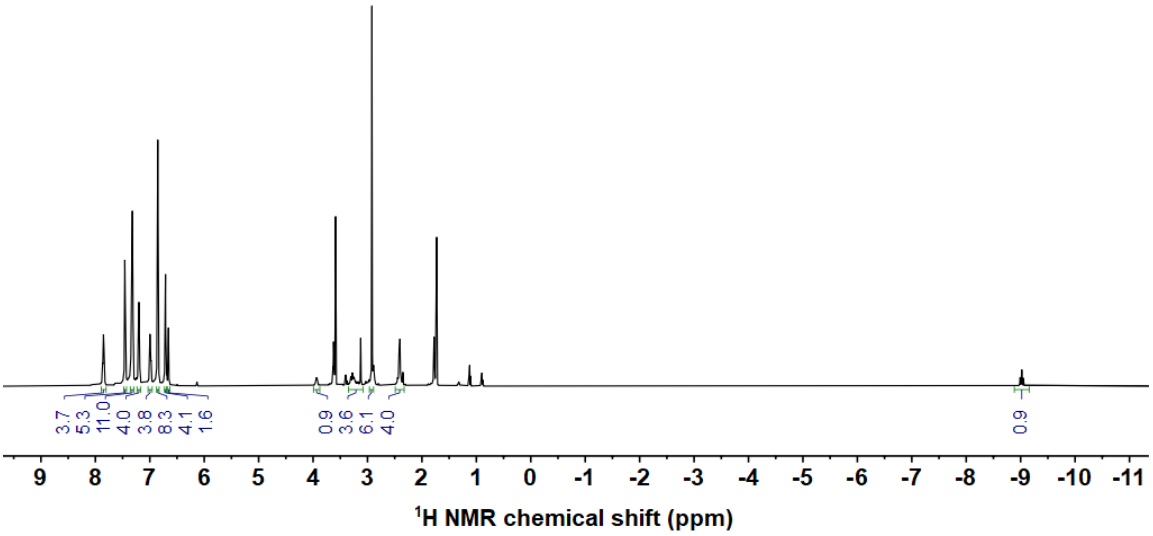

Figure S74. ^{1}H NMR spectrum of **4** in THF-d_8 at 50 °C.

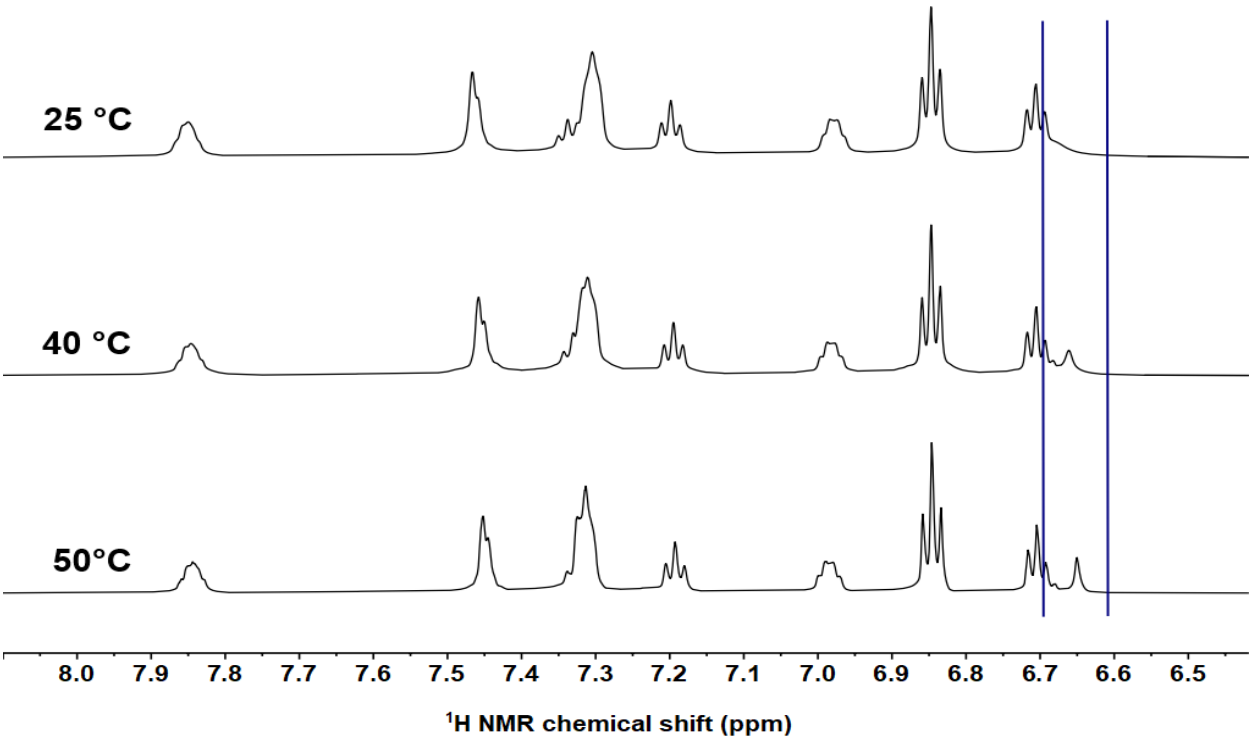

Figure S75. Variable temperature ^{1}H NMR spectrum of **4** in THF-d_8. Blue lines highlight region containing the NHC backbone protons.

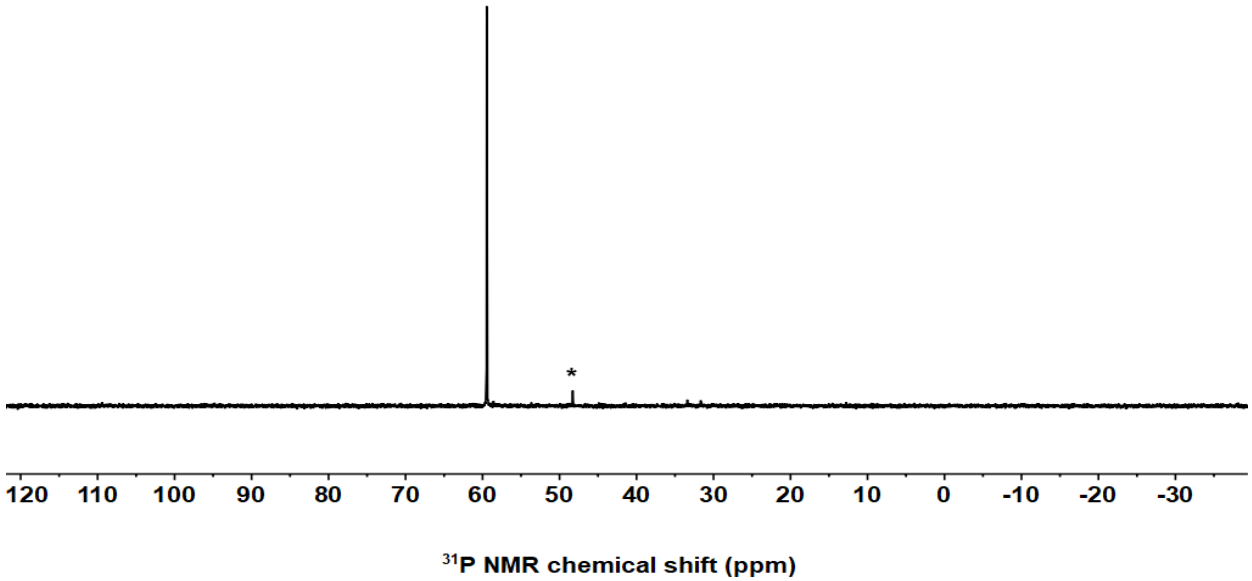

Figure S76. ^{31}P{^{1}H} NMR spectrum of **4** in THF-d_8; [*]: residual impurities.

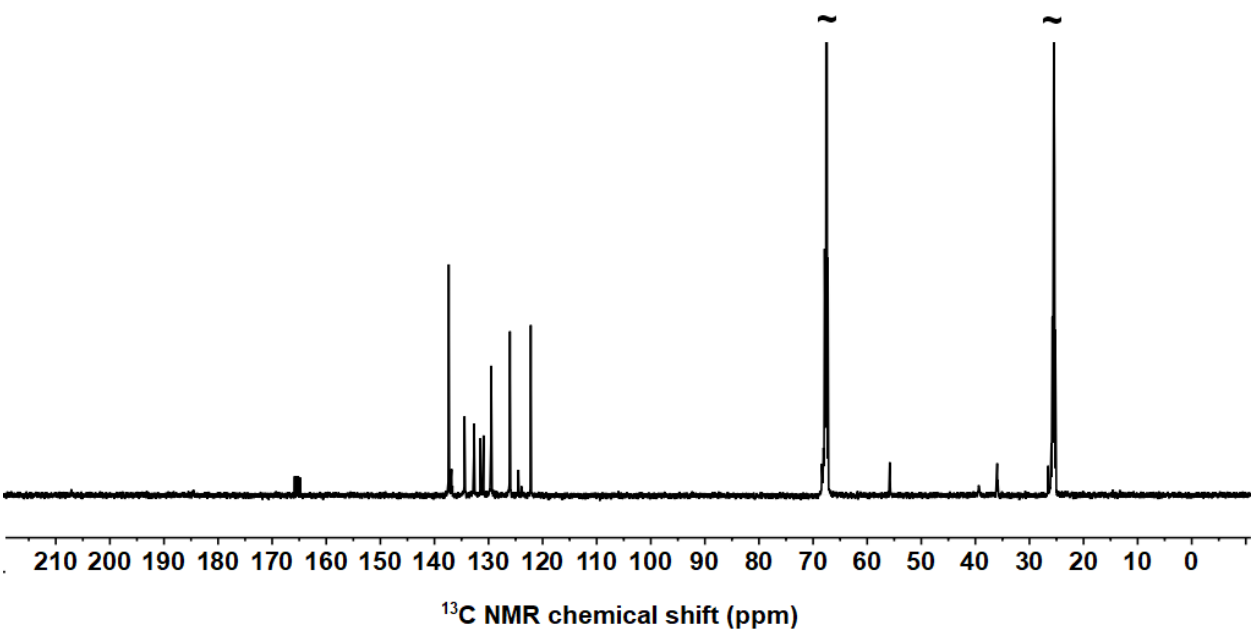

Figure S77. $^{13}C\{^{1}H\}$ NMR spectrum of **4** in THF-d_8.

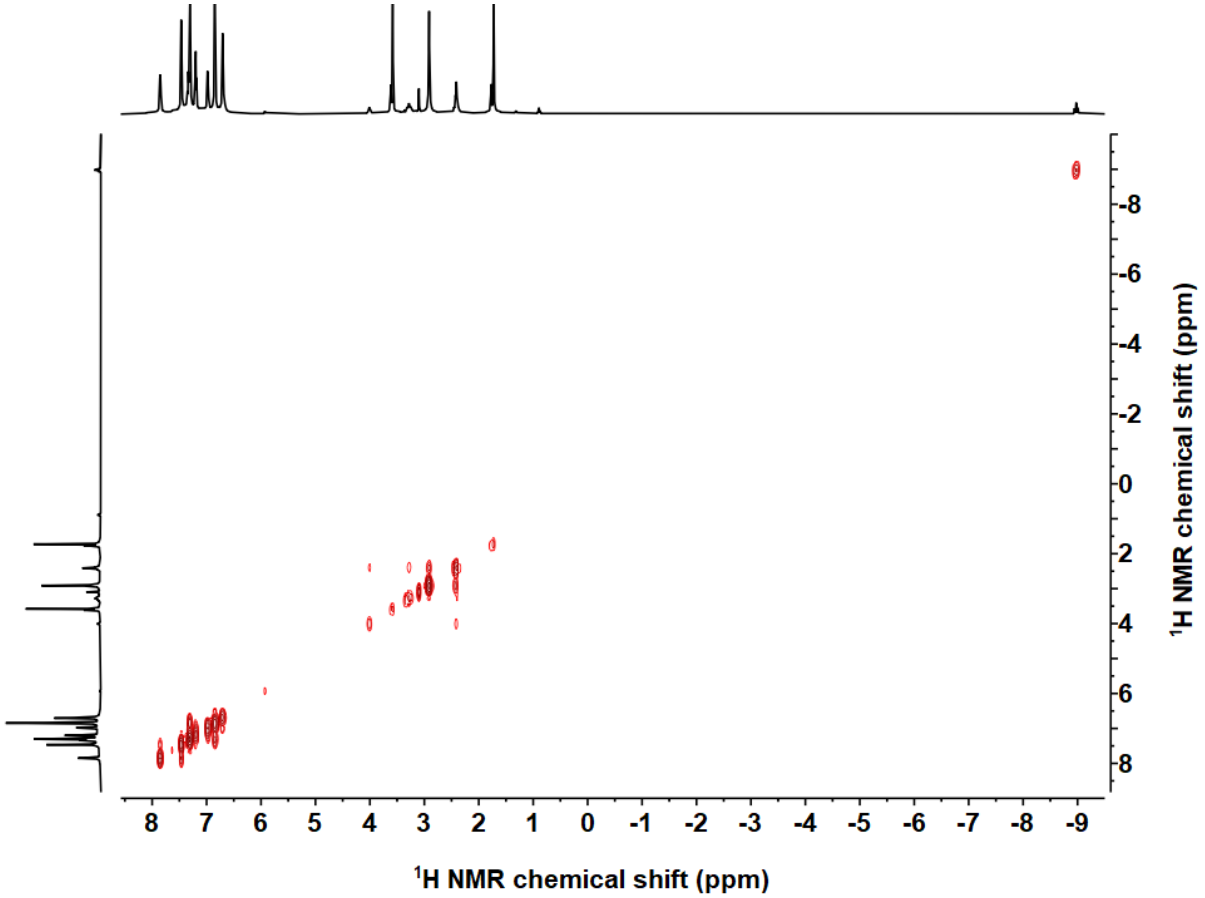

Figure S78. ^{1}H-^{1}H COSY NMR spectrum of **4** in THF-d_8.

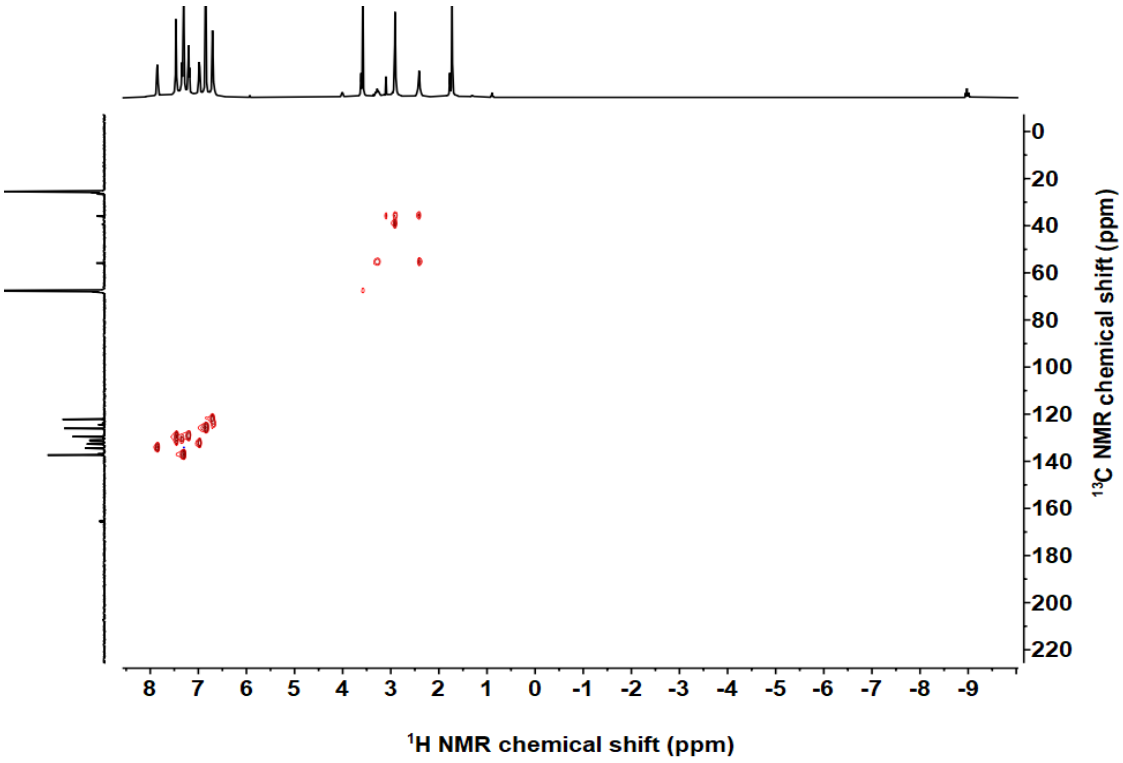

Figure S79. ^{1}H-^{13}C HSQC NMR spectrum of **4** in THF-d_8.

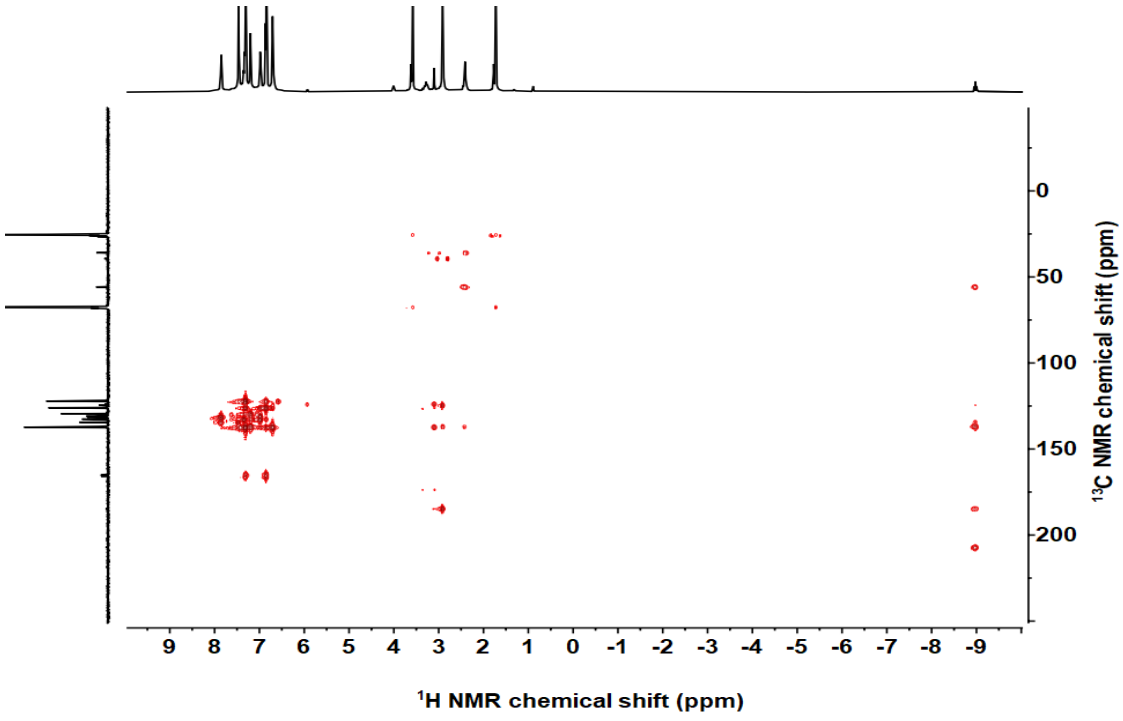

Figure S80. ^{1}H-^{13}C HMBC NMR spectrum of **4** in THF-d_8.

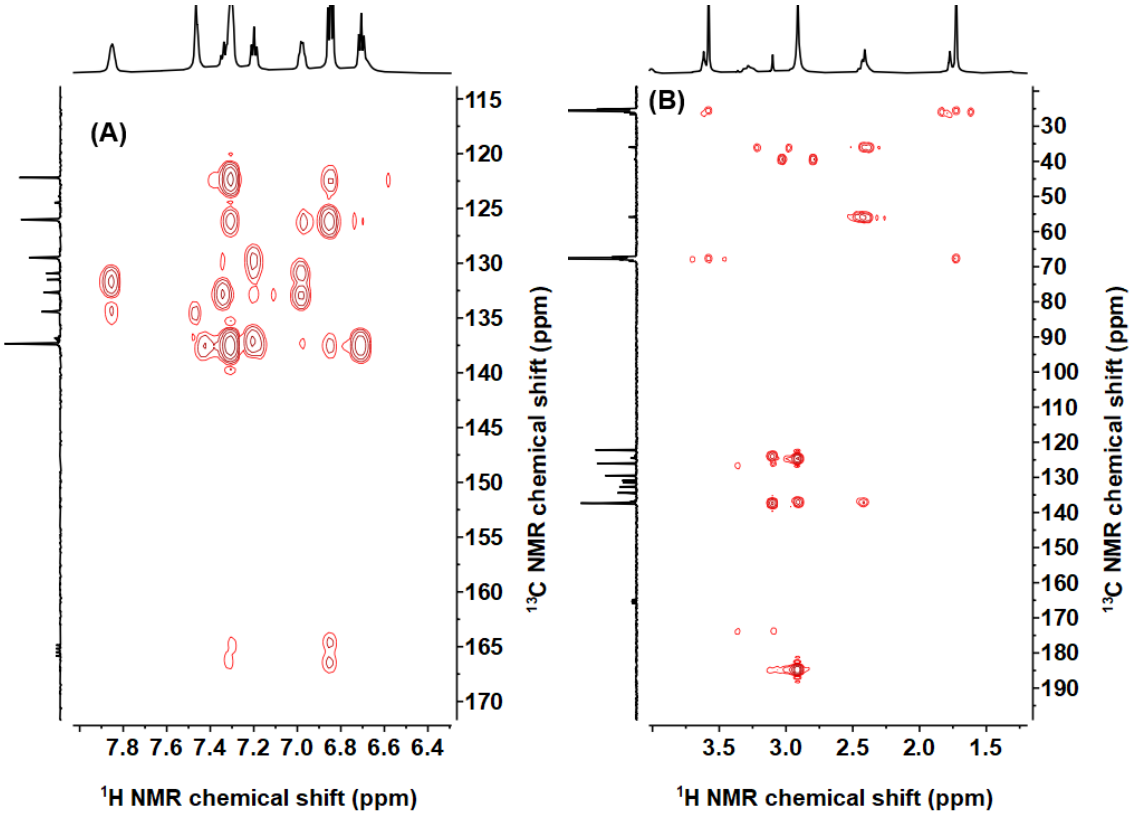

Figure S81. Expansions of the aromatic (A) and aliphatic (B) regions of the ^{1}H-^{13}C HMBC NMR spectrum of **4** in THF-d_8.

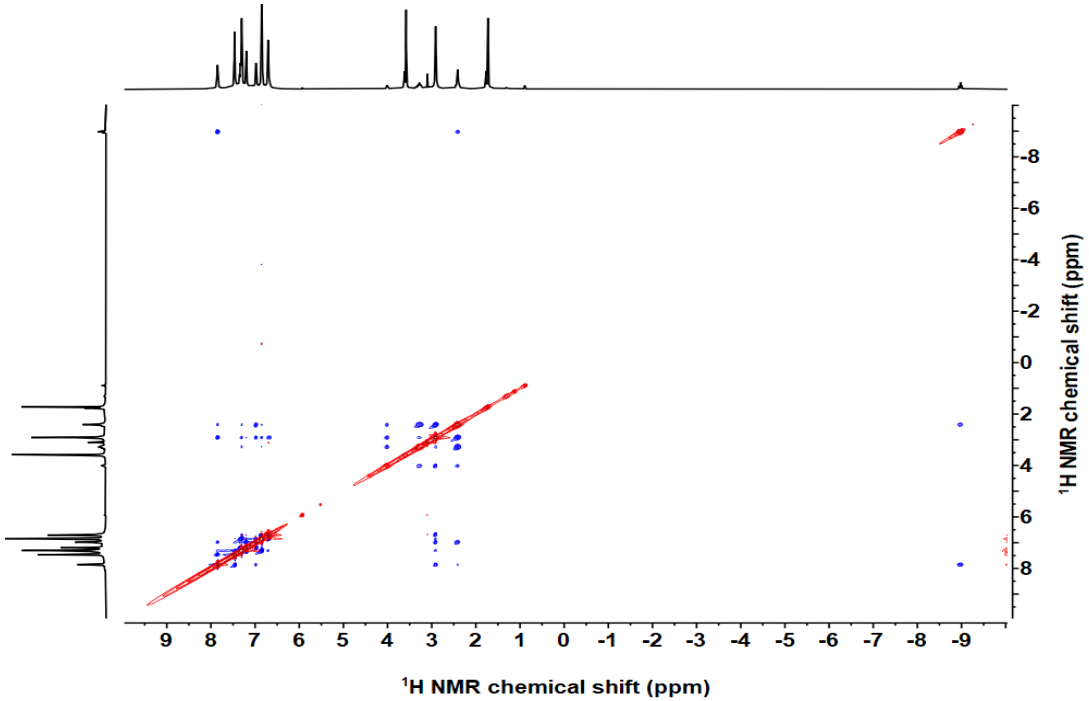

Figure S82. ^{1}H-^{1}H NOSY NMR spectrum of **4** in THF-d_8.

Ligand exchange studies

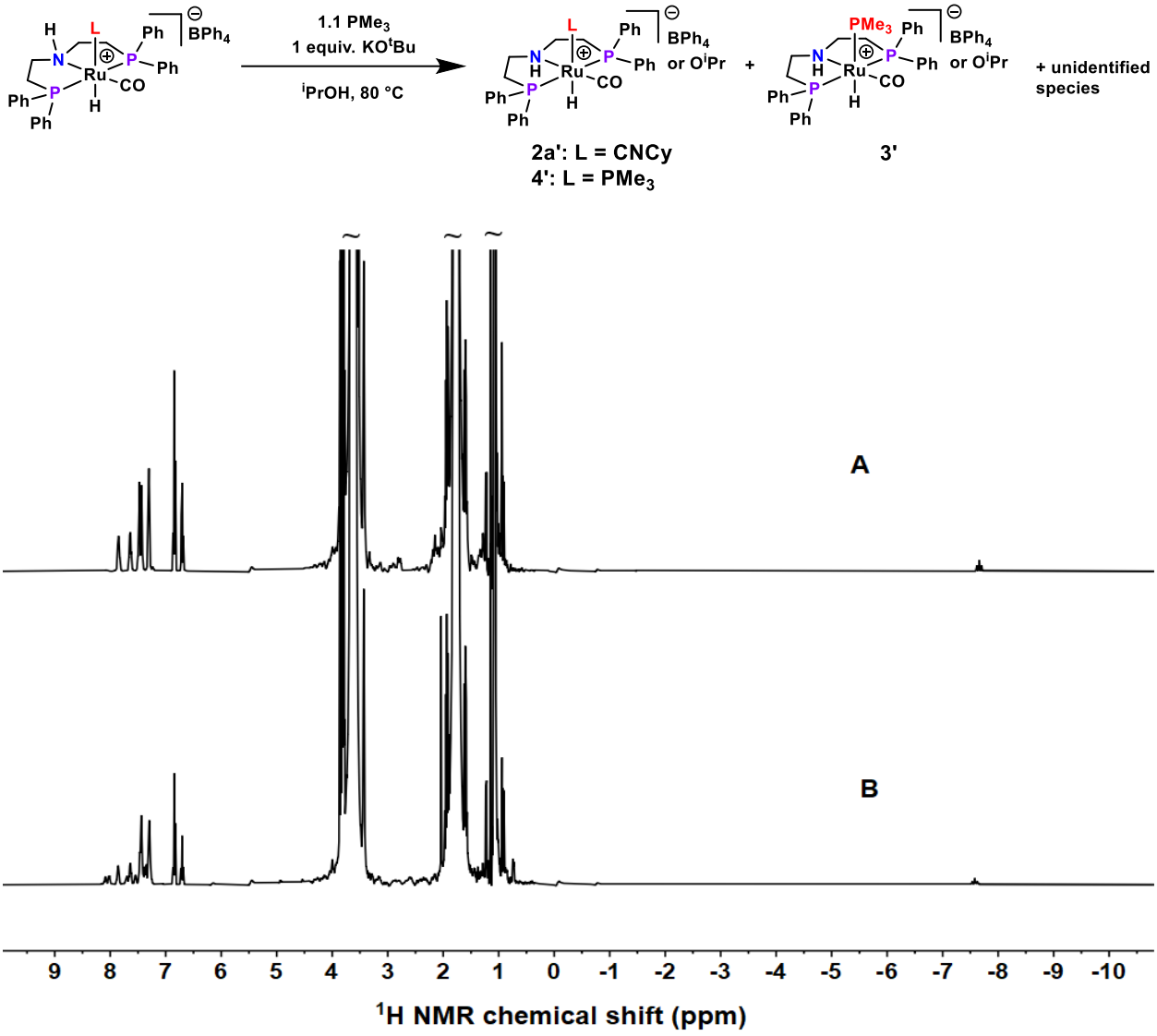

Figure S83. ^{1}H NMR spectra to monitor the progress of the reaction between **2a** and PMe_3. [A] after 30 minutes heating; [B] after addition of KO^{t}Bu followed by 30 minutes heating at 80 °C; ~ = signal cutoff.

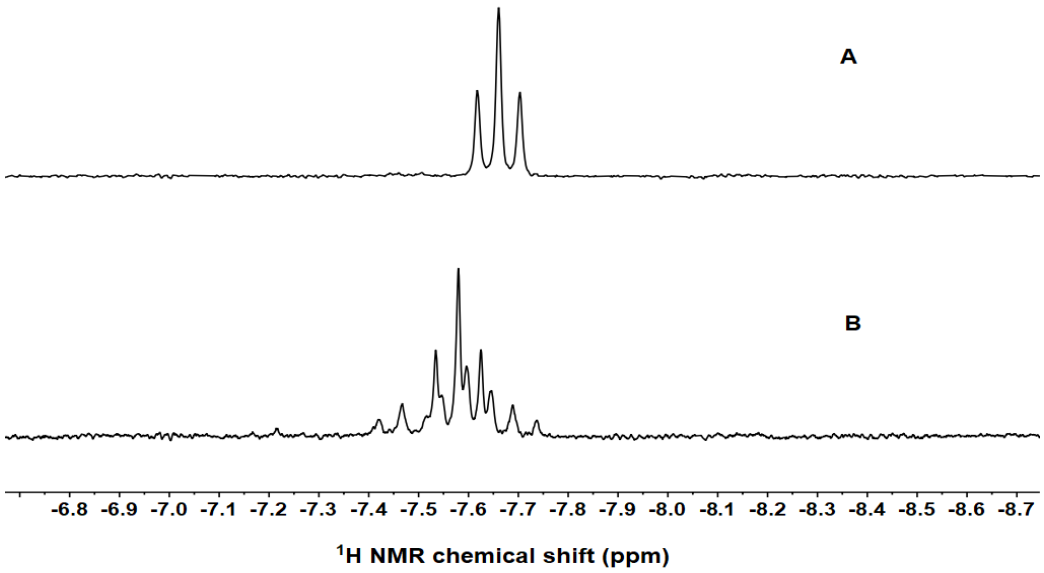

Figure S84. Expansion of the hydride region of the ^{1}H NMR spectra to monitor the progress of the reaction between **2a** and PMe_3. [A] after 30 minutes heating; [B] after addition of KO^tBu followed by 30 minutes heating at 80 °C.

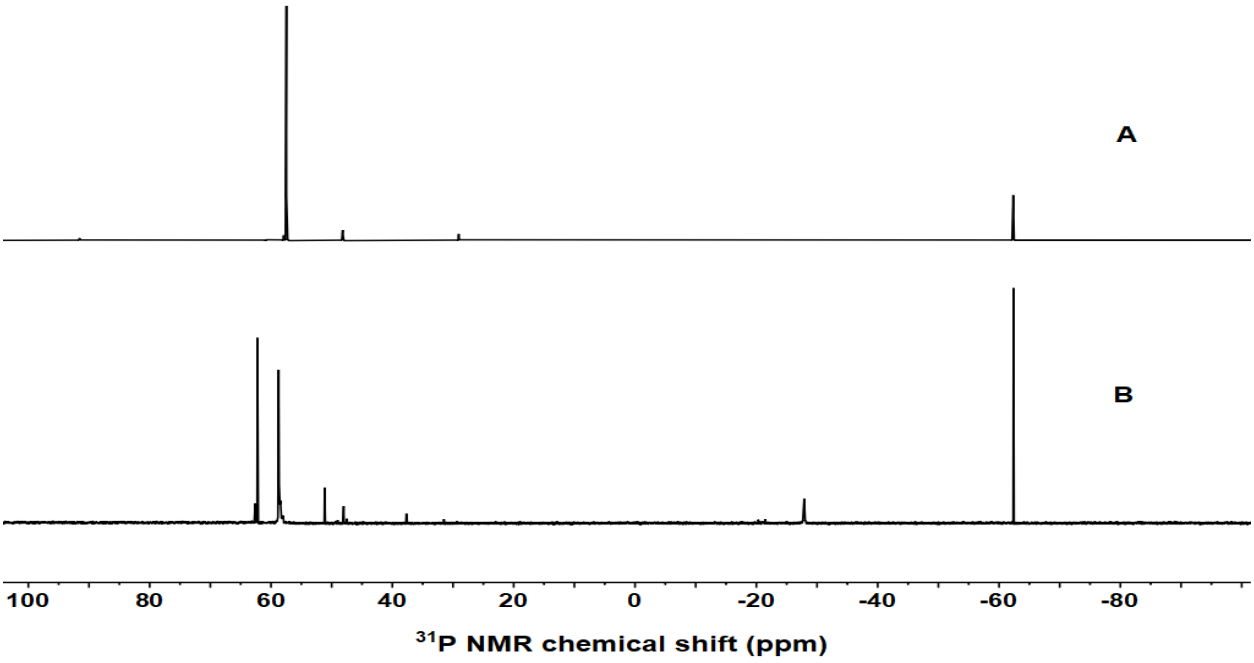

Figure S85. $^{31}P\{^{1}H\}$ NMR spectra to monitor the progress of the reaction between **2a** and PMe_3. [A] after 30 minutes heating; [B] after addition of KO^tBu followed by 30 minutes heating at 80 °C.

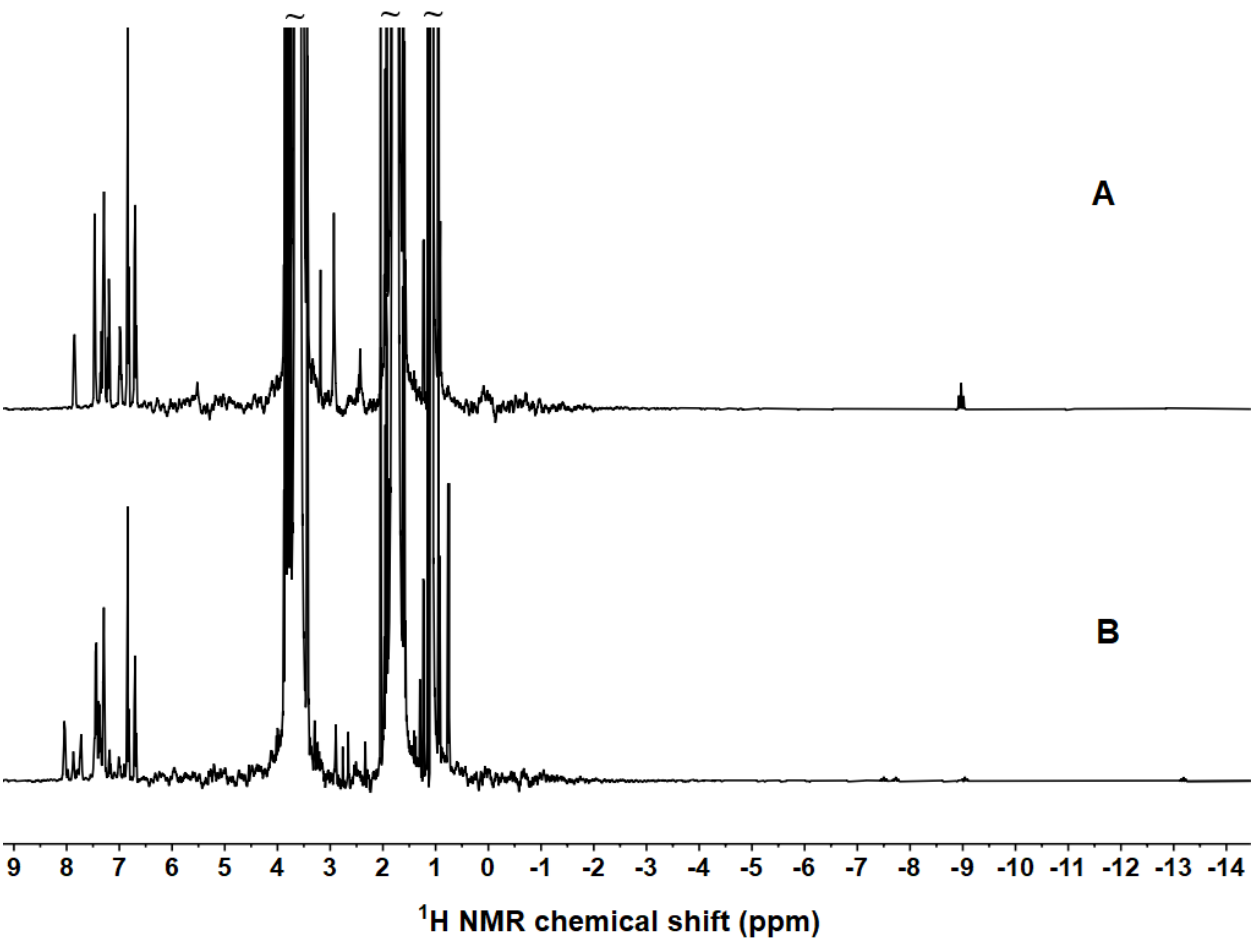

Figure S86. ^{1}H NMR spectra to monitor the progress of the reaction between **4** and PMe_3. [A] after 30 minutes heating; [B] after addition of KO^tBu followed by 30 minutes heating at 80 °C; ~ = signal cutoff.

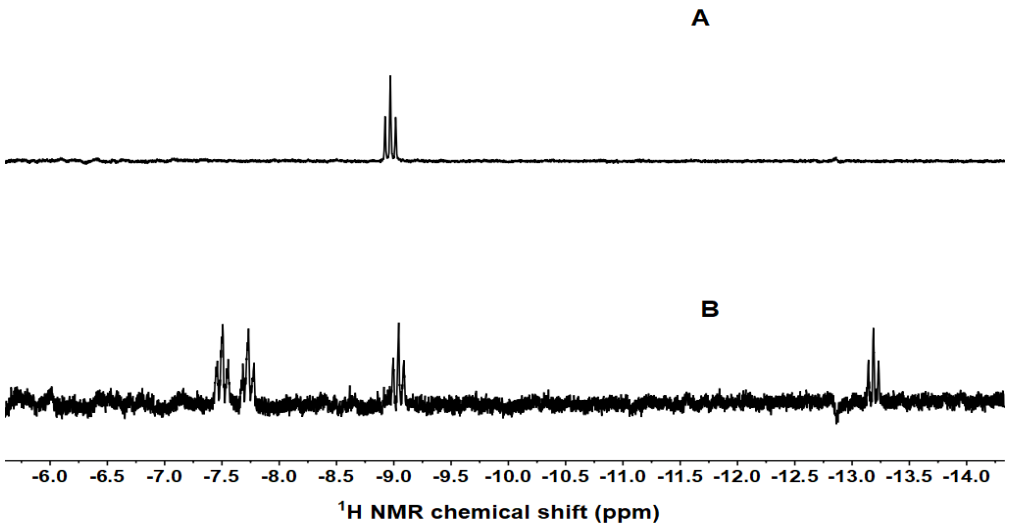

Figure S87. Expansion of the hydride region of the ^{1}H NMR spectra to monitor the progress of the reaction between **4** and PMe_3. [A] after 30 minutes heating; [B] after addition of KO^tBu followed by 30 minutes heating at 80 °C.

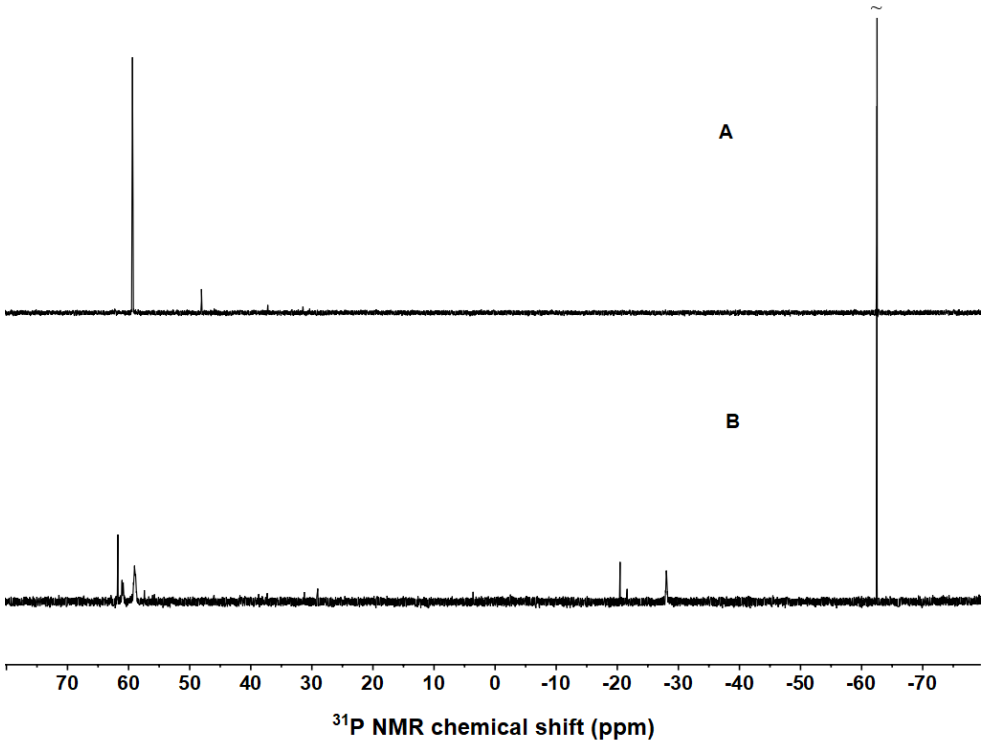

Figure S88. $^{31}P\{^{1}H\}$ NMR spectra to monitor the progress of the reaction between **4** and PMe_3. [A] after 30 minutes heating; [B] after addition of KO^tBu followed by 30 minutes heating at 80 °C. ~ = signal cutoff for PMe_3.